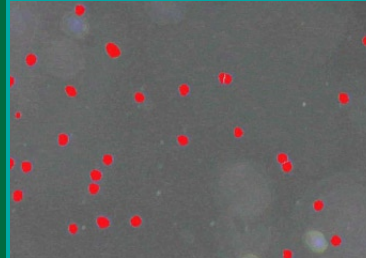




Application of an Image Analysis System to Enumerate and Measure Cyanobacteria



Research Report

31

Application of an Image Analysis System to Enumerate and Measure Cyanobacteria

Catherine Bernard, Peter Baker, Bret Robinson and Paul Monis
Australian Water Quality Centre

Research Report No 31

March 2007

© CRC for Water Quality and Treatment, 2007

DISCLAIMER

- The Cooperative Research Centre for Water Quality and Treatment and individual contributors are not responsible for the outcomes of any actions taken on the basis of information in this research report, nor for any errors and omissions.
- The Cooperative Research Centre for Water Quality and Treatment and individual contributors disclaim all liability to any person in respect of anything, and the consequences of anything, done or omitted to be done by a person in reliance upon the whole or any part of this research report.
- The research report does not purport to be a comprehensive statement and analysis of its subject matter, and if further expert advice is required, the services of a competent professional should be sought.

Cooperative Research Centre for Water Quality and Treatment
Private Mail bag 3
Salisbury
South Australia, 5108
AUSTRALIA

Telephone: + 61 8 8259 0240
Fax: + 61 8 8259 0228
Email: crc@sawater.com.au
Web site: www.waterquality.crc.org.au

Application of an Image Analysis System to Enumerate and Measure Cyanobacteria

Research Report 31
ISBN 1876616563

Foreword

Title: Application of an Image Analysis System to Enumerate and Measure Cyanobacteria

Research Officer: Dr. Catherine Bernard

Project Leader: Dr. Paul Monis

Research Node: Australian Water Quality Centre

CRC for Water Quality and Treatment Project No. 2.3.3.1. – Application of Computer-Assisted Image Analysis Techniques to Counting and Identification of Cyanobacteria

Executive summary

Blooms of noxious cyanobacteria, or blue-green algae, are more and more frequently reported in freshwater environments. Species involved in these blooms can be toxic to animals and humans or can cause taste and odour problems. Toxic species can lead to public health problems and taste and odours represent the major cause of consumer complaints in developed countries. Water utilities then face the challenge to establish effective water quality monitoring programs to detect trends in population growth of noxious species so that appropriate action can be taken to control bloom development. A major difficulty associated with monitoring programs for cyanobacteria arises from the need to identify and enumerate target species. These tasks involve the manual analysis, using a microscope, of water samples by trained experts – a very time-consuming and, therefore, expensive operation.

The aim of this project was to develop and validate an image analysis system able to count and measure species of cyanobacteria in an automatic manner. The study was carried out at the Australian Water Quality Centre (Adelaide, South Australia) and focussed on customizing a user-friendly image analysis system, VideoPro (Leading Edge, Adelaide, Australia).

Research design

The research undertaken focussed essentially on two morphotypes of cyanobacteria: an ovoid/ellipsoid species (e.g., *Microcystis* sp.) and a straight to curved trichome-like species (e.g. *Cylindrospermopsis raciborskii*). This choice was aimed to encompass very commonly found noxious cyanobacteria. The research was carried out by Dr. Catherine Bernard, with the collaboration of Lynn Jarvis, the creator of the image analysis system VideoPro (Leading Edge, Adelaide, Australia).

Study of the morphometric parameters of the two species of cyanobacteria chosen was first undertaken. Computing programs were written to allow selection of the two species of interest in samples. Solutions had to be found to problems encountered on the images analysed such as separating touching cells of *Microcystis* or dealing with overlapping trichomes of *Cylindrospermopsis*. Best means of measuring the cyanobacteria via the image analysis system had to be worked out. Scanning systems were developed to allow rapid and automatic acquisition of images from samples, as well as automatic analyses of the data. Each step was controlled and validated with material from cultures. Towards the end of the project, the user-friendliness of the system was successfully tested when applied to help with acquisition of data in other projects. The image analysis system was also tested with natural samples.

Results

The results showed that an image analysis system can be developed and customized to be used for analysis of culture and natural samples of different morphotypes of cyanobacteria. The results obtained are comparable with those obtained by operators, with a higher reproducibility and higher objectivity. The rapidity and ease of acquisition of the data render the image analysis system a very efficient tool.

The amount and quality of data obtained with such an image analysis system gave valuable information on the best morphometric parameters to choose when measuring and calculating the volume of ellipsoid cells such as *Microcystis*. It also appeared that difficult measurements such as the length of curved trichomes could be rapidly and accurately executed by the image analysis system.

The use of rapid and automated scans appeared to free the operator to attend to other tasks. When using the system with natural samples, however, preliminary work has to be carried out to ensure the programs written are well fitted to the samples and select only the species of interest.

Conclusion

Image analysis, as shown in this project, can improve the efficiency with which water utilities monitor cyanobacteria. It is also becoming a very affordable tool, the use of which is in rapid expansion in all fields using microscopy. Such a system can minimise the time taken during routine surveys of cyanobacteria in water bodies and can provide more accurate calculations of biovolume.

Contents

FOREWORD	3
EXECUTIVE SUMMARY	4
LIST OF FIGURES	7
LIST OF TABLES	8
ABBREVIATIONS	9
1. INTRODUCTION	10
1.1 Aims	10
1.2 Background	10
1.2.1 Noxious cyanobacteria	10
<i>Toxicity problems</i>	10
<i>Taste and odour problems</i>	10
1.2.2 Guidelines	11
1.3 Methods Used	12
1.3.1 Monitoring laboratories	12
1.3.2 Other techniques	12
1.4 Image Analysis	13
1.4.1 Historic	13
<i>Advantages</i>	13
1.4.2 Principles	14
<i>Image acquisition and hardware</i>	14
<i>Image processing techniques: enhancement</i>	14
<i>Segmentation</i>	14
<i>Processing of binary images</i>	15
<i>Feature measurement</i>	15
2. SYSTEM DEVELOPMENT	16
2.1 VideoPro 32 and Set-up	16
2.2 Sample preparation	16
2.2.1 Cyanobacteria cultures	16
2.2.2 Slides	16
2.3 Manual operation	17
2.3.1 Setting-up programs	17
2.3.2 Executive programs	18
2.4 Automation	18
2.4.1 Scan principles	18
4.2 Rapid scan	20
<i>Material and Methods (Jarvis, pers. com.)</i>	20
<i>Preliminary results</i>	20
<i>Discussion</i>	22
2.5 Validation of VideoPro 32	22
2.5.1 Calibration	22
2.5.2 Latex beads	22

3. APPLICATION TO OVOID CELLS.....	23
3.1 Algorithms.....	23
3.1.1 Enumeration.....	23
3.1.2 Measurement	24
3.2 Validations	26
3.2.1 Inter-laboratory measurement validation	26
<i>Material and Methods</i>	26
<i>Results</i>	26
3.2.2 Intra-laboratory validation of enumeration and measurement	27
<i>Materials and Methods</i>	27
<i>Results</i>	27
3.2.3 Using Gene Frames® and fluorescence.....	29
<i>Validation 1</i>	29
<i>Validation 2</i>	30
3.2.4 Discussion.....	31
3.3 Colonial Microcystis.....	31
3.3.1 Material and Methods	32
<i>Samples</i>	32
<i>Disaggregation treatments</i>	32
<i>Image analysis and calculations</i>	33
3.3.2 Results	33
<i>The effect of disaggregation treatment on non-colonial samples</i>	33
<i>The effect of disaggregation treatment on colonial samples</i>	35
3.3.3 Discussion.....	39
4. APPLICATION TO TRICHOMES.....	40
4.1 Algorithms.....	40
4.1.1 Enumeration.....	40
<i>Routine enumeration</i>	40
<i>Image analysis algorithm</i>	40
4.1.2 Measurement	41
<i>Fibre length and fibre width</i>	42
4.2 Validations with laboratory cultures.....	44
4.2.1 Comparison of enumeration techniques	45
4.2.2 Biovolume versus light intensity.....	46
4.2.3 Growth experiment.....	48
<i>Material and Methods</i>	48
<i>Results</i>	49
<i>Discussion</i>	51
4.3. <i>Field experiments</i>	52
4.3.1 Material and Methods	52
4.3.2 Results	54
4.3.3 Discussion.....	56
4.4 <i>Discussion and Conclusion</i>	57
5. DISCUSSION	58
6. RECOMMENDATIONS	60
7. ACKNOWLEDGMENTS	61
8. REFERENCES.....	62

List of Figures

Figure 1-1: Approaches to segmentation.

Figure 1-2: Examples of feature-specific measurements.

Figure 2-1: Diagram detailing the relationships of the programs involved in the automatic scans.

Figure 2-2: Rapid scan: mosaic image obtained after scanning a sample of *Cylindrospermopsis raciborskii* (18000 trichomes.mL⁻¹).

Figure 2-3: Rapid scan: mosaic image obtained after scanning a sample of *Cylindrospermopsis raciborskii* (4700 trichomes.mL⁻¹).

Figure 2-4: Rapid scan: detailed mosaic image after scanning *Microcystis aeruginosa*.

Figure 3-1: Binary images of *Microcystis* using separation of touching cells algorithm.

Figure 3-2: *Microcystis* – photographs showing different cell shapes.

Figure 3-3: *Microcystis* – comparison of data on cell length, width and biovolume.

Figure 3-4: *Microcystis* – comparison of enumeration results obtained with small and large GeneFrame®s.

Figure 3-5: *Microcystis* – disaggregation experiments – examples of acquired images before and after segmentation.

Figure 4-1: *Cylindrospermopsis* – binary image processes to enumerate trichomes.

Figure 4-2: *Cylindrospermopsis* – illustration of the difficulty to measure curved trichome visually.

Figure 4-3: *Cylindrospermopsis* – trichomes width obtained with different techniques.

Figure 4-4: *Cylindrospermopsis* – trichomes biovolume obtained with different techniques.

Figure 4-5: *Cylindrospermopsis* – comparison of three enumeration techniques of one sample in function of the number of fields of view considered.

Figure 4-6: *Cylindrospermopsis* – overtime biovolume changes in function of light intensity.

Figure 4-7: *Cylindrospermopsis* – overtime trichomes length changes in function of light intensity.

Figure 4-8: *Cylindrospermopsis* – growth experiment – morphometric variations overtime.

Figure 4-9: *Cylindrospermopsis* – growth experiment – estimation of cell concentration overtime.

Figure 4-10: *Cylindrospermopsis* – field experiments – map of North Pine Dam (Queensland).

Figure 4-11: *Cylindrospermopsis* – field experiments – variations of density, biomass and length of trichomes at different depths in January 2005 at Site 3.

Figure 4-12: *Cylindrospermopsis* – field experiments – variations of density, biomass and length of trichomes at different depths in February 2005 at Site 3.

List of Tables

Table 2-1: Rapid scan: example of results of speed and efficiency.

Table 2-2: Image analysis validation – calibration of pixel sizes.

Table 2-3: Image analysis validation – performances in measuring latex beads.

Table 3-1: *Microcystis* – inter-laboratory comparison of data of cell length, width and biovolume obtained by different operators and the IA.

Table 3-2: *Microcystis* – intra-laboratory comparison of data of cell length, width obtained by different operators and the IA.

Table 3-3: *Microcystis* – intra-laboratory comparison of data of cell biovolume.

Table 3-4: *Microcystis* – intra-laboratory comparison of enumeration.

Table 3-5: *Microcystis* – intra-laboratory comparison of speed to accomplish measurements and enumeration.

Table 3-6: *Microcystis* – GeneFrame[®] validation of enumeration performances using DIC and fluorescence optics.

Table 3-7: *Microcystis* – GeneFrame[®] validation of enumeration by different techniques.

Table 3-8: *Microcystis* – disaggregation experiments – list of samples used.

Table 3-9: *Microcystis* – disaggregation experiments – results for non-colonial samples exposed to heating treatment.

Table 3-10: *Microcystis* – disaggregation experiments – results for non-colonial samples exposed to grinding treatment.

Table 3-11: *Microcystis* – disaggregation experiments – results for loose/diffuse colonies exposed to heating treatment.

Table 3-12: *Microcystis* – disaggregation experiments – results for loose/diffuse colonies exposed to grinding treatment.

Table 3-13: *Microcystis* – disaggregation experiments – results for compact colonies exposed to heating treatment.

Table 3-14: *Microcystis* – disaggregation experiments – results for compact colonies exposed to grinding treatment.

Table 4-1: *Cylindrospermopsis* – comparison of manual and IA enumeration of triplicate sample.

Table 4-2: *Cylindrospermopsis* – field experiments – list of genera of algae and cyanobacteria present.

Table 4-3: *Cylindrospermopsis* – field experiments – comparison of estimated cell densities at the surface for all sites.

Abbreviations

DIC	Differential interference optics
IA	Image analysis
MIB	2-methylisoborneol
PCR	Polymerase Chain Reaction
WHO	World Health Organisation

1. Introduction

Cyanobacteria, also known as blue-green algae, are the most notorious bloom formers in freshwater environments. Their success is due to their ability to adapt their physiological capacities to compete with other phytoplankton species (e.g., for light and nutrients, Padisák 1997), and the fact that they seem less edible for zooplankton and fish than other non-blooming algae (Gilbert 1996; Reynolds 1998). Cyanobacteria are photosynthetic, oxygen-producing and nitrogen-fixing prokaryotic organisms. They are characterized by the presence of the accessory pigment phycobilin. There are three basic morphological groups: 1) unicells, which may be solitary or aggregated in colonies; 2) undifferentiated non-heterocyst filaments, which also may be solitary or aggregated; and 3) filamentous forms with differentiated cells called heterocysts (Paerl et al. 2001).

As a result of increasing environmental stress on freshwater ecosystems (e.g., eutrophication), blooms are increasing in number and frequency world-wide. Besides health problems due to their toxicity (such as the Caruaru tragedy in Pernambuco state, Brazil, Azevedo 1996), and environmental problems (e.g. fish kills and food web alterations), such blooms may also give rise to water quality and engineering problems such as clogging of filters in water treatment works, coloration of the water or production of tastes and odours (Paerl et al. 2001).

1.1 Aims

A major difficulty in basic research and monitoring programs for noxious cyanobacteria arises from the need to identify and enumerate them. These tasks usually involve the analysis of water samples by trained experts – a very time-consuming and, therefore, expensive operation (Walker 1999). Moreover, such tasks are subject to investigator bias and fatigue.

The aims of this project were to:

- 1) Develop automated protocols to enumerate some types of cyanobacteria;
- 2) Develop protocols to provide biomass data.

1.2 Background

1.2.1 Noxious cyanobacteria

Toxicity problems

Forty-five to ninety percent of cyanobacterial blooms worldwide are of toxin-producing taxa (Anonymous 2003), encompassing about 40 species (Skulberg et al. 1993). These toxins pose a potential risk to humans and livestock (Codd 1999; Bouvy et al. 2001; Carmichael et al. 2001). The most common taxa responsible for noxious blooms worldwide are *Anabaena*, *Cylindrospermopsis*, *Microcystis* and *Planktothrix*. The toxins involved (e.g., peptides, alkaloids, phenols) are secondary metabolites and can be classified as neurotoxins, hepatotoxins and anatoxins (Skulberg et al. 1993).

In Australia, toxic cyanobacterial blooms have been a long-standing problem for agricultural and human drinking water supplies, as well as for the recreational use of water. Livestock poisoning by cyanobacteria was first described in the 19th century near Adelaide (Francis 1878). The species responsible for blooms are mainly *Microcystis aeruginosa*, *Microcystis flos-aquae*, *Anabaena circinalis*, *Cylindrospermopsis raciborskii*, *Aphanizomenon ovalisporum*, *Nostoc* cf. *linkea*, and *Nodularia spumigena*. In three successive summers (1998-2000) in the centre of the City of Adelaide, the Torrens lake (no longer used for water supply) had a heavy bloom of toxic *M. aeruginosa*. This bloom was believed to be the cause of waterfowl deaths. Cases of human and wildlife poisoning are rare, more through avoidance of drinking foul-smelling water than through an absence of toxicity in cyanobacterial blooms (Falconer 2001).

Taste and odour problems

Biogenic tastes and odours are nowadays a major concern for many water utilities around the world. They often represent the major cause of consumer complaints in developed countries (Bruchet and Duguet 2004). Tastes and odours are often due to infinitesimal traces of organic compounds, such as geosmin and 2-methylisoborneol (MIB), produced by some actinomycetes and cyanobacteria (Persson

1996; Young et al. 1996). Geosmin, which gives an earthy-musty odour, and MIB which gives a musty-muddy and camphor-like taste and odour to water are thought to be non-toxic to invertebrates and mammals (Young et al. 1996). Predictability of such problems is low. Little is known about the environmental conditions that trigger their production. Toxicological studies are needed as geosmin and MIB have been shown to be genotoxic and estrogenic to rainbow trout hepatocytes – although at very high concentrations relative to environmental levels (Gagné et al. 1999).

During the last twenty years, many new cyanobacterial species capable of producing tastes and odours have been described (see Izaguirre and Taylor 2004). The genera mainly responsible for the production of geosmin and MIB are: *Anabaena*, *Oscillatoria*, *Phormidium*, *Lyngbya*, *Leptolyngbya*, *Microcoleus*, *Nostoc*, *Planktothrix*, *Pseudanabaena*, *Hyella*, and *Synechococcus* (Izaguirre and Taylor 2004). Tastes and odours are difficult to remove and processes that do so make treatment longer and more costly (Duguet et al. 1995).

Blooms of cyanobacteria have the potential to become a serious issue in terms of a government's ability to supply drinking water that meets the national health standards, not to mention the devastating effects such blooms can have on the environment (Walker 1999). Thus, knowledge of their growth potential in water is of value to water scientists, managers, engineers and water utilities.

1.2.2 Guidelines

Many countries, as well as the World Health Organization (WHO), have established guidelines to determine acceptable levels of noxious cyanobacteria in drinking and recreational waters (Bartram et al. 1999; Falconer et al. 1999; Burch et al. 2003). Up to now, many of these guidelines have only been estimated by enumeration of cells. The abundance based on a numerical census tends to overestimate small cells and underestimate the contribution of large cells (Paasche 1960). Moreover, at the same density, small cells will not represent the same biovolume as large cells, and so cell counts may not be the best representation of the potential health risk. Size and surface area/volume relationships are also important for many processes in algal species: chlorophyll levels per unit cell volume are inversely correlated with mean spherical diameter (Chisholm 1992).

The idea to measure cell dimensions in natural populations arose first in context with biomass determinations of freshwater phytoplankton (Sorokin and Kadota 1972). A standard biomass estimate is essential to: i) compare the relative contribution of different blue green-algae in mixed-taxa samples or between samples and systems (Hillebrand and Sommer 1997), ii) to convert cyanobacteria biovolumes to carbon (Rocha and Duncan 1985) and iii) to estimate the quantity of toxin produced (Long et al. 2001). Toxin concentration appears to be more related to some metabolic pathways and so to the cell biomass than to the number of cells (see Orr and Jones 1998; Lawton et al. 1999).

When estimating algal biomass from microscope counts, two questions must be addressed: i) how to approximate the closest geometrical shape for counted algal units, and ii) how to convert biovolumes into carbon biomass (toxin production?) (Gosselain et al. 2000). Cell dimensions, and hence cell volumes, vary greatly from one species to another and even within the same species as a result of differences between cells in physiological status (e.g., life cycle). Moreover, the methods for cell size measurement are not very good, and all have considerable sources of error. Measurements should be made, where possible, on both fresh and preserved material. As many cells as possible should be measured from a population, but in any event the number should not be less than 25. Because cell size can also vary from one population to another, it is necessary to make original measurements, rather than transpose data from other locations (Bellinger 1974). From microscope data, biomass estimates at the species or genus level are calculated from cell biovolume estimates and generally expressed as fresh weight, considering a cell density of 1.

In Australian drinking water, Alert Level 2 represents the point where operators and health authorities may decide to issue a health warning or notice in relation to suitability of water for consumption. Definitions are given in cell numbers ($\geq 5,000$ cells.mL⁻¹ *Microcystis aeruginosa* or *Anabaena circinalis* - Range: 5,000 - 10,000 cells.mL⁻¹) and in total biovolume for other cyanobacteria (≥ 1 mm³.L⁻¹, Burch et al. 2003). In the case of *Cylindrospermopsis raciborskii*, local or regional thresholds have been developed. A range of 15,000-20,000 cells.mL⁻¹ and also a biovolume of around 1 mm³.L⁻¹ can be adopted to trigger Alert Level 2 actions and investigation.

1.3 Methods Used

1.3.1 Monitoring laboratories

Most monitoring laboratories obtained their density and biovolume data via classical microscopy techniques. These involve counting procedures using chambers such as the Sedgewick-Rafter or the Lund chamber. The protocols and methods to acquire and analyse data are generally described in Guidelines (such as Burch et al. 2003). Measurements are made from a minimum of 30 cells using a calibrated graticule and a high power objective (e.g., $\times 100$). Volume calculations are used following common and simple geometric shapes and formulae. The advantages of these techniques are simplicity, low cost and ease of set up for laboratories. However, the errors in counting and measuring can be as high as 50% and are biased by operator subjectivity and fatigue due to the obligatory long hours at the microscope needed to acquire the data.

1.3.2 Other techniques

Counts of dispersed cells can also be done using images from epifluorescence microscopy (Boulos et al. 1999) or flow cytometry (Suller and Lloyd 1999). Conventional flow-cytometry is rapid for counting and sizing cells, but no identification can be made with the data obtained. Large cells cannot be analysed due to the risk of clogging the probe inlet. Molecular probes can be developed for use in conjunction with flow cytometry for the identification of particular species, but they are not widely used. Moreover, to achieve accurate counts, the samples have to be spiked with fluorescent microspheres to allow the measurement of the volume of sample analysed (Andreatta et al. 2004).

Cell sizing is generally more accurate using imaging cytometry than flow cytometry since size is measured directly from the two-dimensional image. Sieracki and Viles (1998) used imaging cytometry as a validation method of the flow-cytometric analyses. Imaging is used to verify cell identifications and to calibrate the forward scatter signal to biovolume. Imaging cytometry is also more practical for analysis of rarer cells, such as protozoa and larger phytoplankton, which are normally at concentrations below a few hundred cells per millilitre in the environment.

The two most common approaches to determine algal biomass are volumetric biomass determination and chlorophyll-a measurements. For volumetric determination the most common method is to measure the dimensions of a representative number of cells (minimum of 30, but most researchers measure 100 to 200 cells) for each species and calculate an average volume for each species using formulae for geometrical shapes closest to the cell's shape.

There have been many comparisons between techniques for estimating algal biomass (Hallegraeff 1977). Microscopy is essential to identify the algae and to check their condition, although cell dimensions measured are highly dependent on the methods used for image generation (Fry 1988; Fuhrman 1981). Chemical methods, especially those for carbon and chlorophyll analysis, can be informative but may be quite misleading where population numbers are low or cells unhealthy.

Some new technologies combine flow cytometry and image analysis, such as the Flow Cytometer And Microscope (FlowCAM) developed at the Bigelow Laboratory for Ocean Sciences, but they are limited in the size of the particles that can be detected ($> 5 \mu\text{m}$) (Sieracki et al. 1998).

To achieve enumeration, sizing and identification of species of a small size in one sample, image analysis is the most promising technology. Numerous image analysis systems can now be found on the market. They are mostly task orientated and delivered ready to use, especially those aimed at medical or pathology analyses. In aquatic ecology, specialised systems can also be found, such as the Laboratory Universal Computer Image Analysis (LUCIA) system for the image analysis of bacterioplankton (Psenner 1993). Programs for counting phytoplankton have been developed, such as PhytoWin (Windows-Software, Helsinki Commission) or Algamica.exe, but a lot of human intervention is still required to use them.

1.4 Image Analysis

1.4.1 Historic

Image analysis (IA) of microscopic particles was first developed in the 1950s and 1960s for enumeration of coal particles and white cells in blood (see Sieracki et al. 1985). Image analysis was introduced into aquatic microbial ecology more than twenty years later to measure the sizes and determine the biovolumes of fluorescently stained bacteria and protists (see Pernthaler et al. 1997). It has since been used in the enumeration, sizing and identification of viruses (Shopov et al. 2000) and bacteria (Bjørnsen 1986; Meijer et al. 1989; Dubuisson et al. 1994; Bloem et al. 1995), analysis of motion and chemotaxis (Korber et al. 1989), characterisation of filamentous fungi (Thomas and Packer 1990; Morgan et al. 1991; Cox and Thomas 1992; Jones et al. 1993; Paul et al. 1993; Donnelly et al. 1995; Pons et al. 1998) and characterisation of protozoa (Amaral et al. 1999; da Motta 2001). Image analysis has also been used for the enumeration, sizing and identification of phytoplankton (Brown et al. 1989; Estep and MacIntyre 1989; Simpson et al. 1992) and for the systematic analysis of a number of fresh-water algae (Necchi et al. 1993). Image analysis of algae has also been used in environmental monitoring (Hanninen et al. 1993; Wynn-Williams 1994). Water utilities (waste water treatment) have also recently started to use image analysis to help gather data such as measurements of the proportion of filamentous *versus* non-filamentous bacteria in activated sludge plants (Contreras et al. 2004), quantification of some bacteria of interest in activated sludge (Hall et al. 2003) or assessment and monitoring of protozoan and metazoan populations (Amaral et al. 2004).

Since 1990, only a few papers have been written on the application of image analysis to cyanobacteria. Of these, most have been concerned with physiological studies of heterocysts or photosystem complexes (Lelong et al. 1996; Walsby et al. 1998; Ruffle et al. 2000) or with taxa recognition, achieving discrimination between 2-3 genera. However, due to its inherent difficulty, this area of research has seen minimal progress over the last decade, with very little published literature (Walker 2000, 2002).

Cyanobacteria present the image analyst with their own difficulties. Cyanobacteria encompass species with varied shapes and sizes, often similar to other organisms such as algae. Intra-species variation of characteristics (such as size and colony shape) can be large, and is often seasonally dependent (Walker 1999). The types and numbers of objects (bacteria, zooplankton, debris, etc...) that may be present in any one sample of lake water are both unknown and effectively unlimited. As a result, few studies have attempted the enumeration or the measurement of cyanobacteria, and none of these studies involve fully automated systems. Walsby and Avery (1996) described a method based on epifluorescence microscopy for the total length measurement of the straight filaments of *Oscillatoria rubescens* and *Anabaena flos-aquae*. Congestri et al. (2000) evaluated the biomass of Baltic filamentous cyanobacteria by image analysis – but their technique was mainly manual, requiring intervention of the operator for each image and manual circumscription of the cells to be measured.

Advantages

Image analysis has become an increasingly important tool because criteria for quantification can be defined and standardized, and size measurements can be used to estimate microbial biomass (Sieracki et al. 1985). Image analysis is close to the traditional manual technique of microscopy, and the processing of each organism can be followed and controlled step by step. Moreover and unlike a human operator, an automated system is not biased by subjectivity or fatigued by the task, and it reduces the burden on taxonomists rather than replace them completely (Schröder and Krambeck 1991). Therefore, image analysis can offer speed, convenience, and freedom from error due to boredom or fatigue.

The elimination of fatigue constraints means that measurements can be made from a greater number of cells, increasing the precision of the cell count. Once the images have been acquired, the data can be rapidly analysed and basic statistical results presented within a few minutes. Image analysis has been estimated to be able to reduce the time required to count samples by 85%. Such a system can also collect new kinds of data which are impractical to gather manually by eye (Sieracki et al. 1985), such as the accurate length of curved trichomes (see below).

Image analysis systems are developing rapidly and decreasing investment cost has encouraged an expansion in the field of processing microscopic images (see Vanrolleghem and Lee 2003). They are becoming more affordable in price and good software, such as NIH or Scion Images from the National

Institute of Mental Health (U.S.A.), are free on the Internet (see <http://rsb.info.nih.gov/nih-image/about.html>).

1.4.2 Principles

Image analysis is broadly defined as the extraction of information from an image (Glasbey and Horgan 1995) or the extraction of numerical data in the form of simple or complex measurements which are subjected to statistical analysis (Shorey 1993). It encompasses hardware (e.g., microscope, analogue video camera, computer, massive storage device and motorised stage) and software. The software controls the hardware and is considered to be composed of a number of distinct stages: acquisition, correction of defects, enhancement, segmentation, binary processing and feature measurement (Russ 1999).

Image acquisition and hardware

A desktop image analysis system commonly uses a video camera that creates an analogue video signal of a subject that is then converted to a digital image using a frame grabber. Two types of images are generally considered: (i) easy images in which the objects stand out from a background devoid of details and (ii) difficult images with a confusing background. The usual approach is to try to convert difficult images into easy ones, by improvement of the slide: sampling, staining, fixation and illumination (microscopy skills) or by image processing.

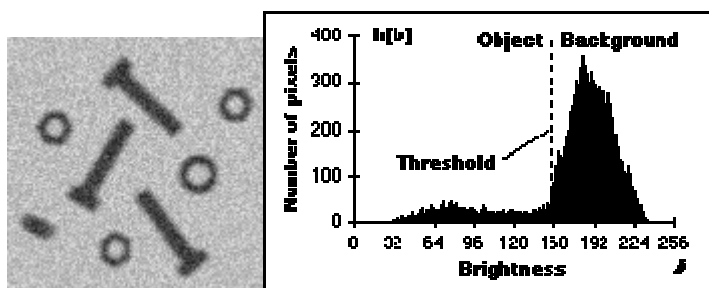
Image processing techniques: enhancement

Image processing is used for two somewhat different purposes: improving the visual appearance of images to a human observer and preparing images for measurement of the features and structures present (Russ 1999). Image enhancement operations aim to increase the visibility of certain aspects or components of an image, although generally at the expense of others whose visibility is diminished (Russ 1995). Image correction methods improve the objective appearance of an image in response to a physical distortion, while image enhancement methods, with which they are often confused, improve their subjective quality. Typical image enhancement operations include: transformations of the grey scale distribution (brightness histogram equalisation), edge enhancement operations and image arithmetic. Edge enhancement procedures use digital filtration to detect edges. Image arithmetic operations may add, subtract, multiply or divide images.

Segmentation

Segmentation is the process of dividing an image into meaningful regions, which ideally correspond to objects or features of interest (Figure 1-1). The end result is a binary image. Segmentation is often the critical step in image analysis. If segmentation is successful then subsequent image processing may be greatly simplified.

Figure 1-1: Pixels below the threshold ($a[m,n] < \theta$) will be labelled as object pixels; those above the threshold will be labelled as background pixels (<http://www.ph.tn.tudelft.nl/Courses/FIP/frames/fip-Segmenta.html>). On the left: image to be *thresholded* and on the right, brightness histogram of the image.



There are three general approaches to segmentation, termed thresholding, edge-based methods and region-based methods. None of these techniques is perfect. Each case requires a study of the best case. In the simplest case, an image may be segmented into only two regions, an object region and a background region, selecting the corresponding pixels by histogram analysis, which determines the brightness values at the minimum between peaks in a bimodal histogram. If the threshold is too high or too low, the area of measurement of the object will be underestimated or exaggerated, respectively (Sieracki et al. 1989).

Processing of binary images

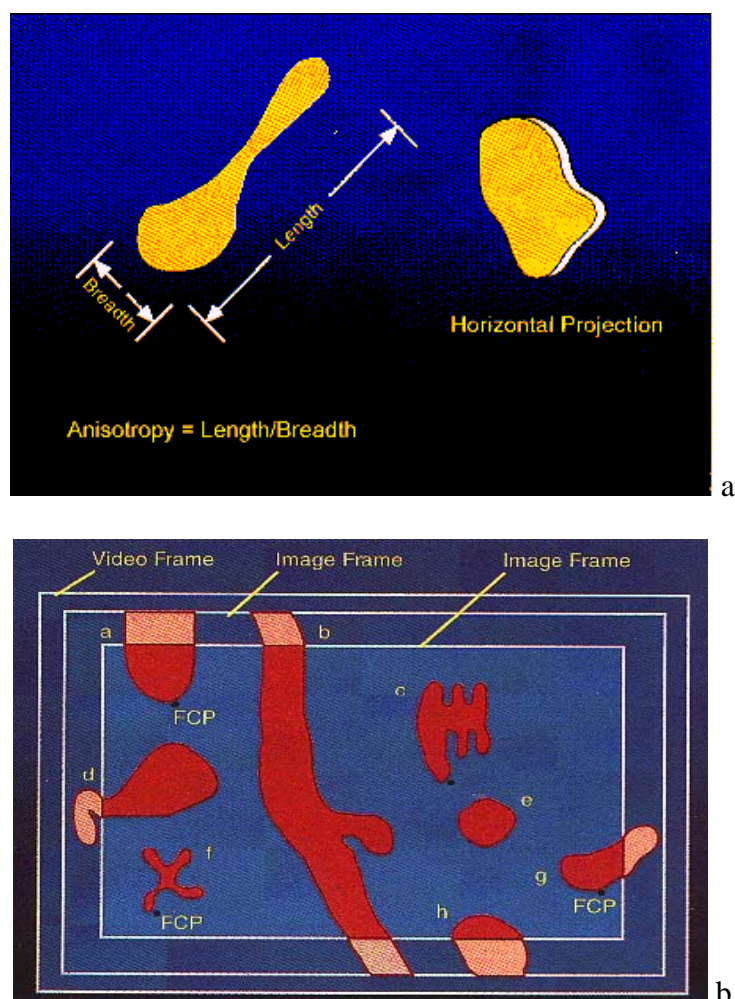
The goal of processing the binary images is to obtain a binary image as close as possible to the real object. Each case is different and may require its own solution. The establishment of a high performance system takes time initially, but once optimised, it provides a very powerful tool. The best approach is to start with simple images, solve any processing issues for these, and then move on to more complicated ones. Processing operations are categorised as either morphological operations, which modify individual pixels in images, or Boolean operations for combining images (Russ 1999). Morphological operations are simply described in terms of adding or removing pixels from a binary image according to certain rules (e.g., erosion, which removes any pixel touching another pixel which is part of the background; thinning, skeletonisation). The Boolean operators AND, NOT, OR, and XOR are used in isolation or in sequence and allow the selective combination of binary images.

Feature measurement

The extraction of quantitative information from binary images is the final stage in the analysis. There are many ways in which features within images may be described. In many cases the selection of features to measure is rather arbitrary (Rohlf 1993) with selections often made because they are analogous to measurements made using conventional techniques. It is usually necessary to capture as much information as possible in the hope of getting the information needed.

There are two types of measurements: the first determines global or scene parameters, and the second involves measuring values for each individual feature that is present. The parameters measured mainly fall into four groups: size, aspect of shape, feature position, or grey scale brightness information (Russ 1999). The enumeration of features is a straightforward procedure providing the features are distinct and a convention is followed when features intersect the edge of the field of view (Russ 1999).

Figure 1-2: (a and b) Examples of feature-specific measurements from (<http://www.metallography.com/technotes/ianalysis/principles.htm>)



2. System Development

2.1 VideoPro 32 and Set-up

VideoPro 32 is a high performance, robust, full colour, image processing and analysis software package for personal computers, developed locally in Adelaide (Leading Edge, Pty Limited, Adelaide SA, Australia). It operates under Microsoft Windows 98 (with more recent releases also able to function under Windows XP). The operation interface is optionally menu or dialog controlled and is complemented by a powerful and easy command program facility which makes it possible for the user to quickly create automated processing routines to solve the highly individual applications typical of image analysis. Extensive image processing, feature discrimination and measurement functions are available, as well as editing and sizing for feature selection. Typical functions used are image processing, discrimination to produce a graphics overlay, binary processing of the overlay, automatic binary segmentation, multi-variable sizing editing, manual editing and field, feature or individual selection measurements.

An upright Olympus BX50 microscope, equipped with UPlanFI objectives (x10, x20, x40 and x100) was dedicated to this project. The microscope was fitted with DIC optics, as well as epifluorescence. Both optics were used during this study.

Til mid-2003, the microscope was coupled to a Panasonic model GP-KR222 black and white ½" format interline transfer CCD camera and grabbed to the computer in 768x576 pixels, 16 bit format, by a video frame grabber card Model VCG (Vision Dynamics, Hemel Hempstead, Herts, England). After that date, the microscope was coupled to a Panasonic WV-CL924 ½" format interline transfer CCD colour camera and grabbed to the computer in 768 x 576, 8 bit format by a Flashpoint 3D Video card. In all cases, care was taken to expose the camera correctly and to keep all objects of interest within the camera's dynamic range. To be able to use the x100 objective, a vibration isolation table was acquired at the end of 2003. With the x100 magnification objective, one pixel typically corresponded to 0.082 to 0.085 µm, which is enough to get a measurable image of very small objects.

Two VideoPro workstations were used, one dedicated to the acquisition of images and coupled to the microscope and another one dedicated to the analysis of the images. Both tasks could then be performed simultaneously on two samples. The computers used were Pentium III's during the first part of the project, upgraded to Pentium IV's in 2003.

Some adjustments had to be made initially on the video parameters (e.g., hue, saturation, brightness, contrast and gain values) as well as on the display of the images onto the monitor (e.g., image position, palette skew). These adjustments were definitive and the same for all further experiments.

2.2 Sample preparation

2.2.1 Cyanobacteria cultures

The cultures used in this project were from the cyanobacteria culture collection held and maintained at the AWQC. Each strain was maintained in tissue culture flasks in ASM- 1 medium (Gorham et al., 2004s), kept in temperature controlled cabinet with a 12:12 light: dark photoperiod.

2.2.2 Slides

The accuracy of cell count depends on the uniformity of their dispersion on the microscope slide, the variation of cell types being enumerated, the amount of foreign material in the sample and the number of cells counted. During the first two years of the project, normal slides and cover slips (22x22) were used to observe and acquire images from the samples. However, these had the disadvantages of holding only very small volumes of sample (ca. 20 µL under a coverslip), and of allowing the sample to dry out if kept too long under the microscope without sealing. In 2004 we adopted the Gene Frame® (ABgene®) system, which utilises double-sided adhesive gaskets that can be sealed and can hold volumes of either 65 µL or 125 µL, enabling observations of the samples for hours without any loss.

2.3 Manual operation

During the first part of the project, and during the writing process of programs, the image analysis system was used manually. The slide containing the sample was put on the stage of the microscope and the microscope set up to get the best resolution and light exposure possible. Once VideoPro was opened, adapting the light intensity of the microscope, choosing a field of view, focusing on the object of interest, freezing the image and saving the image were done manually. To analyse the data, images were opened individually, and either all steps of the algorithms were executed one after the other, or programs were launched manually but several tasks were ran automatically. The data would then be automatically transferred to an Excel file.

Once the algorithms to solve a specific problem (enumeration and/or measurement) were validated, automated processing routines (programs) were written and ran for each of the images analysed. Examples of programs are given later in the text.

All images were stored as TIFF files for the first part of the study and as JPEG files from June 2003. Two types of programs were written. The first type was setting up the conditions of the acquisition of images, parameters limits, etc, the second type being the executive part.

2.3.1 Setting-up programs

These programs were ran initially to set-up the frame of work in which the data would be acquired. Following is an example of such a program:

```
'
'   Program MeasuringBeadsPre-161001
'   Set up VideoPro to measure microspheres
'       on images already acquired.
'   Sizing by length
'
'   Set up frame
'
measure frame width 710
measure frame height 502
measure frame centre
measure frame feature
measure frame edge reject
'
'   Preparing column data
'
data close
data column clear
data column 1 Area
data column 2 Perimeter
data column 3 HullArea
data column 4 HullPerimeter
data column 5 Width
data column 6 Height
data column 7 Length
data column 8 Breadth
data column 9 FeretMax
data column 10 FeretMin
data column 11 Aspect
data column 12 Roundness
data column * record
measure write enable
measure view disable
'
'   Entering unit calibration
'
data units um
'data scale 0.828
'data scale 0.414
data scale 0.208
```

Set up frame inside the field of view to follow the counting convention to avoid counting touching boundary twice during counting a transect – objects in bottom and left-hand boundaries are ignored (Hötzel and Croome 1999).

Set-up columns for and define the type of data to be acquired

In function of the objective used (see below)

' with objective 10
'with objective 20
'with objective 40

```
'data scale 0.082          'with objective 100
data aspect 1.000
'
'   Discriminate objects measured by their size
'
measure sizer variable * disable
measure sizer variable perimeter
measure sizer lower 20      e.g., only objects of perimeter > 20 µm and < 26 µm
measure sizer upper 26      will be taken into account by the program
measure sizer variable length
measure sizer lower 2.4
measure sizer upper 11
measure sizer variable aspect
measure sizer lower 1
measure sizer upper 1.20
measure sizer variable roundness
measure sizer lower 0.5
measure sizer upper 6
'
'Opening a new Excel sheet      open Excel spreadsheet into which data will be
                                automatically transferred
'
data worksheet
```

2.3.2 Executive programs

Operational programs are the 'executive' programs running the tasks and acquiring / generating data. Example of program used to measure beads:

```
'   Program Measuring M6 sample
'   To measure cells of Microcystis
'
'   Measure feature 'select'
'
'   Discrimination with auto global thresholding
'
colour detect black          will detect black objects on a white background
colour auto frequency 4      thresholding mode – binarisation – creates an overlay
binary process holefill      fills holes surrounded by an overlay boundary
binary process clean 1       smooth pixels at the edge of an object
'binary process erode 1       shrinks the overlay by one pixel
'binary process dilate 1      expands overlay by one pixel
```

2.4 Automation

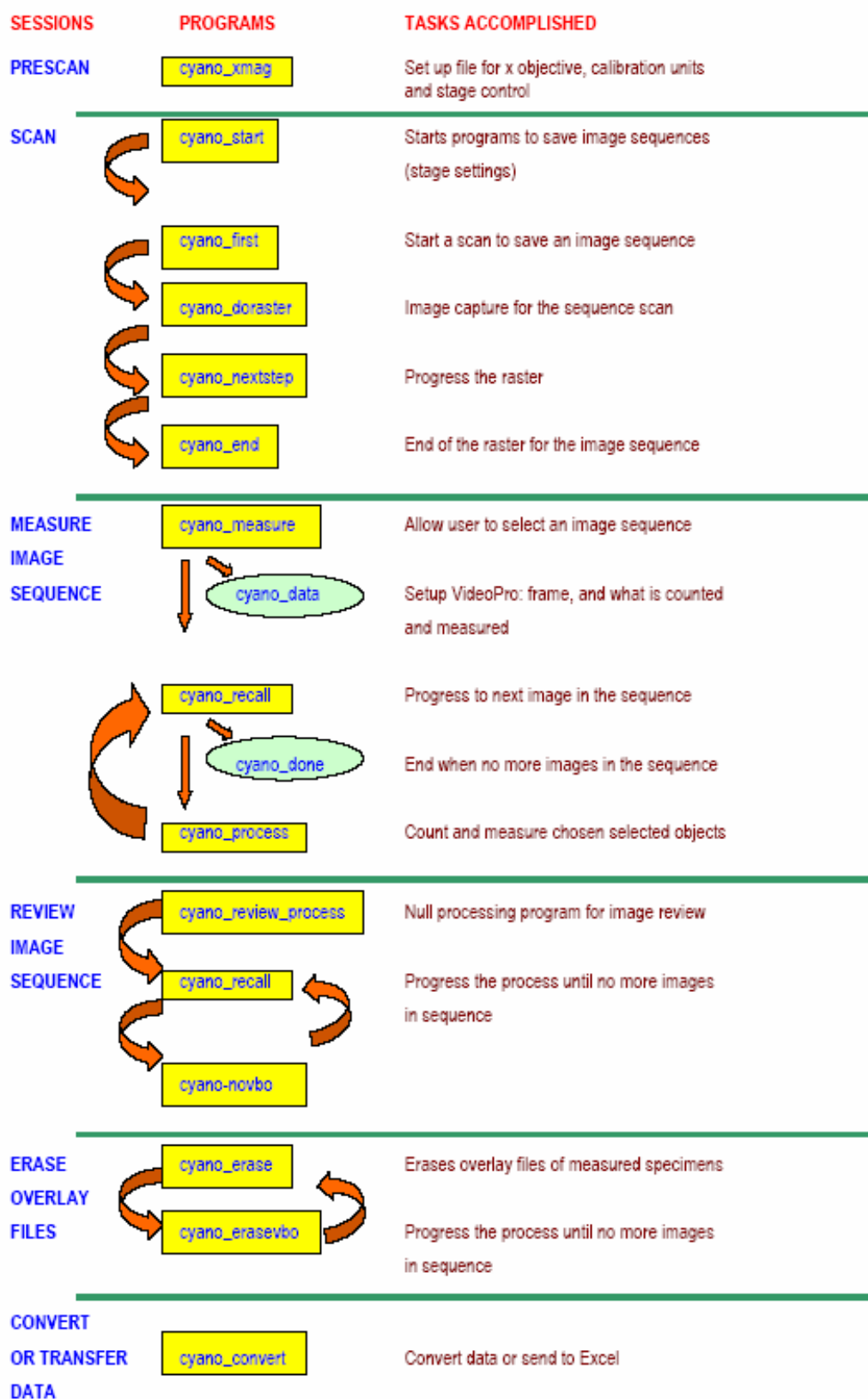
A stage system, with x-y motorised focus control (ProscanTM, Prior Scientific Instruments Ltd., Cambridge, U.K), including a multi-holder motorised stage (4 slides), a stage controller, and a joy stick to drive the stage (3 dimensions), was installed in 2003. The focus was controlled by a stepper motor directly connected to the coarse gear of the microscope. The system's performances are 0.1 µm in resolution and 0.2 µm in accuracy.

2.4.1 Scan principles

Twenty-six linked programs were written to combine all of the tasks necessary to chose the calibration factor, automatically scan a slide, acquire the images as a sequence, analyse data choosing between ovoid cells and trichomes and review the analysis with overlay present or absent (see diagram below). Choices and settings were made via a dialog box. The sequences could be called back at anytime (always done offline) and analysed (including data transfer to an Excel spreadsheet) automatically without any human intervention.

The sequence of images was acquired following a snake raster pattern. The time taken to acquire a sequence of images was dependent upon the frequency with which the system was asked to refocus and upon the size of the sequence (e.g., size of raster) selected in function of the density on the slide of the objects to be analysed.

Figure 2-1: Diagram detailing the different programs used during a scan and the inter-relationships involved in the automation of the enumeration and measurement of ovoid and trichome-like cyanobacteria.



2.4.2 Rapid scan

A new type of scan was developed by Lynn Jarvis (Leading edge) and added to the suite of available programs in August 2004. Its aim was to rapidly screen slides for the presence/absence of a chosen cyanobacterium (generally low density samples) as well as enumerating cells. This rapid scan uses the same hardware and software (VideoPro 32) as the scan described above, but a different set of programs and a new dialog box. Its greater speed of execution is due to its ability to acquire only those images in which the objects of interest are present. This allows the entire slide to be scanned without generating unwanted data (images without objects of interest), which greatly reduces the amount of computer storage space required per slide. The number of images produced depends on how many objects are measured. The main challenge in setting up and validating this new scan was to maintain the focus of the system, even when field of views were empty.

Material and Methods (Jarvis, pers. com.)

The system works by close communication with the stage program used in the scan described above. The dialog window within VideoPro provides the controls needed to scan a specimen: 1) raster and scan preview, 2) type of focus and frequency, 3) file name and path selection, 4) darkfield or brightfield selection, 5) detection sensitivity entry and 6) run scan or cancel options. The calibration was pre-defined for usage with an objective x10, giving a relatively faster speed for the scan. The discrimination of the objects of interest is made based on size and shape. The optimisation of the speed is due to the fact that the stage hardware itself is asynchronous. Images can usually only be acquired if the image is 'frozen'. In this scan, the video image is frozen without transferring any image data. This means that the lengthy image freeze (with data transfer) can happen while the stage is moving. This process avoids movement artefact and optimises the interleave of image processing with stage movement.

Three types of files are generated: mosaic, data and stage files. As objects are measured during the scan, a tile around each object is packed into a 'mosaic' jpeg image (see Figure 2-2). A sequence of these images is produced, the number of which is dependent on how many objects are recognised. The mosaic files provide a map of the objects on the slide and the ability to look at each object individually. When the scan is done a complete map of the scan showing the locations of all cells found can be seen. Zoom is allowed on any of them and erasing of any artefact as necessary can be performed. Counts can be displayed immediately. All object images are compressed into mosaic images, so the total number of images per scan depends on the number of objects measured, not the number of fields. Data files are also generated. They include for each object: screen coordinates of where it was located in the field, location of the tile in the mosaic image, width and height of the tile in the mosaic and scan field number. The associated stage file contains information on the number of moves in X and Y for the raster and the step size per move in X and Y. Given the number of raster moves and the number of steps per move, an image of the entire scan scaled to fit the screen can be constructed (Figure 2-2). The operator can select any field of view in the map image, view its full size, edit the image to erase any unwanted objects, etc.

Focus could be achieved in two ways: ramp focus or auto focus. Preliminary work showed that the latter was the most efficient with a frequency of once every one or two fields. Other areas of validation were to establish the mode of discrimination, and the retrieval and editing of the mosaic images.

Preliminary results

Preliminary results were obtained with cultures of *Cylindrospermopsis raciborskii* and *Microcystis aeruginosa* in Gene Frame slides (Table 2-1, Figures 2-2 to 2-4). Differential Interference Contrast optics was set up to obtain white objects on a dark background. Close to 100 scans were performed to define the best size set-up for discrimination, focus (type, frequency and sensitivity) and the mosaic retrieval and editing techniques.

Table 2-1: Examples of results obtained for *Cylindrospermopsis raciborskii* with the rapid scan, in function of the area scanned and the time necessary to acquire data.

Raster size	Time (min)	Objects detected	% slide scanned
10x10	2.4	109	10.4
15x15	2.5	427	23.4
15x20	6.8	1053	31.2
20x20	8.5	832	41.6
20x30	14.4	609	62.4

Figure 2-2: This figure shows an example of a mosaic image with *Cylindrospermopsis raciborskii* represented as spots. In this particular case, 91% of a small Gene Frame slide was scanned, with a focus frequency of 1 and a sensitivity of 60. The time to run the scan was 22 min and the density of the sample was determined to be 18000 trichomes per mL.

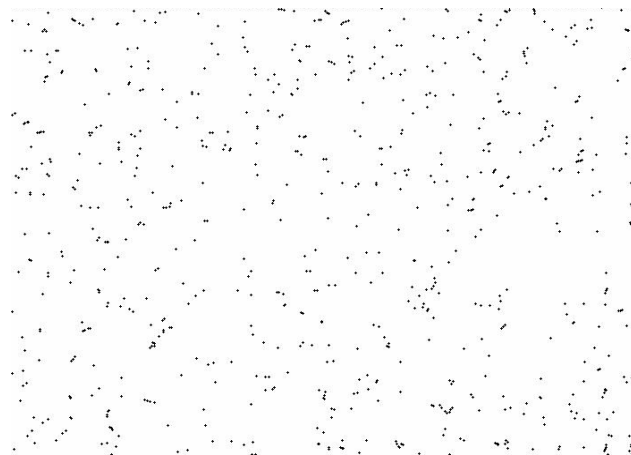


Figure 2-3: This figure shows another example of mosaic image with *Cylindrospermopsis raciborskii* represented as spots. In that case, 31% of a small GeneFrame slide was scanned, with a focus frequency of 1 and a sensitivity of 60. The time to run the scan was 7 min and the density of the sample was determined to be 4700 trichomes per mL. A maximum of 6 fields without objects were encountered and the focus remained well maintained.

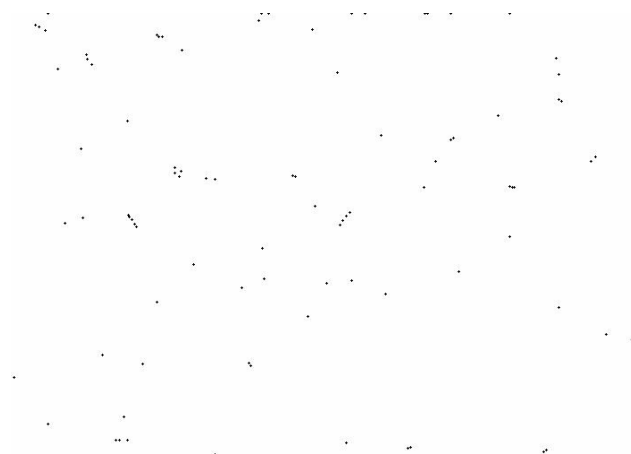


Figure 2-4: Mosaic image obtained with *Microcystis aeruginosa* – raster 10x10 and time to scan the sample 2 min 30 s.



Discussion

For this method there is a trade-off between speed and the maintenance of focus (and hence accuracy) across the slide, with more frequent focussing increasing the scan time. This type of scan becomes more accurate for samples dense in objects (not only objects of interests) as the focus can be more readily maintained across the slide. Samples with low object density are more difficult to scan (hence the lower percentage of the slide scanned in Figure 2-3 compared with Figure 2-2), but we succeeded to maintain focus across 6 empty fields of view. Counting low density samples could be aided by spiking the sample with additional particles (not objects of interest) to facilitate focussing. The time to scan a slide with this method is comparable with that of an operator (see Table 2-1). Although we lacked the time to develop this scan any further, these data illustrate the potential of this type of scan to determine the presence/absence of objects of interest.

2.5 Validation of VideoPro 32

The reliability and accuracy of data obtained by any image analysis system have to be initially validated using objects of known size and shape. The most common method uses fluorescently labelled latex beads of known diameter and concentration to validate the measurement functions and the ability to enumerate the objects of interest in the image (Sieracki et al. 1989). The drawback is that beads have only one shape, spherical. Before validating the system, thorough calibration has to be performed.

2.5.1 Calibration

Calibration of the camera is critical for obtaining repeatable, reliable data. Pixel-based units have to be translated via the calibration routine into real-world units (metric). We calibrated the size of the pixels against scale bars and did so for each objective used. Scale bars were calibrated vertically, horizontally and obliquely for the two video cameras used during the project (Table 2-2).

Table 2-2: Size (in metric) of the pixels calibrated against scale bars for the 4 objectives and for the 2 video cameras used in this study.

Objective	Pixel size (μm)	
	GP-KR222	WV-CL924
10	0.83	0.86
20	0.41	0.43
40	0.21	0.21
100	0.08	0.09

2.5.2 Latex beads

The most common approach to validate the accuracy of the measurements made with image analysis is to use latex microspheres as references. Spheres of 6 μm and 10 μm in diameter were used in this study (Bjørnsen 1986; Sieracki et al. 1989). We validated repeated counts and measurements made with traditional visual methods with those obtained with the image analysis system (Sieracki et al. 1985; Bloem et al. 1995; Sieracki and Viles 1998) (Table 2-3).

Table 2-3: Example of validation of the performance of the image analysis system to measure objects, at different magnifications, compared with performance by classical visual measurement. The beads were from Polysciences, Inc (Fluoresbrite™ Plain, YG 6.0 microns).

	Image analysis			Visual	Manufacturer
	x20	x40	x100	x100	
Diameter	6.220	6.117	6.080	6.270	5.895
Std Dev	0.328	0.347	0.284	0.454	0.375
n	149	193	100	100	n/a

Subsequently, each new program developed (or modified) was tested to verify that only the objects of interest were considered for enumeration and measurement. Data were generally validated against a manual count and by an 'on-screen' count. In addition, a review of the binary images was initially conducted to check which objects were binarised and which were not.

3. Application to Ovoid Cells

The cyanobacterium *Microcystis* Kützing ex Lemmermann 1907 is one of the most common freshwater bloom-forming organisms worldwide and was chosen for this study as an example of cyanobacteria with spherical/ovoid shapes. This genus harbours a diversity of toxic and non-toxic species/strains. Among the toxins produced is the hepatotoxin microcystin. This toxin causes a variety of human illnesses and is responsible for death in native and domestic animals (Falconer et al., 1994; Otsuka et al. 1999). Certain species of this genus have a tendency to form large and visible aggregates or colonies, constrained by an amorphous mucilage or sheath (Holt et al., 1994). The number of cells per colony can reach tens of thousands, but non-colonial strains can also be encountered (Otsuka et al. 2000).

The aim of this chapter was to develop programs to enumerate cells of *Microcystis* spp. at a density as low as possible and to define ways for the image analysis system to measure cell biovolume as accurately as possible. Unless indicated, all experiments were done with cultures of non-colonial strains.

3.1 Algorithms

This chapter focussed on circumscribing the parameters necessary to best describe *Microcystis* to allow its separation from all other objects on the image acquired. To do so, a database was established using data previously known from the literature (mainly length and width of cells), data obtained by manual measurement from cells in cultures and data obtained with the image analysis system from the cultures available at AWQC. At the beginning, a large range of descriptors were used. Results were compared with those obtained with artefacts or dissimilar shaped organisms and finally six parameters were retained, namely Perimeter, Area, Length, FeretMin, Aspect and Ratio. Algorithms were then developed to enumerate the cells and to measure them.

3.1.1 Enumeration

In the last version of the 'National Protocol for Monitoring Cyanobacteria' (Burch et al., 2003), the densities aimed to define the Alert Levels 1, 2 and 3 for *Microcystis aeruginosa* in drinking water sources were 1000-3000 cells.mL⁻¹, . 5000-10 000 cells. mL⁻¹ and ≥ 50 000 cells. mL⁻¹, respectively.

One of the problems that needed to be solved in order to accurately enumerate *Microcystis* was the separation of touching cells. This was best achieved by using watershed algorithms (Russ 1999), as shown below.

Program 3-1: Enumeration of touching cells.

```
'Program Micro-Counting
'To count Microcystis cells allowing to separate touching and overlapping
cells
'
colour process saturate
image store load
filter edge Sobel
image store combine
image store load
'
colour detect grey
colour auto frequency 4
'
binary process erode 1
binary process clean 1
binary process dilate 1
binary store load
'
binary feature separation outline
binary feature overlap 80
```



```

binary feature cycles 20
binary feature segment
binary store blank
binary store retrieve

```

```

measure sizer edit
edit prepare
measure field

```

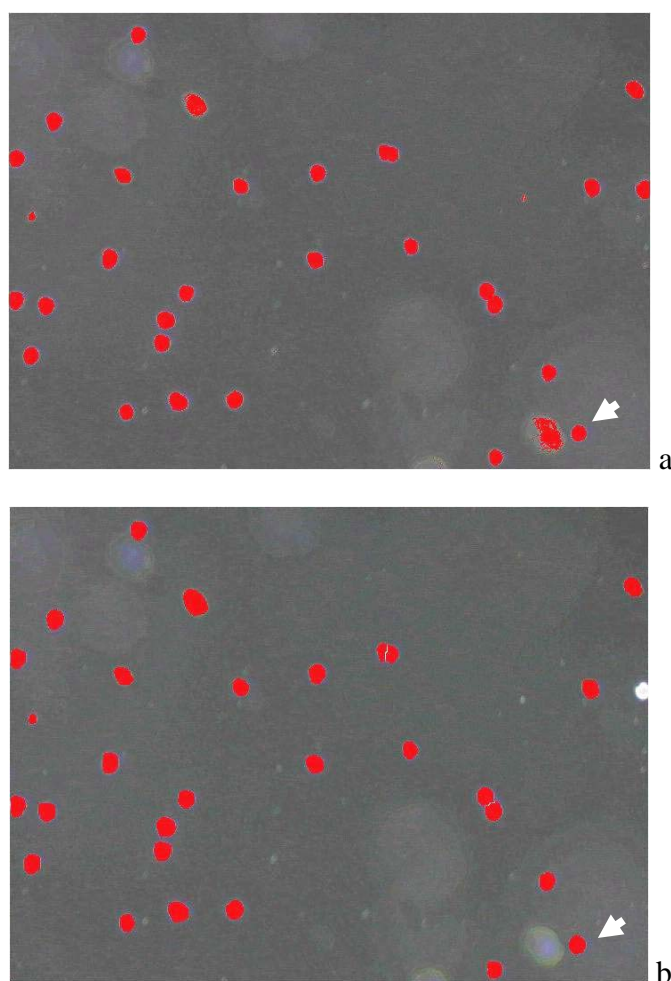
```

'mark rejected feature
'remove rejected feature
'count features remaining

```

The results obtained were quite satisfactory and touching cells (up to 80% of overlapping) were separated and counted as two cells instead of one (Figure 3.1).

Figure 3-1: Binary images of *Microcystis* using separation of touching cells algorithm. Top image (a) shows the image before the algorithm was used and the bottom one (b) afterwards. This also shows artefacts in the image disappearing from the binary image after discrimination parameters and /or frame touching parameters were used (objective x40). In this image, the size of binarised objects has been enlarged.



3.1.2 Measurement

Most articles reporting biovolumes of *Microcystis* cells assume a spherical shape in the calculation of the measurement (Hillebrand et al. 1999; Burch et al. 2003). A sphere requires only a one dimensional measurement to calculate its volume, simplifying the measurement process for routine operators and making it achievable in a relatively short time. However, in reality *Microcystis* cells are rarely spherical and are more commonly ellipsoid in shape (Figure 3-2). As the image analysis system can measure two parameters as rapidly and accurately as one, we chose in this study to compute the volume based on an ellipsoid shape, requiring two measurements: length and width. After testing, the best fit for the width measurement appeared to be the FeretMin parameter.

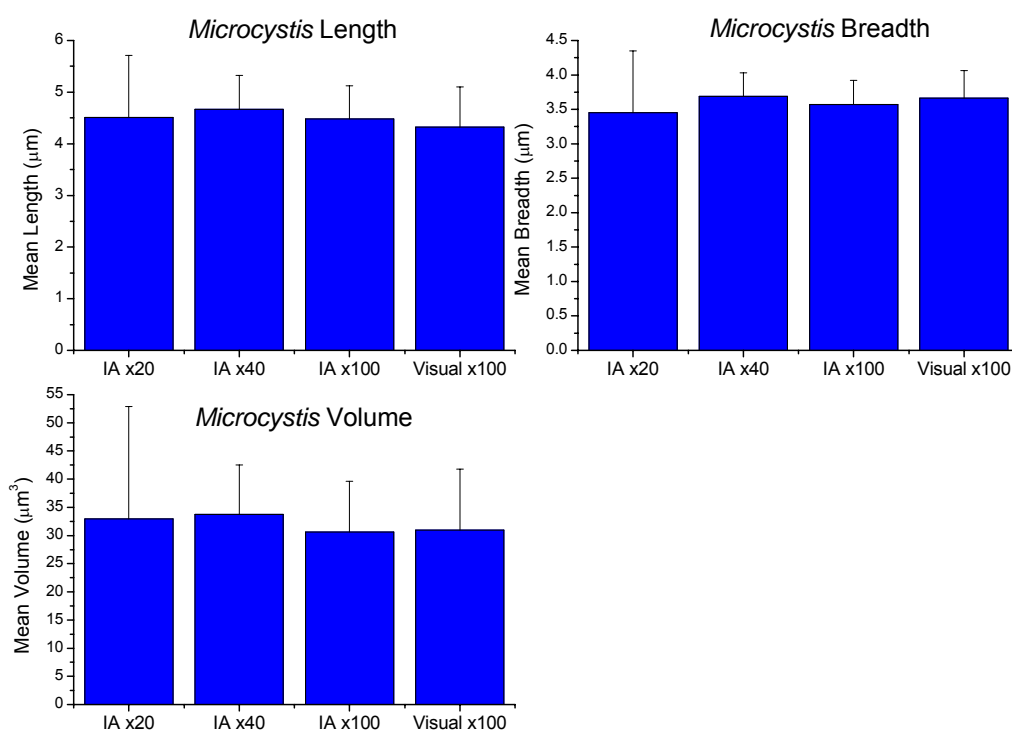
Formula 3-1: $\text{Ellipse} = \pi/6 \times \text{Feret Min.} \times L$

Figure 3-2: Example of *Microcystis* cells showing the divergence between round and ellipsoid shapes (objective x100, bright field optic)



Measurements were made on 50 cells of *Microcystis* in order to compare the accuracy obtained with the image analysis system using different magnification steps and with an ocular micrometer (at x100 objective) (Figure 3-3). The results show that measurements obtained with objectives x40 and x100 are comparable, and that they are also comparable with those obtained by an operator (in this case, the senior author) with x100 being the closest. However, using the lowest magnification (x20 objective), the standard deviation was higher than with x40 and x100 and so the results were less accurate.

Figure 3-3: Histograms comparing measurements of length and width (FeretMin) of *Microcystis* cells by image analysis (with objectives x20, x40 and x100) and by 'eye' by an operator, and subsequent results of calculations of cell volume using Formula 3-1. Fifty cells were measured each time – mean and standard deviation are indicated.



The circularity (Formula 3-2) and shape factor (Formula 3-3), were also calculated from the same cells. The results show a divergence from 1, which indicates that the cells were ovoid (results not shown).

Formula 3-2 Circularity = $P / \sqrt{(4 \times \pi \times A)}$

Formula 3-3 Shape factor = $\pi \times (L + \text{FeretMin}) / 2 \times P$

3.2 Validations

Using the algorithms developed above for enumerating cells and assuming that cells of *Microcystis* were ellipsoid, exercises of validations were undertaken.

3.2.1 Inter-laboratory measurement validation

The samples and the results used for this validation come from an inter-laboratory study called 'Comparison of cell count and cell volume measurement of cyanobacteria between three laboratories' (Hobson, pers. comm.). The variability of biovolume measurements between three laboratories (three different operators) was assessed. The aim of the exercise was to identify what variability could be expected and what influence it would have on the development of guidelines for exposure to cyanobacteria.

Material and Methods

Cultures of *Microcystis aeruginosa* were grown under laboratory conditions (25°C and 15 $\mu\text{mol photons.m}^{-2}.\text{s}^{-1}$, under continuous illumination), harvested in active growth phase and fixed with Lugol's iodine. Measurements were independently carried out on the same samples by two microscopists from Laboratory 1, and one from Laboratory 2. Cell diameter (D) of 30 cells was measured using x100 objectives and oil immersion (Hötzl and Croome 1999). Cell volumes were calculated assuming the shape of a sphere by operators and of an ellipse by the image analysis system (Table 3-1).

The author manually measured 100 cells with x100 objective, but considered both length (L) and breadth (B) of each cell, assuming the shape of an ellipse to calculate the volumes (see above Formula 3-1). With the image analysis system, images were acquired to have a total of 30 cells at different magnifications, using the objectives x20, x40 and x100 (oil immersion). The images were taken under bright field conditions. The parameters measured were: area (A), perimeter (P), width, height, length (L), breadth, FeretMax, FeretMin, aspect and roundness.

Results

The mean length of the cells of *Microcystis* measured by the different operators varied between 3.49 to 4.53 μm (Table 3-1). The mean length obtained by image analysis fell within this range, with a value of 4.32 μm . The same closeness was observed for the measurement of mean breadth. A consequence of the disparity in length measurement is reflected in the more than twofold difference observed in volume calculation between operators 1 and 3. It should be noted that operators 1 and 2 were from the same laboratory, using the same microscope. When volumes were calculated assuming an ellipsoid shape, they were located in between the two extremes observed.

Table 3-1: Measurements of 30 cells acquired either by operators or by the image analysis system at different magnification. The author and the image analysis system considered the cells as ellipsoid and measured 2 dimensions for each cell. The volumes were calculated accordingly.

	Mean length (μm)	Mean breadth (μm)	Volume of single cell (μm^3)
Operator 1	4.5	Not done	50.3
Operator 2	3.7	Not done	26.6
Operator 3	3.5	Not done	22.3
Author	4.5	3.6	31.0
Image analysis	4.3	3.7	30.6

These results show that the measurements obtained by different operators in different laboratories can vary and have a great influence on the calculation of the volume of cyanobacteria. It also shows that the results obtained with the image analysis system give comparable results to those obtained by operators.

3.2.2 Intra-laboratory validation of enumeration and measurement

Intra-laboratory validation experiments were carried out in 2003 at AWQC. The people involved were: three trained operators in the NATA accredited AWQC Algal Monitoring laboratory, experts in counting and measuring cyanobacteria, and the senior author of this report. The aim of this validation study was to confirm the earlier study, namely that the image analysis system was as efficient and accurate as a human operator for enumerating and measuring cells of *Microcystis*, and in addition to compare the speed of image analysis versus human operators. Following the results of the previous study, it was decided that the operators would measure two dimensions for each cell of *Microcystis*.

Materials and Methods

A culture of *Microcystis* (Mic-337, AWQC), maintained as above (2.2.1.) was chosen for use in this study. The initial concentration of cells was determined by enumeration in a Sedgewick-Rafter chamber and found to be 1.9×10^6 cells.mL⁻¹. The sample was fixed with Lugol's and vials with 10^4 , 10^5 and 10^6 cells.mL⁻¹ were established, each in triplicate. To enumerate and measure the cells, operators used a compound microscope (Olympus BX 40) with eye piece micrometer and Whipple grid as an area of reference. Twenty-eight μ L were put on a slide and covered with a 22x22 mm coverslip. The slide preparation was carried out in an identical way by each operator.

The long and short dimensions of 100 cells were considered for each sub-sample, with individual cells only being measured once. Cells were visualised using brightfield optics and an objective x100 under oil immersion. Only the first 100 cells acquired by the image analysis were measured with x20 (raster 10X, 6Y) and x40 objectives (raster 20X, 10Y). The volume of the cells was calculated as an ellipsoid as above.

Cell counts were done in triplicate (3 separate sub-samples) for each sample. To alleviate sources of errors and to provide consistency between operators, cells in division were considered as one unit, and clumped cells were counted individually. Phase contrast with an objective x20 was used by operators 1-3. The protocol to enumerate the cells was pre-established and followed by each operator (also by the author): a Whipple grid was randomly moved on the slide (taking care of sampling through the whole slide) or transects were followed, 400 cells had to be counted. For image analysis, a x10 objective and DIC optics were used to obtain white cells on a black background for all samples. Images with a total of at least 400 cells were acquired, raster sizes were 6X, 5Y for the 10^6 sample, 10X, 10Y for the sample 10^5 , and 20X, 20Y for sample 10^4 . The duration of each task performed by each operator and by the image analysis system was recorded.

Results

Measurements varied between operators both for length and width (see Table 3-2). On average, the results obtained with the image analysis system were higher, also with higher standard deviations. When calculating the volumes (Figure 3-4), the tendency observed in linear measurements became more visible. However, although higher, the volume obtained by image analysis (x40 objective) remained in the range obtained by operators (Table 3-3).

Table 3-2: Intra-laboratory comparison of length and width measurements of *Microcystis aeruginosa* made with 4 operators and the image analysis system.

	Length (μ m)		Width (μ m)	
	Mean	Std Dev	Mean	Std Dev
IA x20	6.3	1.4	4.6	1.2
IA x40	5.6	1.0	4.4	0.6
x100 Operator 1	4.5	0.7	4.1	0.5
x100 Operator 2	5.1	0.6	4.2	0.3
x100 Operator 3	4.6	0.6	4.0	0.5
x100 Author	5.0	1.1	4.1	0.7

Table 3-3: Intra-laboratory comparison of biovolume of *Microcystis aeruginosa* calculated from results shown in Table 3-2.

	Biovolume (mean in μm^3)	Standard deviation (μm^3)
IA x20	78.4	49.0
IA x40	59.6	23.5
x100		
Operator 1	40.5	14.8
x100		
Operator 2	47.0	13.2
x100		
Operator 3	39.8	14.5
x100 Author	48.0	21.0

Enumeration of the samples was made by only 3 operators and the image analysis system. The results obtained by the operators were always lower than the results obtained initially with the Sedgewick-Rafter chamber (Table 3-4). The differences between operators increased as the concentration of the samples decreased. For the most concentrated samples (10^6 and 10^5), image analysis led to higher results than those obtained by the operators – and for the less concentrated sample (10^4), the results became unreliable due to the dirtiness of the sample, displaying too many artefacts similar in size and shape to *Microcystis*.

Table 3-4: Intra-laboratory comparison of enumeration of samples of different concentrations of *Microcystis aeruginosa* calculated from results shown in Table 3-2.

		Sample 1 (10^6)	Sample 2 (10^5)	Sample 3 (10^4)
1 μl subsample	Sedgewick-Rafter Operator 1	$2.3 \times 10^6 \pm 6.8 \times 10^4$	$2.3 \times 10^5 \pm 8.8 \times 10^3$	$2.2 \times 10^4 \pm 2.4 \times 10^3$
28 μl subsample	Image analysis	$1.8 \times 10^6 \pm 1.1 \times 10^5$	$2.8 \times 10^5 \pm 7.9 \times 10^4$	$3.9 \times 10^6 \pm 1.3 \times 10^6$
	Operator 1	$1.6 \times 10^6 \pm 2.2 \times 10^5$	$1.9 \times 10^5 \pm 1.7 \times 10^4$	$1.5 \times 10^4 \pm 1.6 \times 10^3$
	Operator 2	$1.5 \times 10^6 \pm 1.4 \times 10^5$	$1.1 \times 10^5 \pm 8.2 \times 10^3$	$1.4 \times 10^4 \pm 1.8 \times 10^3$
	Operator 3	$1.5 \times 10^6 \pm 3.2 \times 10^5$	$1.2 \times 10^5 \pm 4.0 \times 10^4$	$6.0 \times 10^3 \pm 3.0 \times 10^3$

The times recorded to accomplish each task show large differences between image analysis and operators (Table 3-5). When enumerating, time differences observed between operators for one sample was not much different than those found for one operator across the range of 3 samples, so that samples with high or low cell density took similar times to be enumerated by an operator. A large difference was observed when samples were enumerated by the image analysis system, the denser samples being the most rapid (1'30'') to be enumerated due to the very small size of the scan needed to obtain the 400 cells. It is to be noted that despite counts for sample 3 being much slower, it was not dramatically slower than the time taken by the operators. When measuring individual cells of *Microcystis* in two linear dimensions, the image analysis system was very rapid (0h02') compared with the time taken by the operators (over an hour).

Table 3-5: Intra-laboratory comparison of times to accomplish tasks such as enumeration and measurements of samples of *Microcystis*.

Counts	Sample 1	Sample 2	Sample 3
IA	1' 30"	9'	38'
Operator 1	26'	24'	15'
Operator 2	10'	22'	26'
Operator 3	13'	19'	18'

Measurements	Acquisition	Data Entry	Total
IA	0h 01'	1'	0h 02'
Operator 1	1h 15'	6'	1h 21'
Operator 2	0h 55'	6'	1h 01'
Operator 3	0h 56'	6'	1h 02'

This study showed the limitation of the image analysis system when using samples of low concentration. It is difficult for the system to distinguish the difference between a few cells (relatively small in size) and the presence of many small artefacts as was the case for Sample 3. The small volume of samples analysed with the image analysis system (under a 22x22 coverslip) emphasized this problem. However, the comparison of the duration of each task carried out by an operator and the image analysis system, especially for the measurement of cells, show the enormous advantage given by the latter.

3.2.3 Using Gene Frames® and fluorescence

The earlier validation studies demonstrated the limitations of the standard sample preparation method of dispensing a drop of sample (generally around 20 µl) under a coverslip (22x22 mm). The limitations of such preparation are that it contributes to the large errors observed when counting samples of low concentration and that the sample evaporates when running long scans (see above 3.2.2). The aim of this section was to develop better sample processing methods to increase the sample volume analysed and to overcome sample storage issues related to evaporation.

Gene Frames® are slide covers developed by ABgene® (Epsom, U.K.) for use in molecular biology. They comprise a gasket (frame) with a dual adhesive coating and a transparent plastic cover. The frame can be stuck onto a standard microscope slide, and the thin plastic cover (or a coverslip depending on the size of the frame) can then be stuck to the top of the frame after filling it up with the appropriate volume, sealing the sample completely inside the frame. The focal depth is larger than that of the former system using a coverslip. Two frame sizes with capacities of 65 µl (10x10 mm internal) and 125 µl (17x28 mm internal) were chosen for evaluation. The advantages of these frames were larger volume for samples and reduction of evaporation to almost nil. Frames could be kept for up to a week without any entry of air. Two validation experiments were carried out. A preliminary experiment was conducted out to determine the time needed for the cells of *Microcystis* to sediment to the bottom of the frame; this time appeared to be over an hour (results not shown).

Validation 1

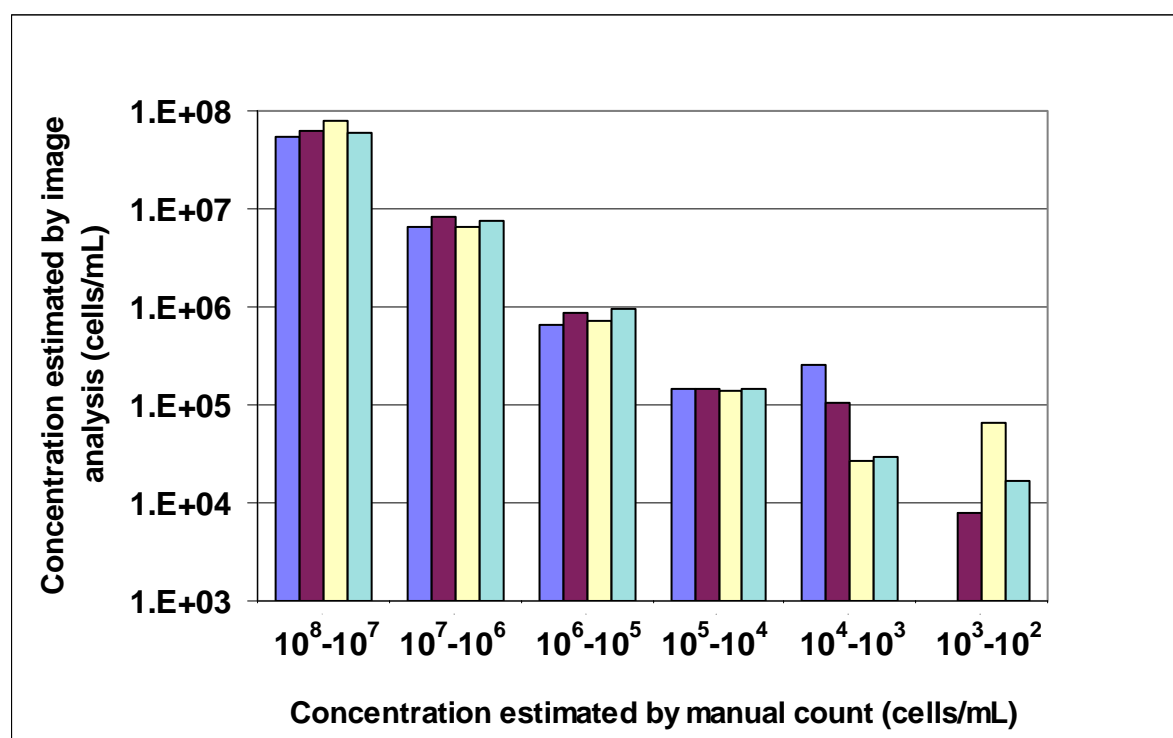
Preliminary experiments were done to compare usage of DIC optics and fluorescence using Gene Frames®. The initial concentration was obtained by counting the cells fixed in Lugol's in a Sedgewick-Rafter chamber with phase contrast. Manual counts were done in triplicate and acquisition of the data was also done in triplicate with both DIC optics and fluorescence. The results are shown in Table 3-6. These results show that the DIC manual and image analysis counts were similar but they differed with the original counts made with the Sedgewick-Rafter chamber (7.18×10^6). In both cases, counts obtained with fluorescence were lower than counts obtained with DIC, although the difference was smaller for the manual counts. It should be noted that more cells were counted by image analysis than by manual counting.

Table 3-6: Results of preliminary experiments using small Gene Frames® comparing manual and automatic counts, in both fluorescence and DIC optics (both with objective x20). When using DIC, size and shape discrimination were applied in the programs – no discrimination was used with fluorescence.

	Visual			Image Analysis	
	Lugol's	Fluorescence	DIC	Fluorescence	DIC
$\times 10^6$ cells/mL	7.2	9.0	9.3	6.1	9.8
Cells counted	898	346	376	2506	4016
Std Dev ($\times 10^6$ cells/mL)	n/a	2.6	6.6	4.2	1.1

An experiment was conducted to determine whether Gene Frames would give more robust data at low cell densities compared to the previous method. A series of diluted samples were sedimented in small and large Gene Frames. Figure 3-4 shows the results. Enumerations at high densities were efficient, but the lower the density (approx 10^4 - 10^3 and 10^3 - 10^2), the less accurate the results were. Fluorescence gave better results, probably due to the removal of artefacts visible by DIC or phase contrast optics and which the image analysis system cannot differentiate from cells.

Figure 3-4: Enumeration of *Microcystis* cells – comparison of results obtained in small and large Gene Frames for different concentration of samples. From left to right: DIC Large frame, Fluorescence Large Frame, DIC Small Frame, Fluorescence Small Frame.



Validation 2

Another experiment was carried out with small Gene Frames to see whether using fluorescence would improve the enumeration of *Microcystis*. The same culture as above was used. Three sub-samples were enumerated. The manual counts were obtained with a Sedgewick-Rafter chamber and compared with those obtained with the image analysis system. The results show that the counts made with the DIC optics were much higher than those obtained either manually or with the image analysis system using fluorescence optics. The difference between the manual counts and the results obtained with fluorescence are probably due to the number of dying/dead cells still present that would not be visible in the samples using fluorescence. The standard deviation obtained with the analysis system using fluorescence demonstrated good reproducibility with that system. In future work, the use of fluorescence to count small cells should be considered.

Table 3-7: Comparison of results obtained between manual counts (phase contrast) and image analysis (DIC and Fluorescence) ones for triplicates

Counting Method	Cells counted ($\times 10^5$)				
	Sample 1	Sample 2	Sample 3	Average	Std. Dev.
Manual	5.6	6.4	4.9	5.6	0.7
IA - Fluorescence	4.4	4.5	4.6	4.5	0.1
IA - DIC	8.5	8.2	11.7	9.5	2

3.2.4 Discussion

This study is the first using image analysis to measure and enumerate cells of *Microcystis* in an automated manner. In Australian guidelines, the shape to apply to *Microcystis* is a sphere (Burch et al. 2003). Burch et al. (2003) indicate that the average volume of *M. aeruginosa* is $87 \mu\text{m}^3$. The results presented in this study (Tables 3-1 and 3-3) are in general much lower, and the variations are large, mainly due to the differences observed in linear measurements. The current volumes found in the literature are probably overestimated and using an ellipsoid shape to calculate volume would certainly lead to more accurate results. The speed with which results were obtained, combined with the quality of the data (2 dimensions instead of one, precision of $0.5 \mu\text{m}$), place the image analysis system ahead of manual measurement by an operator.

Enumeration of *Microcystis* cells gave mixed results, due to the small size of the cells and other considerations: technical and biological. However, good results were obtained for the separation of adjoining cells and for counting when fluorescence was used. The volume of the sub-sample analysed is important. The smaller the volume, the less precise the count can be (potentially because there are fewer cells per field of view). In all of the experiments above, initial enumeration was made with a Sedgewick-Rafter chamber, the volume of which is 1 mL. In the first part of this work, sub-samples used for image analysis were in the order of $20 \mu\text{L}$. This explains the discrepancy between results obtained between high and low concentrations. Because of the small size of the cells, when concentrations get low, the proportion of artefacts can become higher and thus counts become unreliable. Using the new frames, we were able to increase the volume of sub-sample, and counts done in large frames were more reliable than those done in small frames. A large frame increases the volume analysed by 5 fold compared to the original method using coverslips. Using fluorescence for counting by image analysis is an advantage at low concentrations because it detects only objects of interests. A drawback is that it might be more difficult to compare with counts done in phase contrast or DIC, which take into account dead cells as well as living cells. Fluorescence counts were systematically lower than DIC counts by 20-30%. Cell counts by standard visual microscopy methods yield Coefficient Variations in the order of 10-20% (Kirchman et al. 1982).

3.3 Colonial *Microcystis*

The collection of representative samples of cyanobacteria and the determination of reliable estimates of their abundance by microscopy can be complicated in some species due to the natural formation of colonial or filamentous aggregates of cells. Certain species of *Microcystis* commonly form large colonial aggregates constrained by an amorphous mucilage or sheath (Holt et al. 1994). The number of cells per colony can reach tens of thousands in a three dimensional matrix. Fluctuations of up to an order of magnitude in mean colony volume can be observed seasonally: for example, *Microcystis aeruginosa* Kützing can have mean colony volumes ranging from $30,000 \mu\text{m}^3$ to $2,500,000 \mu\text{m}^3$ (see Reynolds and Jaworski 1978; Box 1981). In Australian drinking water, the recommended concentration of toxic *Microcystis aeruginosa* should not exceed $2,000 \text{ cells.L}^{-1}$, or an equivalent biovolume of $0.2 \text{ mm}^3 \text{ L}^{-1}$, for human health considerations (Burch et al. 2003). This can effectively constitute the presence of only a few colonies per mL of sample. In such cases, the accuracy of cell density estimates is compromised by the chance detection of a large aggregate.

A common procedure for enumerating large aggregates by microscopy without interfering with the natural morphology of the aggregate involves the use of an eyepiece graticule (e.g., Whipple Grid) to super-impose "standard unit areas" over the field of view. Cell density is estimated in a portion of the colony and the total number of cells per colony is extrapolated from the total number of "standard unit areas" in the colony (Burch et al. 2003). This method of enumeration is highly subjective due to the variable thickness of colonies and the inability to visualize individual cells. Whereas counting errors of

$\pm 20\text{-}30\%$ are generally acceptable for most cyanobacteria (Burch et al., 2003), the level of uncertainty in abundance estimates of *Microcystis* is much higher for an equivalent counting effort.

An accepted approach for improving the accuracy of counts is to disaggregate colonies of *Microcystis* to individual cells or small aggregates (Burch et al., 2003). Different disaggregation techniques have been evaluated, including suspension in deionised water, ultrasonication (Reynolds and Jaworski 1978), alkaline hydrolysis (Reynolds and Jaworski 1978) and heating/vortexing (Humphries and Widjaja 1979). These techniques were reviewed by Box (1981), who concluded that heat treatment was the most efficient and reliable of all, preserving both the number and the integrity of the cells. It was especially efficient for the disaggregation of *Microcystis* colonies, although the success of the technique was very much dependent on the strain used. The technique of grinding, which is generally used to homogenise tissues, has more recently been adapted to mechanically disrupt colonies of *Microcystis* into smaller subunits, resulting in counting errors of around $\pm 5\%$ (Falconer et al., 1994). However, the efficiency of the grinding technique has not yet been validated (e.g., potential for cell loss), nor has it been compared with other techniques.

In this study, we compared the grinding technique with the heating/vortex technique of Box (1981) for the disaggregation of colonies of *Microcystis* using image analysis. Assessment of the efficiency of the disaggregation techniques on colonies was achieved by directly measuring the number and size of the cells/aggregates of *Microcystis*. The more efficient the technique, the higher the number of objects in the sample and the smaller their size. Such measurements, especially of the size of the cells/aggregates would be very time consuming and difficult to obtain solely by manual microscopy.

3.3.1 Material and Methods

Samples

Two species of *Microcystis* were used in these experiments: *M. aeruginosa* Kützinger and *M. flos-aquae* (Wittrock) Kirchner (see Table 3-8), which differentiate by certain aspects of cell and colony morphology, but both forming large aggregates of cells bound by a mucilaginous sheath. Eight independent environmental samples were used and all but one (#4) were identified to the species level. All samples originated from Australian waters, and all but two (#7 & #9) had been fixed with Lugol's iodine solution (1% final concentration). Samples #8 and #10 were sub-samples of #7 and #9 respectively that were subsequently fixed. Fixed samples were kept at room temperature. Unfixed samples were strains isolated from the original environmental sample cultured in ASM-1 medium (Carmichael and Gorham 1974), with a 12-hour dark-light cycle in a temperature-controlled cabinet (25°C). Half of the samples were non-colonial and composed of single cells or very small aggregates (2-5 cells). These were used as controls to check whether the different treatments caused any cell loss. The colonies in the remaining samples were macroscopically visible and varied from soft and diffuse aggregates (#1) to well-delimited, strong and compact aggregates of several mm in diameter (#9/10).

Table 3-8: List of Samples used in disaggregation experiments

#	Species	Status	Aspect	Lugol's fixed	Time fixed
1	<i>M. flos-aquae</i>	Colonial	Loose, diffuse	Yes	22 months
2	<i>M. aeruginosa</i>	Colonial	Loose, diffuse	Yes	55 months
3	<i>M. flos-aquae</i>	Unicellular**		Yes	8 months
4	<i>Microcystis</i> sp.	Unicellular**		Yes	-
5	<i>M. aeruginosa</i>	Colonial	Loose, small	Yes	10 months
6	<i>M. aeruginosa</i>	Unicellular**		Yes	46 months
7	<i>M. flos-aquae</i> *	Unicellular		No	n/a
8	<i>M. flos-aquae</i> *	Unicellular		Yes	24 hours
9	<i>M. aeruginosa</i> *	Colonial	Compact, large	No	n/a
10	<i>M. aeruginosa</i> *	Colonial	Compact, large	Yes	24 hours

* Cultured isolates in ASM-1 medium (Carmichael and Gorham 1974)

** Unicells include a high proportion of paired dividing cells

Disaggregation treatments

The heating/vortexing and grinding time course experiments were performed in consecutive months. Where possible, the experimental design was the same for both techniques. Prior to each experiment,

samples were mixed thoroughly by inverting 20 times and 10 mL sub-samples were poured into capped-glass tubes. Each sub-sample was gently mixed 20 times and a 100 μ L aliquot was placed on a slide and covered with a coverslip for analysis.

For the heat treatment, capped-glass tubes were placed in an 80°C water bath. At each time-point (30, 60, 120 and 180 min), tubes were removed from the water bath, vortexed for 20 s (Vortex, IKA-Labortechnik, Germany), and a 100 μ L aliquot was placed on a slide with a coverslip for analysis.

For the grinding treatment, samples in capped-glass tubes were gently mixed by inversion 20 times and 2 mL sub-samples were placed in the grinding chamber of a Potter-Elvehjem tissue grinder with 101.6 μ m of clearance between chamber walls and tissue grinder surface (Wheaton, U.S.A.). Each 2 mL aliquot was then homogenised in a manual and constant grinding motion with a Teflon® pestle for 1, 2, 3, 4, or 5 min, after which 100 μ L aliquots were placed on slides with a coverslip.

Image analysis and calculations

The DIC optics was set to obtain white objects against a black background. Thirty images were acquired for each sub-sample immediately after the slide had been set; in total, 3300 images were acquired and saved.

The best thresholds to use for the automatic segmentation were determined for each time course experiment. Processing of the binary images consisted of single steps of cleaning and eroding. Data acquired were the area of each image occupied by the *Microcystis* units and their number. The area occupied by these units was representative of the size. Each field of view had a total area of $2.43 \times 10^5 \mu\text{m}^2$. Calculations of (i) the total area occupied by the cyanobacteria in a field of view divided by the number of units to obtain the average area per object and (ii) mean and standard deviations, were made from 30 captured images at each elapsed time during the experiments. It took less than 2 minutes to extract data from 30 images. Hereafter, references to size of cells or aggregates will refer to their area in μm^2 . Statistical analyses (ANOVA) were conducted using Analyse-it for Microsoft Excel (version 1.68, Analyse-it Software Ltd., Leeds UK).

3.3.2 Results

The effect of disaggregation treatment on non-colonial samples

Non-colonial samples were exposed to the disaggregation treatment regimes to investigate any possible effects on cell integrity that could result in a decrease in cell numbers. The results are given in Table 3-9 for heating treatment and Table 3-10 for grinding treatment. The sizes of the *Microcystis* 'units' were comparable at $t=0$ for both treatments except for sample #3, which had significantly ($p < 0.0001$) larger units in the sub-sample exposed to heating (Table 3-9) compared with the sub-sample exposed to grinding (Table 3-10). The number of units were comparable at $t=0$ between the two sets of treatment sub-samples for samples #3 and #4. For the other samples, the number of units in sub-samples were significantly different ($p = 0.0005$ or less). The difference between sub-samples for #7 in particular were large, with three fold more cells in the sub-sample used in the heating experiments compared with the sub-sample used for the grinding experiment.

Table 3-9: Mean object numbers and mean object areas for non-colonial samples exposed to heating treatment (n=30±standard deviation, nd=not done)

#	Measurement	Heating treatment time (minutes)				
		0	30	60	120	180
3	Mean object number	$1.5 \times 10^2 \pm 4.3 \times 10^1$	$1.3 \times 10^2 \pm 2.9 \times 10^1$	$1.1 \times 10^2 \pm 2.1 \times 10^1$	$1.8 \times 10^2 \pm 5.8 \times 10^1$	$1.7 \times 10^2 \pm 5.1 \times 10^1$
	Mean area (μm^2)	$3.9 \times 10^1 \pm 4.9 \times 10^0$	$4.3 \times 10^1 \pm 4.3 \times 10^0$	$3.2 \times 10^1 \pm 4.8 \times 10^0$	$2.0 \times 10^1 \pm 3.9 \times 10^0$	$1.6 \times 10^1 \pm 7.2 \times 10^0$
4	Mean object number	$1.3 \times 10^1 \pm 5.5 \times 10^0$	nd	$1.4 \times 10^1 \pm 1.2 \times 10^1$	$8.5 \times 10^0 \pm 2.3 \times 10^0$	$1.4 \times 10^1 \pm 1.5 \times 10^1$
	Mean area (μm^2)	$2.2 \times 10^1 \pm 1.1 \times 10^1$	nd	$2.4 \times 10^1 \pm 1.1 \times 10^1$	$3.2 \times 10^1 \pm 3.4 \times 10^1$	$2.3 \times 10^1 \pm 1.4 \times 10^1$
6	Mean object number	$4.9 \times 10^1 \pm 1.2 \times 10^1$	$5.3 \times 10^1 \pm 1.4 \times 10^1$	$5.8 \times 10^1 \pm 3.1 \times 10^1$	$6.3 \times 10^1 \pm 1.6 \times 10^1$	$7.2 \times 10^1 \pm 2.5 \times 10^1$
	Mean area (μm^2)	$1.8 \times 10^1 \pm 4.8 \times 10^0$	$1.5 \times 10^1 \pm 4.3 \times 10^0$	$2.4 \times 10^1 \pm 4.8 \times 10^0$	$2.3 \times 10^1 \pm 7.5 \times 10^0$	$9.5 \times 10^0 \pm 1.7 \times 10^0$
7	Mean object number	$9.7 \times 10^1 \pm 1.2 \times 10^1$	$7.9 \times 10^1 \pm 1.7 \times 10^1$	$5.7 \times 10^1 \pm 1.3 \times 10^1$	$5.5 \times 10^1 \pm 1.2 \times 10^1$	$6.2 \times 10^1 \pm 1.8 \times 10^1$
	Mean area (μm^2)	$1.2 \times 10^1 \pm 5.6 \times 10^0$	$8.2 \times 10^0 \pm 2.6 \times 10^0$	$5.3 \times 10^0 \pm 1.0 \times 10^0$	$5.5 \times 10^0 \pm 1.7 \times 10^0$	$5.5 \times 10^0 \pm 0.9 \times 10^0$
8	Mean object number	$8.8 \times 10^1 \pm 1.6 \times 10^1$	$5.3 \times 10^1 \pm 9.4 \times 10^0$	$5.3 \times 10^1 \pm 8.5 \times 10^0$	$3.2 \times 10^1 \pm 6.5 \times 10^0$	$4.2 \times 10^1 \pm 9.2 \times 10^0$
	Mean area (μm^2)	$5.7 \times 10^1 \pm 1.3 \times 10^0$	$5.6 \times 10^0 \pm 1.1 \times 10^0$	$5.3 \times 10^0 \pm 0.9 \times 10^0$	$8.9 \times 10^0 \pm 3.4 \times 10^0$	$1.0 \times 10^1 \pm 4.9 \times 10^0$

Table 3-10: Mean object numbers and mean object areas for non-colonial samples exposed to grinding treatment (n=30±standard deviation)

#	Measurement	Grinding treatment time (minutes)					
		0	1	2	3	4	5
3	Mean object number	$1.6 \times 10^2 \pm 3.1 \times 10^1$	$1.7 \times 10^2 \pm 2.9 \times 10^1$	$1.5 \times 10^2 \pm 2.7 \times 10^1$	$1.6 \times 10^2 \pm 2.5 \times 10^1$	$1.3 \times 10^2 \pm 2.4 \times 10^1$	$1.3 \times 10^2 \pm 2.4 \times 10^1$
	Mean area (μm^2)	$1.2 \times 10^1 \pm 0.9 \times 10^0$	$1.1 \times 10^1 \pm 0.7 \times 10^0$	$1.1 \times 10^1 \pm 0.9 \times 10^0$	$1.1 \times 10^1 \pm 0.8 \times 10^0$	$1.0 \times 10^1 \pm 0.7 \times 10^0$	$1.0 \times 10^1 \pm 0.8 \times 10^0$
4	Mean object number	$1.1 \times 10^1 \pm 4.4 \times 10^0$	$9.7 \times 10^0 \pm 2.3 \times 10^0$	$8.4 \times 10^0 \pm 3.9 \times 10^0$	$1.0 \times 10^1 \pm 3.5 \times 10^0$	$1.1 \times 10^1 \pm 3.5 \times 10^0$	$9.9 \times 10^0 \pm 3.2 \times 10^0$
	Mean area (μm^2)	$2.4 \times 10^1 \pm 1.6 \times 10^1$	$2.5 \times 10^1 \pm 1.6 \times 10^1$	$3.3 \times 10^1 \pm 3.5 \times 10^1$	$2.2 \times 10^1 \pm 6.6 \times 10^0$	$1.8 \times 10^1 \pm 5.5 \times 10^0$	$1.8 \times 10^1 \pm 5.5 \times 10^0$
6	Mean object number	$3.5 \times 10^1 \pm 1.2 \times 10^1$	$5.2 \times 10^1 \pm 7.9 \times 10^0$	$4.4 \times 10^1 \pm 1.1 \times 10^1$	$4.9 \times 10^1 \pm 1.1 \times 10^1$	$5.3 \times 10^1 \pm 1.6 \times 10^1$	$4.5 \times 10^1 \pm 9.2 \times 10^0$
	Mean area (μm^2)	$2.2 \times 10^1 \pm 8.5 \times 10^0$	$1.8 \times 10^1 \pm 2.3 \times 10^0$	$1.7 \times 10^1 \pm 2.6 \times 10^0$	$2.0 \times 10^1 \pm 8.5 \times 10^0$	$1.9 \times 10^1 \pm 4.6 \times 10^0$	$2.0 \times 10^1 \pm 2.9 \times 10^0$
7	Mean object number	$2.8 \times 10^1 \pm 7.5 \times 10^0$	$2.4 \times 10^1 \pm 7.3 \times 10^0$	$2.5 \times 10^1 \pm 7.8 \times 10^0$	$2.9 \times 10^1 \pm 6.6 \times 10^0$	$2.7 \times 10^1 \pm 7.0 \times 10^0$	$3.2 \times 10^1 \pm 6.2 \times 10^0$
	Mean area (μm^2)	$9.0 \times 10^0 \pm 5.4 \times 10^0$	$8.4 \times 10^0 \pm 6.2 \times 10^0$	$7.0 \times 10^0 \pm 3.3 \times 10^0$	$7.4 \times 10^0 \pm 2.4 \times 10^0$	$7.3 \times 10^0 \pm 2.3 \times 10^0$	$8.2 \times 10^0 \pm 3.1 \times 10^0$
8	Mean object number	$7.4 \times 10^1 \pm 1.5 \times 10^1$	$8.2 \times 10^1 \pm 1.6 \times 10^1$	$8.4 \times 10^1 \pm 1.4 \times 10^1$	$8.4 \times 10^1 \pm 1.7 \times 10^1$	$5.7 \times 10^1 \pm 1.1 \times 10^1$	$8.2 \times 10^1 \pm 1.7 \times 10^1$
	Mean area (μm^2)	$6.6 \times 10^0 \pm 1.9 \times 10^0$	$6.5 \times 10^0 \pm 1.3 \times 10^0$	$6.5 \times 10^0 \pm 0.9 \times 10^0$	$6.3 \times 10^0 \pm 0.8 \times 10^0$	$6.9 \times 10^0 \pm 1.4 \times 10^0$	$6.5 \times 10^0 \pm 0.9 \times 10^0$

In general, there was no major effect observed for samples exposed to the grinding treatment (Table 3-10). In the case of sample #3, there were significantly fewer cells after 4 min of grinding ($p < 0.0001$) and there was a slight but significant decrease in area after 1 min grinding ($p = 0.008$). In contrast, sample #6, which was composed of unicells and paired dividing cells, had a significant increase in the number of cells ($p < 0.0001$) but no significant change in cell size. Following 4 min of grinding sample #8 appeared to have fewer cells compared with the other time points, but overall the number of cells appeared to increase after grinding although the area did not appear to change.

With the exception of sample #4, the heat treatment appeared to have more of an effect on the cells, resulting in more variation between $t=0$ and treated sub-samples. For sample #3, the number of units varied significantly between some of the time points (e.g. for $t=0$ versus $t=60$, $p < 0.0001$) but not for others (e.g. $t=0$ versus $t=180$, $p = 0.27$). However, there was a significant decrease in the size of units after 60 min of heating ($p < 0.0001$), suggesting that some of the paired dividing cells present were being disaggregated. Similarly, for sample #6 the number of cells increased and the area decreased significantly when comparing $t=0$ and $t=180$ ($p < 0.0001$). In contrast, the mean number of units significantly decreased ($p < 0.0001$) after 30 min of heat exposure for samples #7 and #8 (Table 3-10). The mean area of units for sample #7 also decreased with increased heat exposure.

The effect of disaggregation treatment on colonial samples

The application of both treatments on loosely formed colonies of *Microcystis* resulted in a decrease of the size of the aggregates and an increase in the number of units in the field of view, indicating disaggregation (Tables 3-11 & 3-12). At $t=0$, the mean size of the aggregates varied between the sub-samples used for the two treatments. However, with the exception of sample #2 ($p = 0.0295$), this variation was not significant. Statistical analysis was made difficult by the large standard deviations, which were a major source of error variance within sub-samples. These large standard deviations demonstrate the large amount of variation in the size of aggregates even within a single sample. The number of units in each sub-sample appeared to be similar at $t=0$, although statistical analysis for sub-sample of #2 indicated a significant difference in the counts.

With heating, maximum disaggregation as assessed by changes in cell number was achieved within 30 min (samples #1 and #5, $p < 0.0001$) or 60 min (sample #2). In the case of sample #5, longer heat treatment appeared to significantly decrease ($p < 0.0001$) the number of objects (Table 3-11). The area of the objects decreased significantly for sample #5 ($p = 0.02$), but although the areas of the other samples also decreased after disaggregation the changes were not significant on account of the large standard deviations of the $t=0$ samples.

For the sub-samples treated by grinding, samples #2 and #5 reached maximum disaggregation after 1 min as assessed by changes in cell number (Table 3-12). In the case of sample #2 the number of objects began to decrease after 4 min but the numbers in sample #5 were not affected. Sample #1 achieved maximum disaggregation after 4 min of grinding. The maximum number of cells after disaggregation appeared to be less after grinding compared with heating treatment for samples #1 and #5. The area measurements suggested that heating was more effective for disaggregating sample #1 ($p < 0.0001$) but that grinding was more efficient for sample #2 ($p = 0.0004$). There appeared to be no difference between either method in the mean area after disaggregation for sample #5.

Samples #9 and #10 were well defined compact colonies, fresh for the former and fixed 24 hours in Lugol's iodine solution for the latter (Table 3-8). The average sizes of the colonies were comparable for the two samples but the standard deviations were large. Examples of the images acquired during the grinding treatment of sample #10 for $t=0$ and $t=1$ min, along with the binarised images that were analysed to calculate the number and area of objects, are illustrated in Figure 3-5.

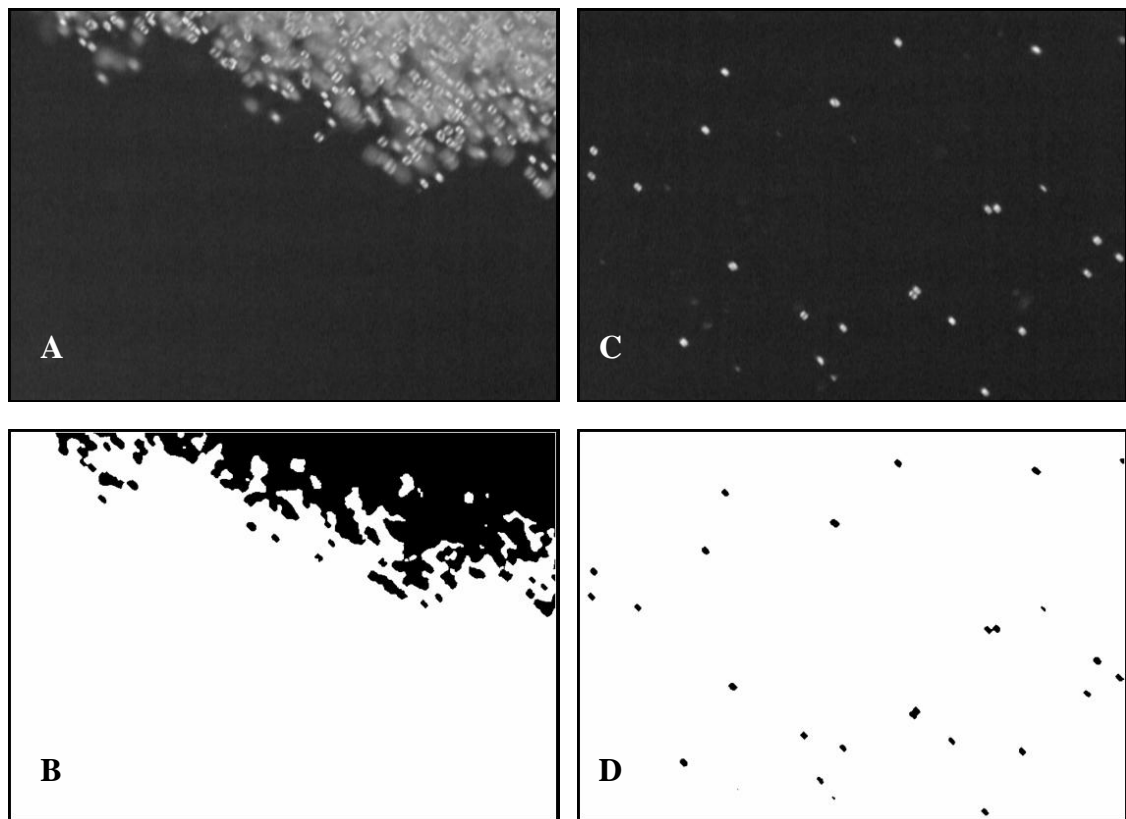
Table 3-11: Mean object numbers and mean object areas for loose/diffuse colonial samples exposed to heating treatment (n=30±standard deviation)

#	Measurement	Heating treatment time (minutes)				
		0	30	60	120	180
1	Mean object number	$1.4 \times 10^2 \pm 3.1 \times 10^1$	$4.5 \times 10^2 \pm 8.5 \times 10^1$	$3.4 \times 10^2 \pm 1.0 \times 10^2$	$4.6 \times 10^2 \pm 1.4 \times 10^2$	$4.6 \times 10^2 \pm 1.5 \times 10^2$
	Mean area (μm^2)	$8.0 \times 10^1 \pm 1.4 \times 10^2$	$2.9 \times 10^1 \pm 9.9 \times 10^0$	$2.6 \times 10^1 \pm 9.3 \times 10^0$	$3.1 \times 10^1 \pm 3.5 \times 10^1$	$2.7 \times 10^1 \pm 3.1 \times 10^0$
2	Mean object number	$7.8 \times 10^1 \pm 1.1 \times 10^2$	$3.9 \times 10^1 \pm 2.2 \times 10^1$	$7.5 \times 10^1 \pm 7.8 \times 10^2$	$1.0 \times 10^2 \pm 4.0 \times 10^2$	$1.9 \times 10^2 \pm 1.7 \times 10^2$
	Mean area (μm^2)	$7.6 \times 10^3 \pm 1.6 \times 10^4$	$3.6 \times 10^3 \pm 8.0 \times 10^3$	$1.1 \times 10^2 \pm 1.0 \times 10^2$	$2.2 \times 10^2 \pm 4.7 \times 10^2$	$1.0 \times 10^2 \pm 7.3 \times 10^1$
5	Mean object number	$1.4 \times 10^1 \pm 4.3 \times 10^0$	$1.0 \times 10^2 \pm 1.5 \times 10^1$	$2.2 \times 10^1 \pm 7.9 \times 10^0$	$6.1 \times 10^1 \pm 2.1 \times 10^1$	$5.7 \times 10^1 \pm 1.5 \times 10^1$
	Mean area (μm^2)	$5.2 \times 10^2 \pm 1.1 \times 10^3$	$3.9 \times 10^1 \pm 1.5 \times 10^1$	$3.1 \times 10^1 \pm 1.7 \times 10^1$	$2.9 \times 10^1 \pm 9.2 \times 10^0$	$2.7 \times 10^1 \pm 8.5 \times 10^0$

Table 3-12: Mean object numbers and mean object areas for loose/diffuse colonial samples exposed to grinding treatment (n=30±standard deviation)

#	Measurement	Grinding treatment time (minutes)					
		0	1	2	3	4	5
1	Mean object number	$1.3 \times 10^2 \pm 2.9 \times 10^1$	$1.9 \times 10^2 \pm 2.8 \times 10^1$	$2.0 \times 10^2 \pm 3.2 \times 10^1$	$2.2 \times 10^2 \pm 2.3 \times 10^1$	$3.4 \times 10^2 \pm 4.0 \times 10^1$	$2.6 \times 10^2 \pm 2.8 \times 10^1$
	Mean area (μm^2)	$1.9 \times 10^2 \pm 3.9 \times 10^2$	$9.8 \times 10^1 \pm 6.2 \times 10^1$	$1.1 \times 10^2 \pm 8.7 \times 10^1$	$1.2 \times 10^2 \pm 7.0 \times 10^1$	$6.4 \times 10^1 \pm 2.4 \times 10^1$	$1.0 \times 10^2 \pm 6.3 \times 10^1$
2	Mean object number	$3.3 \times 10^1 \pm 1.4 \times 10^1$	$1.7 \times 10^2 \pm 8.3 \times 10^1$	$1.7 \times 10^2 \pm 5.9 \times 10^1$	$1.7 \times 10^2 \pm 5.3 \times 10^1$	$1.4 \times 10^2 \pm 3.5 \times 10^1$	$1.1 \times 10^2 \pm 7.5 \times 10^1$
	Mean area (μm^2)	$5.9 \times 10^2 \pm 1.0 \times 10^3$	$5.9 \times 10^1 \pm 4.6 \times 10^1$	$4.7 \times 10^1 \pm 1.9 \times 10^1$	$5.5 \times 10^1 \pm 4.5 \times 10^1$	$7.4 \times 10^1 \pm 7.0 \times 10^1$	$9.1 \times 10^1 \pm 1.0 \times 10^2$
5	Mean object number	$1.5 \times 10^1 \pm 5.5 \times 10^0$	$4.7 \times 10^1 \pm 1.6 \times 10^1$	$4.4 \times 10^1 \pm 1.3 \times 10^1$	$4.0 \times 10^1 \pm 1.8 \times 10^1$	$4.4 \times 10^1 \pm 1.5 \times 10^1$	$5.4 \times 10^1 \pm 1.9 \times 10^1$
	Mean area (μm^2)	$1.6 \times 10^2 \pm 2.5 \times 10^2$	$4.5 \times 10^1 \pm 1.7 \times 10^1$	$4.3 \times 10^1 \pm 2.3 \times 10^1$	$4.5 \times 10^1 \pm 2.9 \times 10^1$	$3.3 \times 10^1 \pm 1.9 \times 10^1$	$4.2 \times 10^1 \pm 2.1 \times 10^1$

Figure 3-5: Example of images acquired during the grinding time course experiments of sample #10. Images A and B were taken at t=0, with A the original image showing part of a colony and B the same image after binarisation – Images C and D were taken after 1 min of grinding, with C showing the singlets and doublets after disaggregation and D the same image after binarisation. Optics = DIC, Magnification = x600.



In the case of sample #9, both heating and grinding were equally effective at disaggregating the colonies (Tables 3-13 & 3-14). Maximum disaggregation of sample #9 was achieved after 1 min of grinding or 120 min of heating, and in each case the number and area of objects were not significantly different from each other (e.g., $p=0.58$ for the comparison of object area).

The grinding technique also disaggregated sample #10 with a similar efficiency (in terms of cell number and area) compared with sample #9 (Table 3-14), except that 2 min of grinding were required for maximum disaggregation. However, the heating technique failed to disaggregate colonies of sample #10 and the mean area and number of objects remained the same after treatment compared with the t=0 control (Table 3-13).

Table 3-13: Mean object numbers and mean object areas for compact colonial samples exposed to heating treatment (n=30±standard deviation)

#	Measurement	Heating treatment time (minutes)				
		0	30	60	120	180
9	Mean object number	$3.1 \times 10^0 \pm 4.3 \times 10^0$	$5.6 \times 10^0 \pm 4.3 \times 10^0$	$1.5 \times 10^1 \pm 3.5 \times 10^1$	$8.1 \times 10^0 \pm 5.0 \times 10^0$	$9.7 \times 10^0 \pm 5.4 \times 10^0$
	Mean area (μm^2)	$3.5 \times 10^4 \pm 8.6 \times 10^4$	$2.5 \times 10^3 \pm 7.7 \times 10^3$	$6.6 \times 10^1 \pm 7.6 \times 10^1$	$3.2 \times 10^1 \pm 2.4 \times 10^1$	$4.2 \times 10^1 \pm 4.3 \times 10^1$
10	Mean object number	$9.0 \times 10^0 \pm 1.2 \times 10^1$	$4.4 \times 10^0 \pm 8.9 \times 10^0$	$2.7 \times 10^0 \pm 3.1 \times 10^0$	$5.0 \times 10^0 \pm 6.2 \times 10^0$	$8.3 \times 10^0 \pm 1.3 \times 10^1$
	Mean area (μm^2)	$2.8 \times 10^4 \pm 7.6 \times 10^4$	$1.3 \times 10^4 \pm 4.9 \times 10^4$	$2.7 \times 10^4 \pm 7.1 \times 10^4$	$1.8 \times 10^4 \pm 6.3 \times 10^4$	$1.9 \times 10^4 \pm 6.3 \times 10^4$

Table 3-14: Mean object numbers and mean object areas for compact colonial samples exposed to grinding treatment (n=30±standard deviation)

#	Measurement	Grinding treatment time (minutes)					
		0	1	2	3	4	5
9	Mean object number	$2.8 \times 10^0 \pm 5.3 \times 10^0$	$9.3 \times 10^0 \pm 5.7 \times 10^0$	$1.4 \times 10^1 \pm 1.5 \times 10^1$	$1.4 \times 10^1 \pm 5.8 \times 10^0$	$1.5 \times 10^1 \pm 4.6 \times 10^0$	$7.9 \times 10^0 \pm 3.5 \times 10^0$
	Mean area (μm^2)	$2.8 \times 10^4 \pm 7.6 \times 10^4$	$3.7 \times 10^1 \pm 2.5 \times 10^1$	$3.2 \times 10^1 \pm 1.2 \times 10^1$	$2.9 \times 10^1 \pm 7.6 \times 10^0$	$3.0 \times 10^1 \pm 7.3 \times 10^0$	$3.0 \times 10^1 \pm 7.9 \times 10^0$
10	Mean object number	$2.7 \times 10^0 \pm 3.6 \times 10^0$	$2.3 \times 10^1 \pm 1.4 \times 10^1$	$1.7 \times 10^1 \pm 9.9 \times 10^0$	$2.0 \times 10^1 \pm 7.4 \times 10^0$	$1.4 \times 10^1 \pm 3.6 \times 10^0$	$1.9 \times 10^1 \pm 4.9 \times 10^0$
	Mean area (μm^2)	$2.9 \times 10^4 \pm 6.9 \times 10^4$	$1.4 \times 10^2 \pm 3.6 \times 10^2$	$5.8 \times 10^1 \pm 4.3 \times 10^1$	$7.3 \times 10^1 \pm 5.5 \times 10^1$	$4.3 \times 10^1 \pm 1.4 \times 10^1$	$4.8 \times 10^1 \pm 1.7 \times 10^1$

3.3.3 Discussion

This study reports the use of image analysis for estimating the size and cell number of colonial cyanobacteria, and in particular, an assessment of two techniques for disaggregating colonies of *Microcystis* as a preparatory step in enumeration. A major advantage of the image analysis system was the ability to directly and easily calculate the number and size of the *Microcystis* units (unicells, paired dividing cells and aggregates), which provided a measure of the success of disaggregation. In earlier studies (see Box 1981), the effectiveness of disaggregation was assessed by comparing the number of cells detected following treatment with the number of cells calculated from a theoretical regression, assuming that the number of cells in a healthy quasi-spherical colony can be approximated from its diameter. This has several drawbacks: (i) the colonies are not always spherical or quasi-spherical, (ii) the spacing of cells within the mucilage envelope is highly variable, and (iii) the relationship does not hold for populations in which there is a wide variation in colony diameter (Reynolds and Jaworski 1978).

A potential limitation of image analysis systems is the size of the field of view that can be acquired by the camera (i.e., 243,000 μm^2 at the magnification used with the system described herein), which determines the size of the objects that can be analysed. This did not appear to affect our results. Non-colonial strains were used as controls to determine whether the disaggregation treatments resulted in the loss of any cells. Overall, neither treatment appeared to have a negative effect on cell numbers, although in some instances (e.g., sample #3) excessive disaggregation treatment led to the loss of cells. In the case of samples #3 and #6, the cell number increased and the mean object area decreased, suggesting that paired dividing cells and small aggregates were being disaggregated. Separation of the aggregates within sample #3 during mixing could explain the slightly higher number and smaller mean object area observed in sub-sample #3 which was used in the grinding experiment. In general, grinding produced more homogeneous data with smaller standard deviations compared with heating. Our results for heating/vortexing are consistent with previous studies, which found no associated losses when used on *Microcystis* (see review by Box 1981). In addition, the size of the unicells measured in the non-colonial samples, except for sample #4, were consistent with that reported in natural populations in Australia (Baker 1992).

Sub-samples of the colonial strains exhibited differences in the size and number of aggregates. This observation can be explained by the extreme patchiness of the samples. The times required for disaggregation of colonies by heating treatment in this study (30 - 120 min) were at least twice as long as those considered adequate by Box (1981). The response of the colonial samples to the disaggregation treatments appeared to be related to the structure of the colonies. Colonies that were loose/diffuse required less grinding or heating treatment for maximum disaggregation compared with compact colonies. The grinding technique was equally efficient for the disaggregation of fixed compact colonies and fresh compact colonies. However, the heating treatment, while effective for disaggregating fresh compact colonies, could not disaggregate fixed compact colonies. Our findings are consistent with the observation made by Box (1981) that colonies of *M. aeruginosa*, fixed overnight with Lugol's iodine, were less susceptible to disaggregation under heating at 80°C than unfixed colonies. These data suggest different modes of action for the disaggregation treatments - physical for grinding and chemical for heating (although heating may also exert some physical effect as well). Fixation appears to enhance the thermal stability of the mucilage but does not confer any additional ability for the colonies to withstand mechanical disruption. The type of fixative may be an important factor in determining colony stability, but this was not investigated. Colonies of both cultured and field samples of *M. aeruginosa* fixed in acidified Lugol's iodine appeared to be partially reduced to single cells (Box 1981). The Lugol's iodine solution used in this study was alkaline. The success of heating / vortexing obtained for other taxa of cyanobacteria has been extremely variable, with some strains requiring additional hydrolysis in 0.1M NaOH (Box 1981). The grinding technique may be better for these species because it has the advantage of being a physical technique and is not affected by the chemical composition of the mucilage. However, it is not known yet what the performance of the grinding technique is on other taxa.

In conclusion, this study shows that (i) image analysis is a rapid and efficient way to assess disaggregation of colonies of *Microcystis* spp. by measuring the area and number of units in fields of view of a microscope, (ii) the grinding technique is an effective and rapid technique (1-2 min treatment required) to disassociate all types of colonies of *Microcystis*, fresh or fixed, without associated loss and that (iii) the heating technique at 80°C followed by vortexing is not reliable for all types of colonies of *Microcystis* (especially the compact and fixed ones) and is a considerably longer and more involved process than the grinding technique. The success of the grinding technique warrants further testing on colonial strains of other species of cyanobacteria.

4. Application to Trichomes

Noxious trichome-shaped cyanobacteria encompass genera such as *Planktothrix*, *Phormidium* and *Cylindrospermopsis* (straight and flexuous trichomes). As a model in this study, we chose *Cylindrospermopsis raciborskii* (Woloszynska) Seenaya and Subba Raju (Nostocales, Seenaya and Subba Raju, 1972) because of its wide distribution (Padisák 1997; Briand et al. 2004) and its potential toxicity (Hawkins et al. 1985; Humpage et al. 2000). Its toxicity involves hepatotoxins (Ohtani et al. 1992) and neurotoxins (Lagos et al. 1999). *Cylindrospermopsis raciborskii* is also causing increasing concern because of its invasive behaviour (Briand et al. 2004).

Image analysis has been previously reported as a tool to measure the total length of the straight filaments of *Oscillatoria rubescens* and *Anabaena flos-aquae* (Walsby and Avery 1996). Congestri et al. (2000) evaluated the biomass of Baltic filamentous cyanobacteria by image analysis. Both studies required manual intervention on each of the trichomes.

The aim of this chapter was to develop programs to enumerate trichomes of *Cylindrospermopsis* at a density as low as possible and to define ways for the image analysis system to measure trichome biovolume as accurately as possible. All studies described below were based on trichomes obtained from the extensive collection of *Cylindrospermopsis* strains, both toxic and non-toxic, harboured at the Australian Water Quality Centre. Cultures were grown in ASM medium (Gorham et al. 1964) on a 12:12 light-dark cycle in a 25 °C constant temperature cabinet.

4.1 Algorithms

4.1.1 Enumeration

Routine enumeration

Cylindrospermopsis raciborskii is a difficult species to enumerate as the cells in the trichomes are poorly defined. Moreover, the length of the trichomes varies widely in natural populations and it cannot be assumed that a trichome contains an 'average' number of cells. The average cell length varies between 4 and 10 µm. Cells of *C. raciborskii* are generally enumerated as follows: the number of cells is determined for a defined number of trichomes in the sample (generally high magnification is used), the number of trichomes in the sample is determined following the statistics of Laslett et al. (1997) and the average number of cells per trichome is multiplied by the total number of trichomes. To achieve a $\pm 20\%$ precision, 50 trichomes need to be counted; to achieve a $\pm 30\%$ precision, 23 trichomes need to be counted. In either case, the number of cells for each trichome counted must also be determined.

Image analysis algorithm

Due to the variations of the length of the trichomes and length of the cells in each trichome, and to minimise errors, our approach has been to base our algorithms on enumerating trichomes and calculating their biovolume. One of the problems that needed to be solved was how to deal with trichomes that overlapped following sedimentation on to a slide. We had to develop algorithms which allowed the image analysis system to count trichomes in a sample even when they overlapped in dense samples. This was achieved using the skeleton technique and reducing the skeleton obtained to end dots, which were then magnified. The algorithm was then set up to count the number of dots remaining. The final number of trichomes corresponds to half the final number of dots (see Figure 4-1).

The best optics for analysis was found to be DIC, which provided a white object on a dark background (Figure 4-1). In experiments the number of trichomes counted was often much higher than recommended due to the easiness of data acquisition. Recognition of trichomes was defined after analysing hundreds of cells and noting the image analysis parameters that best defined the trichomes relative to other objects and artefacts on the slide. The parameters retained in the study were perimeter, area, roundness and aspect.

Basic Executive program

```

colour process saturate
image store load
filter edge Sobel           improves the definition of edges
image store combine
image store load
'

colour detect grey
colour auto frequency 4
'

binary process erode 1
binary process clean 1
binary store load
'

measure features
binary store load
'

binary store And
binary conditional skeleton reduces the overlay to a centred one-pixel thick line
binary conditional ends    isolates the ends of branches of the skeleton (see Figure 4-1)
'

measure field

```

Figure 4-1: Example of image quality (DIC optic) used to enumerate trichomes of *Cylindrospermopsis raciborskii* – the final overlay is represented by dots at the ends of the trichomes. The executive programs finally counts the number of these dots.



4.1.2 Measurement

The aim of measuring trichomes is to be able to calculate their biovolume. In the Australian guidelines, the shape attributed to *Cylindrospermopsis raciborskii* is a cylinder (Hillebrand et al. 1999; Burch et al. 2003) requiring the measurement of the two parameters width and length. This is a time consuming but relatively easy task when the trichome is straight, but becomes arbitrary when the trichome is curved as the length is then estimated by integrating chosen straight section (Figure 4-2). Hoogveld and Moed (1993) designed a digitising tablet to help measuring the length of filamentous cyanobacteria. Their comparison of the classic technique and by digitising (although manually) led to discrepancies of more than 10% when the filaments were curved.

Figure 4-2: Example of a curve trichome of *Cylindrospermopsis raciborskii* showing the difficulty to accurately measure the total length of the trichome. The lines illustrate the two-steps operation needed to measure the total length ($\times 100$ objective).



In this chapter we described means of accurately measuring the width and length of straight and curved trichomes and calculating their biovolume, in an automatic manner.

Some tests were initially performed to determine which of the parameters measured by the image analysis system would fit best the definition of width and length of the trichome.

Fibre length and fibre width

We chose to compare two formulae describing shapes similar to that of trichomes of *Cylindrospermopsis*, namely a cylinder shape and a rod shape.

Formula 1 (from Hillebrand et al. 1999) Cylinder = $\pi/4 \times W^2 \times L$
Where W is the width of the trichome and L is its length

Formula 2 (from Massana et al. 1997) Rod = $(\pi/4) \times W^2 \times (L - W/3)$
Where W is the width of the trichome and L its length.

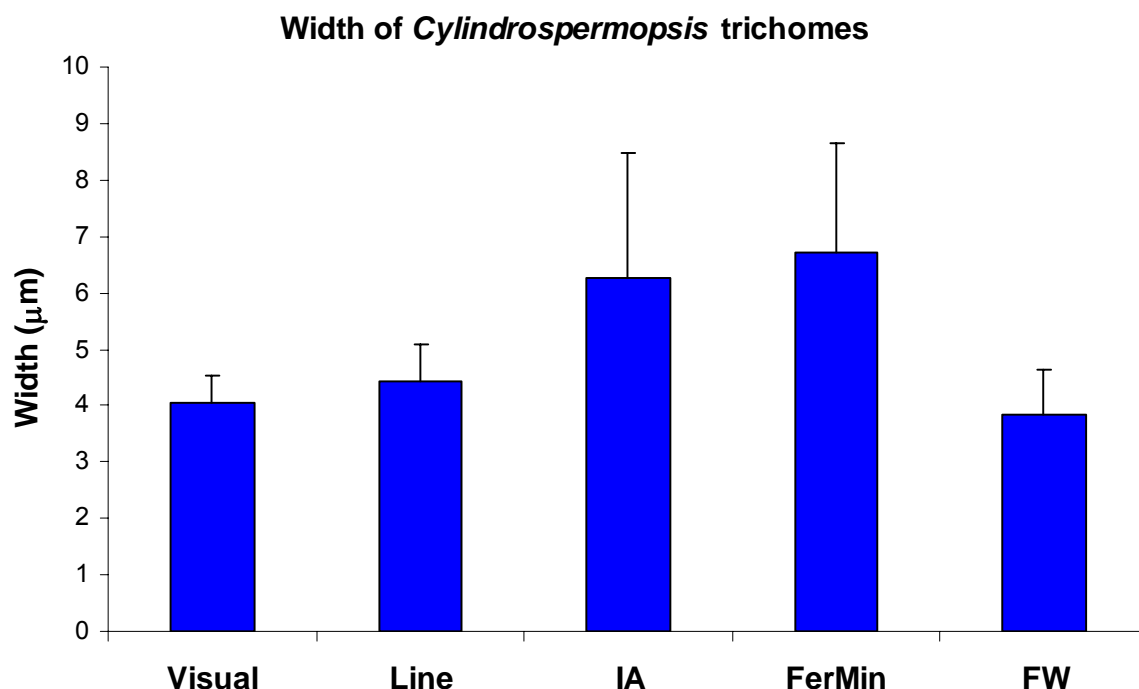
Because of the potential curvature of the trichome, the best parameter found to match the length was the Fibre Length (FL), which is the only parameter taking into account the curvature.

Formula 3 (from Russ 1999) Fibre Length (FL) = $P/2 - 2 \times A/P$
Where P is the perimeter of the trichome and A its area.

The measurement of Fibre Width (FW) (Formula 4) gave the closest fit ($3.84 \pm 0.788 \mu\text{m}$) with the visual measurement ($4.05 \pm 0.488 \mu\text{m}$) and the line one ($4.44 \pm 0.650 \mu\text{m}$).

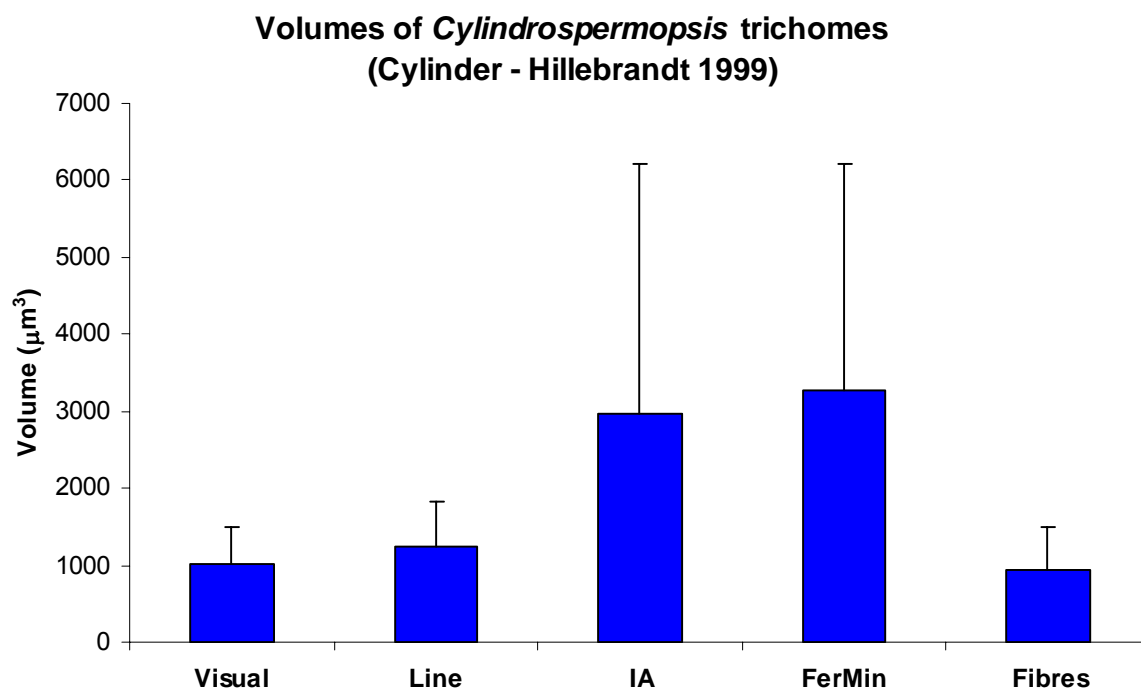
Formula 4 (from Russ 1999) FW = A / FL

Figure 4-3: Width measurements of *Cylindrospermopsis* trichomes (n=50) obtained using different techniques. 'Visual': 'manual' measurement using a calibrated graticule, 'Line': manual point-to-point distance measurement of each trichome carried out using the image analysis system, 'IA' automatic measurements made by image analysis programs considering the width of a parallelepiped fitting the boundary of the object (see Figure 1-2), 'FerMin': Feret Minimum and 'FW': Fibre Width (see above).



The calculations of Fibre Length and Fibre Width require accurate measurements of the area and perimeter of the trichomes. These measurements can be obtained easily with the image analysis system. The biovolume calculations obtained with formulae 1 and 2 were very similar (data for formula 2 not shown). Volumes obtained with fibre length and width were the closest to those obtained by routine (visual) measurements (Figure 4-4).

Figure 4-4: Biovolumes of *Cylindrospermopsis* trichomes (n=50) calculated using Formula 1 and length and width obtained with different measurement techniques: 'Visual': 'manual' measurement using a calibrated graticule, 'Line': manual point-to-point distance measurement carried out with the image analysis system, 'IA' automatic measurement of width made by image analysis programs considering the width and the length of a parallelepiped fitting the boundary of the object (see Figure 1-2), 'FerMin': Feret Minimum and 'Fibres': fibre width and length.



In further programs, the shape parameters Roundness and Aspect were selected as the most appropriate parameters to differentiate trichome shapes from non-trichome objects in the samples.

Formula 5 $\text{Roundness} = 4 \times A / \pi \times \text{FL}^2$
Where A is the area of the trichome and FL its fibre length

The Roundness gives a value of 1.0 for a perfect circle. Using the length of the object, it makes it more sensitive to how elongated the object is, rather than how irregular its outline may be.

Formula 6 $\text{Aspect ratio} = \text{FL} / \text{FW}$
Where FL is the Fibre Length and FW the Fibre Width

The aspect ratio makes no assumption about the shape of the object, but is used to indicate the degree with which an object's dimension approaches a sphere. In the case of *Cylindrospermopsis*, differentiation was generally successful with a Roundness factor above 57 and an Aspect ratio between 4 and 30.

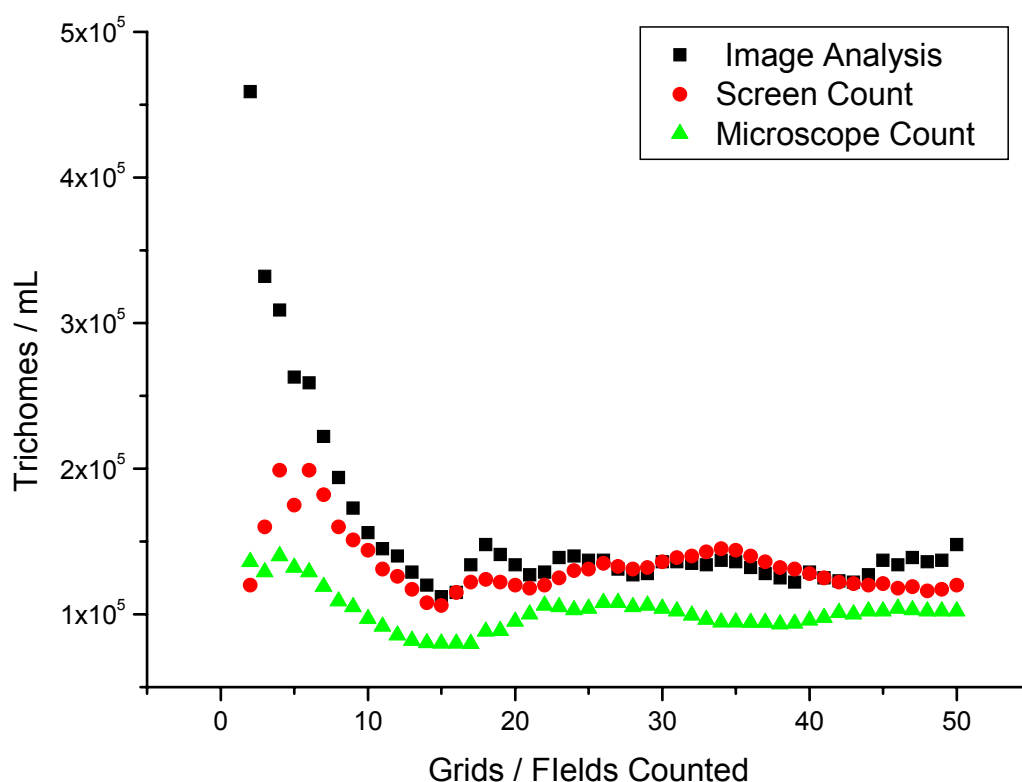
4.2 Validations with laboratory cultures

Numerous validations were performed with culture material, both to enumerate and measure/calculate the biovolume of *Cylindrospermopsis*. From the same run of the programs, it was eventually possible to obtain both the concentration of trichomes per mL and the volume of each trichome present in any field of view, leading to the acquisition of numerous data. To calculate the volumes, Formula 1 was chosen. Two examples of results are presented hereafter.

4.2.1 Comparison of enumeration techniques

In the first example, the results obtained by the image analysis system were compared with that obtained 'manually' by microscopy, but also with counts made from each image acquired manually from the image displayed on a computer monitor (Figure 4-5). The enumeration was carried out in August 2001, with the strain AWT-205 (AWQC). Fifty fields of view were acquired and analysed one by one. For routine counts, fields of view are represented by a calibrated grid (see above) placed in the ocular, and for the image analysis, a field was defined as the size of the image acquired minus the frame (see above). The DIC optics were used to obtain white bright trichomes on a black background, and the x20 objective was used. In this example, discrimination was based on an object length $> 7 \mu\text{m}$ and object roundness > 50 .

Figure 4-5: Enumeration of *Cylindrospermopsis raciborskii* (strain AWT-205) comparing three modes of data acquisition: manual by microscopy (triangles), image analysis system (squares) and on-screen manual count (circles).



The data obtained during this experiment display the expected trend of a decrease of the trichome concentration as the number of fields counted increases to reach a plateau. These data show that the image analysis system is very reliable for counting trichomes. The manual counts were always slightly lower than the two others, but after 50 fields the concentration plateaued at around 1.02×10^5 trichomes.mL⁻¹ for the manual count compared with 1.48×10^5 trichomes.mL⁻¹ for the image analysis results. This difference could be explained by the difference in size of the fields of view considered during enumeration: a frame of view analysed by the image analysis is relatively small ($60\,674.18 \mu\text{m}^2$ at the magnification used) compared with the grid area ($250\,000 \mu\text{m}^2$) used manually. The smaller the area, the less volume of sample considered, and so the higher the chance of error occurring in the count. However, the results obtained with the image analysis system were very similar with that obtained by manually counting trichomes from each image analysed, showing the reliability of the system for counting from the images that it acquires.

The second example was from a much later experiment (end of 2004) conducted using larger volumes of sample in Gene Frames (see above) and comparing manual counts with image analysis counts

using both DIC and fluorescence optics. The culture used was AWT-205 (see above). Pre-cultures of the strain were grown in autoclaved 500 mL Pyrex Erlenmeyer flasks containing ASM medium (Gorham et al., 1964). An initial count using a Sedgewick-Rafter chamber was made to determine the original concentration of the culture (1.24×10^5 trichomes.mL⁻¹) to subsequently dilute it to obtain ca. 50000 trichomes.mL⁻¹. Fifty mL were then transferred into a cell culture vial to facilitate mixing before sub-sampling. The vial was then inverted 20 times before sub-sampling: sub-samples were taken in triplicate to count trichomes:

- 1) in Sedgewick-rafter chambers after fixing with Lugol's and sedimentation, with phase contrast, x20 objective to count the number of trichomes and the number of cells per trichome in a defined number of trichomes. This part was carried out by someone other than the main author;
- 2) in small Gene Frames slides for acquisition of images with fluorescence first and with DIC subsequently using the same raster (20x20, 400 images per raster), x10 objective. Each scan took ca. 20 min. Images were analysed later off-line, with no discrimination when images were acquired with fluorescence and discriminated on length (threshold of 7 μ m) and roundness (threshold of 30) values when images were acquired with DIC optics. Around 1000 trichomes per sub-sample were analysed. The results are displayed in the following Table 4-1.

Table 4-1: *Cylindrospermopsis* counts by manual and IA methods (estimated original concentration 50000 trichomes.mL⁻¹)

	Sample 1	Sample 2	Sample 3	Average +/-	Std. Dev.
Manual counts					
(Phase Contrast))	49500	52950	46900	49783	3035
IA – Fluorescence	40333	35786	45435	40518	4827
IA – DIC	32828	32939	40888	35552	4622
PCR (# gene copies)	238764	222818	296624	252735	38836

The results obtained by image analysis using DIC optics were generally lower than those obtained 'manually' using a Sedgewick –Rafter chamber, but comparable for those obtained by image analysis using fluorescence. The results obtained with DIC were always found to be lower (but not significantly) than those obtained with fluorescence. This can be explained by the discrimination value used when images were acquired with DIC optics, leaving out very short trichomes or parts of trichomes still containing pigments. Our preliminary studies showed that with DIC, many artefacts of short length could be mistaken for short parts of trichomes. The differences between manual counts and IA-fluorescence are less than 20% although it reaches almost 30% between manual counts and IA-DIC. It has to be kept in mind that the manual counts are not absolute and that they probably include some of the objects refused by the discrimination made with DIC.

Despite the differences observed between DIC and fluorescence, we estimated that parts of trichomes < 7 μ m, corresponding roughly to 1 cell and a bit, could be dismissed as dying or broken trichomes, and for practical reasons, only analysis in DIC was carried out for field experiments.

4.2.2 Biovolume versus light intensity

The programs of the image analysis system were consequently adapted in order to assist in a project where a large number of samples of *Cylindrospermopsis* had to be analysed. The project intended to study the light preference and growth of a strain (020A – straight to curved) isolated from Palm Island (Queensland). This study was part of an AWWA Research Foundation Project 2976 on 'Reservoir management strategies for control and degradation of algal toxins' (Regel and Brookes 2005). The difficulty of precisely counting the number of cells in trichomes is well known and the requirement to monitor the changes of biomass of *Cylindrospermopsis* provided a good opportunity to test the image analysis system under real experimental conditions and with a new trained user, Dr. Rudi Regel.

Samples were maintained under 12:12 dark: light photoperiod and at a constant temperature of 25°C. To acquire images, the best thresholds were determined for the automatic segmentation for each set of analysed samples. Processing of the binary images consisted of single steps of cleaning and eroding. For each light treatment, approximately 30 trichomes were measured, in triplicate, for 44 days. The trichomes were measured individually from isolated images, the data were saved and the biovolume of each trichome was calculated instantaneously in an Excel spread sheet.

The results are summarised in the graphs below and more details and discussion can be obtained in Regel and Brookes (2005). Figure 4-6 shows that growth is dependent upon light intensity, and that

positive growth was recorded for the 44 days at low-medium intensity of light ($10\text{--}30\ \mu\text{mol}\cdot\text{m}^{-2}\cdot\text{s}^{-1}$). For light intensity $> 30\ \mu\text{mol}\cdot\text{m}^{-2}\cdot\text{s}^{-1}$, positive growth was only recorded during the first 6 days.

Figure 4-6: Changes in *Cylindrospermopsis* biovolume over time at different light intensities ($\mu\text{mol}\cdot\text{m}^{-2}\cdot\text{s}^{-1}$). Total biovolume was determined from fibre length and fibre width parameters. Total biovolume was calculated by multiplying volume by trichome concentration. (from Regal and Brookes 2005).

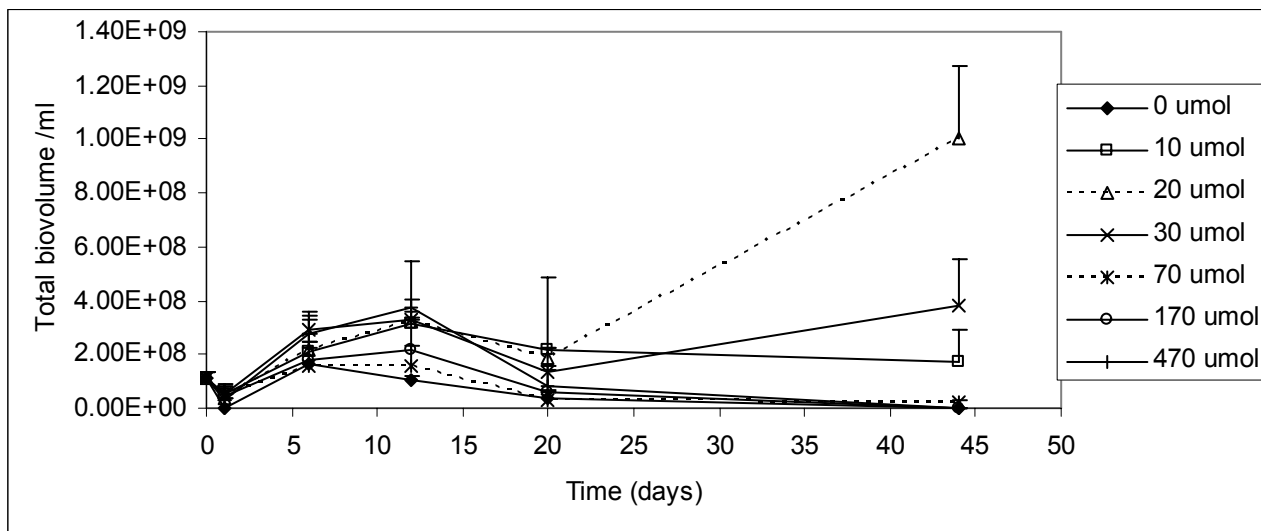
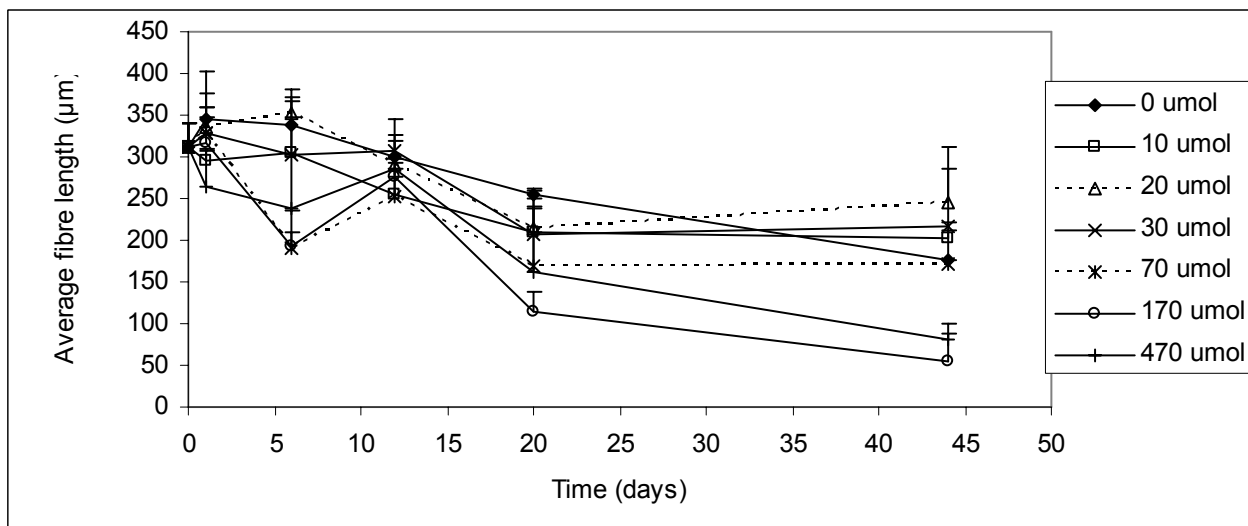


Figure 4-7 below shows the changes in the average length of the trichomes in function of the different light treatments. The average length, of $310\ \mu\text{m}$ at the beginning of the experiment decreased through time for all treatments. The higher the light intensity the stronger decrease in length of the trichomes.

Figure 4-7: Changes in *Cylindrospermopsis* trichome length over time at different light intensities ($\mu\text{mol}\cdot\text{m}^{-2}\cdot\text{s}^{-1}$) (from Regal and Brookes 2005).



This study shows that the analysis system is user-friendly and can be learnt to be used quite easily. In this case, it saved a lot of time and gave the assurance of quality data. Moreover, for this study image analysis allowed the rapid and accurate acquisition of data that are generally not gathered when studying *Cylindrospermopsis* or other cyanobacteria, such as fibre length and fibre width, which would have been very time consuming if done manually and probably not as accurate since trichomes can be curved and error of the measurement of width is important.

The data identified a possible relationship between light intensity and the average length of the trichomes in culture over time. These results triggered more interest in acquiring additional morphometric data on *Cylindrospermopsis* during a long-term study of its growth.

4.2.3 Growth experiment

Image analysis appeared to be a good tool to rapidly and accurately obtain data on the morphometry of trichomes, in this case of *Cylindrospermopsis*. The aim of this part of the study was to conduct a controlled growth rate experiment using the image analysis system to follow the changes in morphometry of the trichomes through time (length, width and biovolume).

Material and Methods

The growth experiments were carried out over 40 days throughout June to August 2005. Only part of the data have been analysed to date and so only partial data will be presented here. The strain used in this study was the same as that used in the preliminary experiment above. At the beginning of the first day of the growth experiment (day 1), a sample was taken, fixed with Lugol's, sedimented in a Sedgewick-Rafter chamber and subsequently enumerated by the method of McAlice (1971), with a result of 5.79×10^6 trichomes.mL⁻¹ (n=579). Three Schott® bottles of 2 litres each, A, B and C, were started with 500 mL of ASM medium with the aim to have a concentration of 5000 trichomes.mL⁻¹. Each subsequent sub-sample from bottles A, B and C was analysed in triplicate. During the experiment, the three bottles were placed in a culture cabinet with constant temperature of 25°C and a 12:12 h light:dark photoperiod. The light intensity was measured at the beginning and at the end of the experiment with a LiCor LI-1000 linked to a Quantum Sensor and placed at the bottom of the bottles. It was found to vary between 19.5 and 23.0 $\mu\text{mol.s}^{-2}.\text{s}^{-1}$.

Sub-sampling was generally performed at the same time in the morning. Prior to sampling, samples were mixed by inversion (20 times) and then 10 mL was sampled from each bottle and placed into a 100 mL plastic tube. Each plastic tube was again inverted 20 times before further sub-samples were taken. For image analysis, 130 μL was further sub-sampled and placed in a large Gene Frame® slide (65 μL in a small Gene Frame® after the 16th of June) for scanning. Three mL of each sub-sample was fixed with Lugol's and kept in the dark at room temperature until further analysis by microscopy.

The Gene Frame® slides were left to sediment for an hour before scanning by IA. The $\times 10$ objective was used and the DIC optics was set up to obtain white objects against a dark background. The size of each raster varied with the density of trichomes per field of view to obtain images of at least 400 trichomes: 20x25 (500 images) of 20 min duration down to 10x10 (100 images) of 5 min duration towards the end of the experiment. Analysis of the images was conducted later off line. The programs used were similar to those used previously with values of the discrimination parameters (e.g., length, roundness and aspect) tested on a set of images taken from the same culture. The enhancement and processes of the binary images were slightly modified relative to former experiments to accommodate the quality of the images as shown below:

Extract of the 'processing' program used:

```
'          Used for DNA standards DIC (9 December 04 - CB)
binary process clean 3
binary process holefill
binary dilate 1          'growth experiment 270505
binary erode 1           'growth experiment 270505
...
'          Original
'binary conditional thin 2      ' retain small spots
'binary process dilate 1      ' restore size
'binary process clean 4
'
'          Remove bumps on the larger features
'          Used for DNA standards (9 December 04 - CB)
'
binary store load          ' save original
binary feature interval 2
binary feature bsmooth     ' remove bumps
binary process clean
binary store swap          ' original back
'binary feature miss       ' remove processed features
```

```
'binary store or          ' and combine them
'binary plane store 0
'binary store load        ' save detected overlay
'image store retrieve      ' significant features remain
```

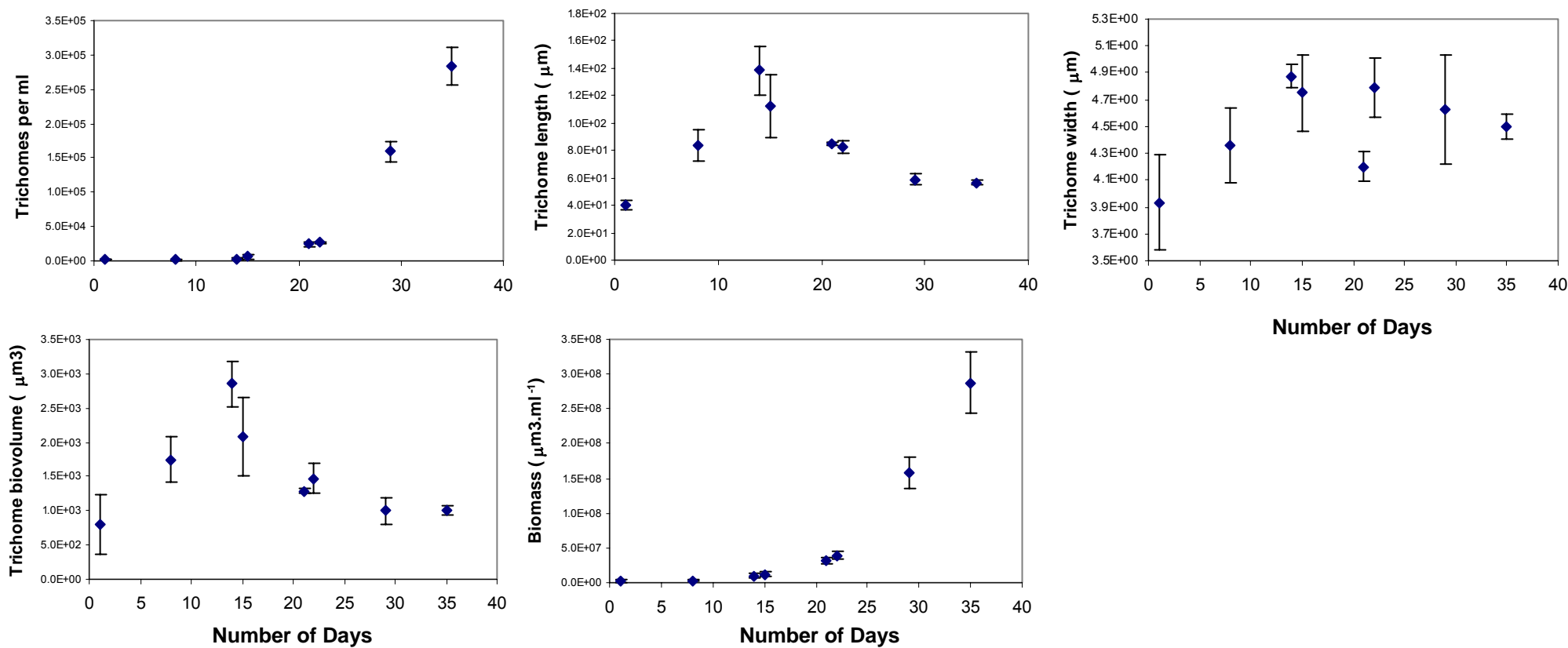
The main changes were relative to the number of cleaning, dilating and eroding steps, as well as to the removal of bumps (smoothing) on large objects, increasing the accuracy of parameters such as area and perimeter needed to calculate the fibre length and width (see above). The programs were tested on a subset of images until the discrimination was satisfactory.

Results

The speed at which data were acquired passed from 20 min for the first 4 curve points to 5 min towards the end when the number of trichomes in the culture became large. The number of trichomes analysed ranged from 279 on day 1 to 5866 on day 35.

The variations of the parameters measured during the study are shown Figure 4-8. The parameters followed the typical variations observed during a growth experiment with a lag phase followed by exponential growth (the plateau is not shown here). Although the number of trichomes per mL increased through time as well as the total biomass of *Cylindrospermopsis* per volume unit, the volume of individual trichomes through time follows a different pattern. The average volume of the trichomes increased during the lag phase to reach a maximum just as the trichome number and biomass entered exponential phase. From then, the volume of the trichomes decreased through time as their numbers increased. The changes in volume of individual trichomes were mainly due to changes in length, although the average width varied during the study, but without following the same trend. However, through time, it seems that the width of the trichome increased.

Figure 4.8. Morphometric parameters obtained for *Cylindrospermopsis raciborskii* during a 40 day growth experiment. Each point represents triplicate samples; each sample average data on at least 400 trichomes (except for the first 3 sample dates).



Discussion

The image analysis system again demonstrated its utility by rapidly obtaining enumeration and morphometric data on a very large number of trichomes (> 5000 for one sample). This allowed a more comprehensive study than previously attempted using conventional manual microscopy. For example, Hawkins et al. (2001) had to consider at least 50 trichomes during their study to keep the coefficient of variation of the mean population estimate to $\pm 28\%$ or less (Laslett et al. 1997). Moreover, many of the parameters taken into account by image analysis are generally not measured due to the difficulty of obtaining them and the variability observed between operators.

Morphometric data

There are not many studies on the morphometry of *Cylindrospermopsis* in the literature (e.g., Chonudomkul et al. 2004). The length and width of vegetative cells are known to change in the presence of an appropriate nitrogen source but more significantly with cell density. The width of cells corresponds to that of the trichomes and so we can therefore try to make a comparison with data from the literature. A progressive decrease in cell breadth from 5 μm in a nitrate-replete culture to 2.5 μm at stationary phase was observed by Hawkins et al. (2001). The accurate measurement of trichome width is important for the calculation of the biovolume of the trichome. Due to its relative small size compared to its length, errors leading to inaccuracy are easily made during the measurement of trichome width. It has been stated that the cell width of filamentous cyanobacteria is generally the most stable morphological characteristic (Campbell 1985), but it may vary between different populations (Komárek and Kling 1991) and so it is better to measure it for each new sample.

Both zooplankton activity and nutrient concentrations may affect cyanobacteria length distribution (see Hoogveld and Moed 1993). Another complication of the measurement of length is trichome curvature. Previously, there has only been one reported attempt at solving this problem (Hoogveld and Moed 1993). The IA system used herein has been able to readily measure both trichome width and length, the latter using the calculated fibre length as the length measurement to account for trichome curvature.

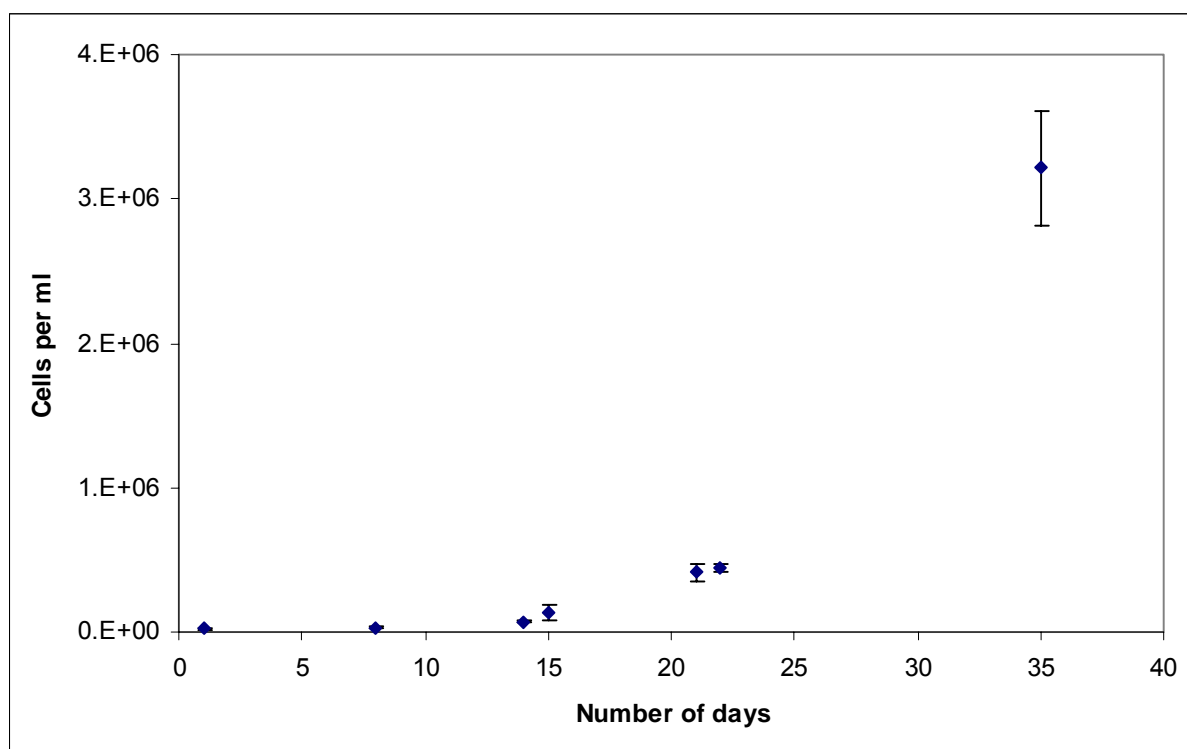
In our study, both the average width and length of trichomes increased during the lag phase, which is reflected in the increase of the biovolume of individual trichomes. When the exponential phase starts, the width plateaued while the length and the trichome biovolume decreased. The temperature and light were constant during the study but no new culture medium was added. While the biomass of *Cylindrospermopsis* was increasing, the availability in nutrients is likely to have decreased.

In McGregor and Fabbro (2000), measurements of the width of cells in straight trichomes were found between 2.0-3.2 μm , which were smaller than those recorded in this study, which range from 3.93 μm during the lag phase to a maximum of 4.87 μm at the beginning of the exponential phase. However, our results are in the range found by Chonudomkul et al. (2004), who reported cell widths varying from 1.9 μm to 6.3 μm . The length of filaments is not often reported in morphometric studies. We found that the average trichome length, at a quite low light intensity such as that of our growth experiment, diminished from 310 μm to around 250 μm . Changes in length have been found to be dependent upon cell division rates. Short filament lengths in cyanobacteria may be at least partially due to nutrient stress (Smith and Gilbert 1995). A somewhat similar growth pattern, in which mean filament length first increased and then declined as mean cell concentration increased, was also observed by Smith and Gilbert (1995) in both field and laboratory studies. One ecological benefit of shorter trichome length could be a reduced entanglement of trichomes. As the number of trichomes increases and the availability of light reduces in the culture vial, changes could occur in trichome morphometry to maximize light harvesting efficiency (Hawkins et al. 2001). The average trichome volume decreased from 2000 to 400 μm^3 as shorter trichomes (made up of smaller cells) gradually came to dominate the cultures (Hawkins et al. 2001). The same type of pattern was observed during this study.

Growth rate

Growth rate studies of *Cylindrospermopsis* and other cyanobacteria generally use cells per mL as the unit of measure. It is therefore difficult to directly compare our data with those found in the literature. However, if we consider an average cell length of 5 μm , we can try to extrapolate the number of cells from the data obtained on the average length and the number of trichomes (Figure 4-9).

Figure 4-9: Estimation of the concentration of cells of *Cylindrospermopsis raciborskii* during a growth experiment. The calculations were made estimating the average size of a cell at 5 μm (Baker 1991).



These results follow the same trend as the total biomass and trichome concentration, as they are related parameters. Calculations led to a growth rate of 0.146 day^{-1} and to a doubling time of 4.74 days. This growth rate is much lower than that of the maximum growth rates ($0.60\text{--}1.40 \text{ divisions day}^{-1}$) of pure cultures grown in the laboratory (Saker and Griffiths 2001). However, Regel and Brookes (2005) found growth rates ranging from 0.03 to 0.18 d^{-1} which were also substantially lower than previously reported in the literature. For straight forms, Saker et al. (1999) reported growth rates of 0.33 to 0.54 d^{-1} for irradiances between 6 and $433 \mu\text{mol photons.m}^{-2}.\text{s}^{-1}$. Positive growth was also reported by Briand et al. (2004) over light intensities ranging from $30\text{--}400 \mu\text{mol photons.m}^{-2}.\text{s}^{-1}$. Shafik et al. (1997) found a maximal growth rate at $30 \mu\text{mol photons.m}^{-2}.\text{s}^{-1}$, as in Regel and Brookes (2005). In our study, the light intensity was quite low (between 19.5 to $23.0 \mu\text{mol photons.m}^{-2}.\text{s}^{-1}$), which might explain the slow growth rate of the cultures.

4.3. Field experiments

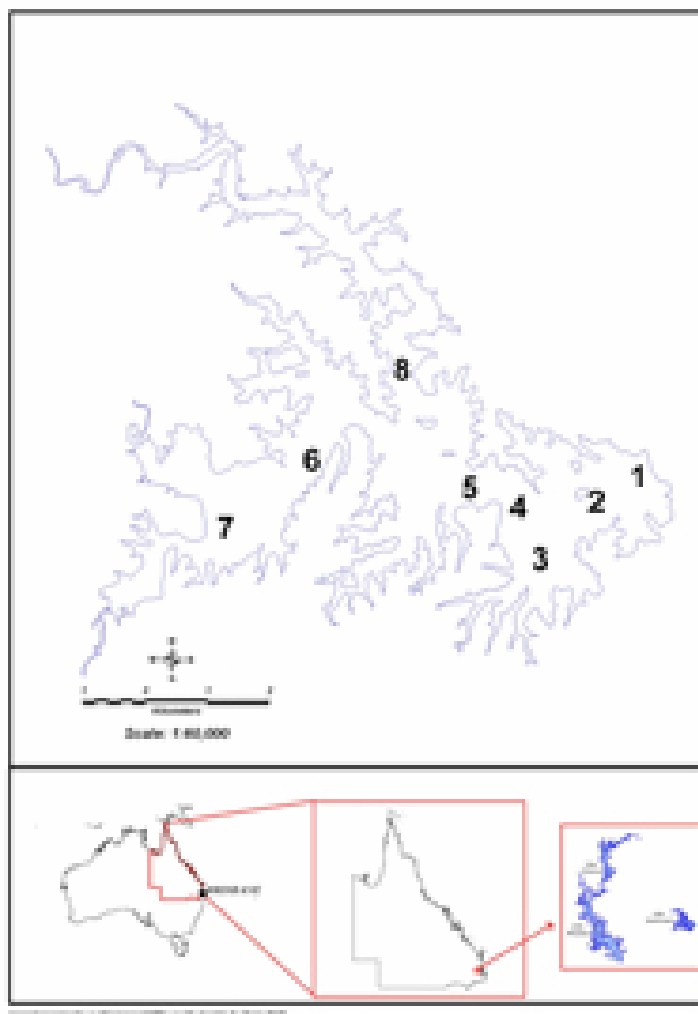
In the summer of 2005, samples from two consecutive field experiments during blooms of *Cylindrospermopsis raciborskii* in Queensland became available. The image analysis system was used to gather counts of trichomes as well as morphometric data. Data were compared with that obtained by classical microscopy.

4.3.1 Material and Methods

Two expeditions were organised during the summer of 2005 when blooms of *Cylindrospermopsis raciborskii* were present in the North Pine Dam and Lake Samsonvale (Queensland, Australia) (see Figure 4-10). These were part of a CRC project (2.3.0.4.) 'Early detection of cyanobacterial toxins using genetic methods'. Seven sites were chosen and samples from both the surface and different depths were carried out on two occasions in January and February 2005. Biological samples were taken with a Van Dorn sampler, at the same time environmental parameters such as conductivity, dissolved oxygen, pH and turbidity were recorded by using a Hydrolab sonde.

Figure 4-10: Map showing the location of the sites sampled during the blooms of *Cylindrospermopsis raciborskii* observed during the summer of 2005.

North Pine Dam / Lake Samsonvale



Samples from the surface were initially observed by microscopy at AWQC by an experienced biologist to determine the diversity of algae and cyanobacteria present in the samples (Table 4-2). *Cylindrospermopsis raciborskii* dominated the population and biomass.

Table 4-2: List of the genera of algae/cyanobacteria encountered, besides *Cylindrospermopsis raciborskii*, in the samples of North Pine Dam (Queensland) in January 2005. The genera have been listed by alphabetical order.

Anabaena circinalis
Anabaenopsis
Aphanizomenon
Aphanocapsa
Aphanocapsa
Aulacoseira
Crucigenia
Cryptomonas
Cyclotella
Dictyosphaerium
Glenodinium
Peridinium
Scenedesmus
Sphaerocystis
Staurastrum

The samples were fixed in Lugol's before being transported to AWQC, where they were kept at room temperature in the dark until further analysis. Depending on the sample density, either small or large Gene Frames were used to carry out the scan. In January, 37 samples were analysed. It took between 20-25 minutes to scan each slide. Four hundred images per slide were automatically acquired and saved. It took an average of 7 minutes to analyse them. In February, 23 samples were analysed. It took 40 minutes for each automatic scan of 800 images to be performed and 14 minutes to analyse each of them. On both occasions, morphometric data and the total biovolume of *C. raciborskii* were obtained. Thousands of trichomes were analysed.

The programs used to carry out the analyses were the same as those used in preceding chapters. The discrimination parameters (length, roundness and aspect) were determined using some of the first samples obtained to make sure the objects of interests were all taken into account. Of the other genera present in the samples, all but *Aphanizomenon* and *Aulacoseira* were automatically eliminated by the image analysis system on the ground of their trichome-like shape. *Aulacoseira* was eliminated from the analyses due to its width, which was close to 10 μm (limit of the system imposed was 7 μm). *Aphanizomenon* might have accidentally been counted by the image analysis system due to the similarity of their size and shape with that of *C. raciborskii*. However, their density in the samples was extremely low compared with that of *Cylindrospermopsis* and would have had made no statistical difference in the results obtained.

4.3.2 Results

The populations of *Cylindrospermopsis raciborskii* responsible for the blooms observed at North Pine Dam were mainly straight trichomes, although sometimes slightly curved ones were observed. Only partial data, relative to site 3, are going to be shown below. The results obtained in January were representative of a quite homogeneous environment. The biovolume, length and width of the trichomes were not showing great variations between sites or at one site between the different depths sampled (Figure 4-8). No correlation was found between the distribution of *C. raciborskii* and environmental parameters. The whole dam was quite well mixed during the event. Morphometric data did not show large variations either (see Figure 4-8): at site 3, the average biovolume per trichome varied from 785 μm^3 at 2 m to 1230 μm^3 at 1 m and the average width varied from 3.64 μm at 5 m to 4.07 μm at 10 m.

A comparison of the results obtained by traditional microscopy and by the image analysis system is presented in Table 4-3 for the surface samples. The results obtained by traditional microscopy were obtained counting cells in 15 trichomes. We considered an average cell size of 5 μm as in the previous chapter when estimating cell numbers from trichome length data. The results were very much comparable, the largest difference being observed at site 6, but these differences were smaller than those observed generally between operators (see Chapter 3.2.2).

Figure 4-11: Example of data on *Cylindrospermopsis raciborskii* obtained at site 3 during the first expedition (11 January 2005) to North Pine Dam (Queensland). It shows a mixed environment and the homogeneity of the data.

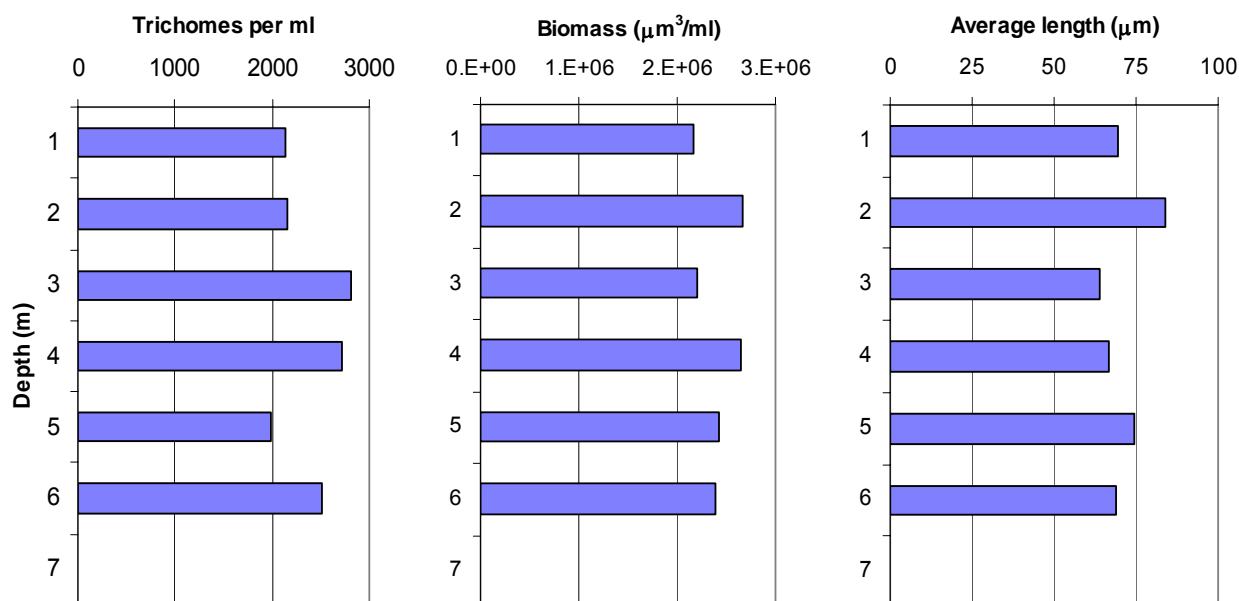
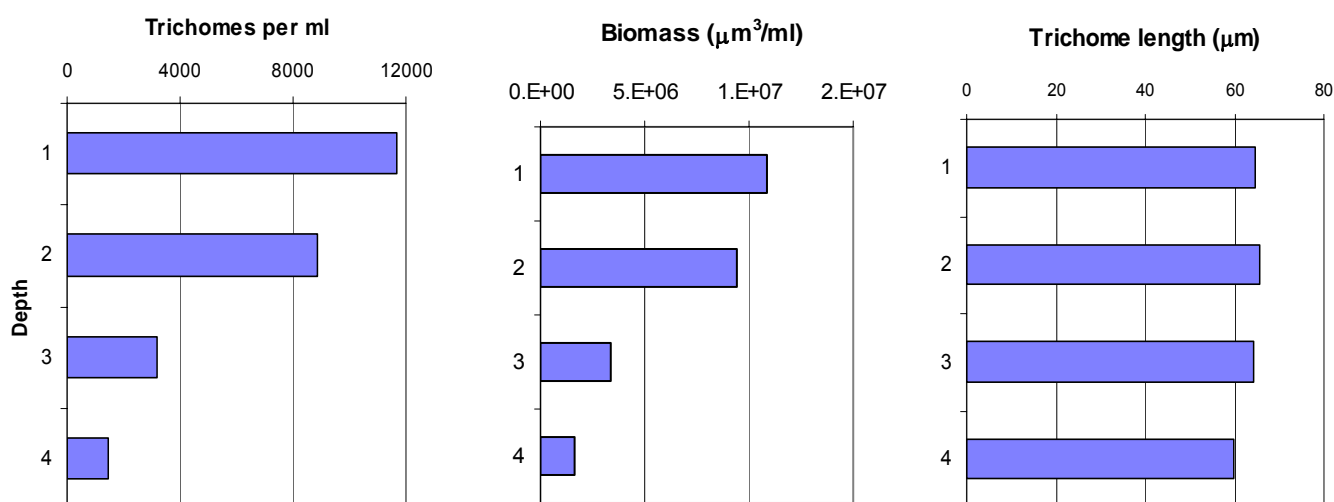


Table 4-3: Comparison of results obtained via manual counting and via image analysis at the surface of North Pine dam (January 2005) for all the sites sampled.

	Site 1	Site 2	Site 3	Site 4	Site 5	Site 6	Site 7
Cells.mL⁻¹ (Visual)	n/a	27607	27950	57855	73670	71290	73625
Cells.trichomes⁻¹ (mean of 15 trichomes)	12	13	14	12	15	13	15
Cells.mL⁻¹ (calculated from IA)	29816	23721	29604	55227	69627	55997	82621

A month later, on the 11th of February, the data suggested that a more stratified environment was present at all sites. Not as many depths were sampled compared with the first field trip in January. All sites but site 1 showed strong stratification. However, for example at site 3, although the number of trichomes per mL varied greatly between the surface and particular depths (5-8 m), the average biovolume per trichome remained quite constant ($933 \mu\text{m}^3$ at the surface to $1107 \mu\text{m}^3$ at 8 m), as did the average length (Figure 4-9) and width ($4.00 \mu\text{m}$ at 0 m to $4.32 \mu\text{m}$ at 8 m) of the trichomes. Figure 4-9 shows the results obtained for site 3.

Figure 4-12: Example of data obtained for *Cylindrospermopsis raciborskii* at site 3 during the second expedition (11 February 2005) to North Pine Dam.



At site 3, the number of trichomes per mL decreased greatly between the surface (11667 trichomes.mL⁻¹) and 8 m (1468 trichomes.mL⁻¹), as did the total biomass. However, the average volume of individual trichome showed an increase between the surface (933 μm^3) and 8 m (1107 μm^3). This was due to an increase in the width of the trichomes (4.00 μm to 4.32 μm).

4.3.3 Discussion

The image analysis system, as used in this field study, showed that it was possible to rapidly and reliably obtain a large amount of data on morphometric parameters of *Cylindrospermopsis raciborskii*, giving insights into the ecology of organisms. The results were very different between January and February, with a large surface/subsurface bloom developing by February where the concentration of the trichomes ranged from 1125 per mL at 8 m (site 5) to 14946 at the surface (site 6).

If we assume an average number of 13 cells per trichome (see above), the concentrations of *C. raciborskii* encountered during this study were ranging from 14625 to 194298 cells per mL, or > 2 mm³ per litre. These correspond to a Level 2 alert for *Cylindrospermopsis* (Burch et al. 2003), and are in the order of biomass found during blooms studied in Queensland (see McGregor and Fabbro 2000). In Lake Julius (Queensland), Saker and Griffiths (2001) also recorded cell concentrations which corresponded approximately to 14 cells per trichome. However, assuming a constant average number of cells per trichome is not always reliable. First, the number of cells per trichome is very difficult to estimate and second, the natural variation in the number of cells per trichome should be taken into account. In the more stratified environment, biometry parameters of the trichomes seem more stable irrespective of the depth and the amount of light.

There are few published studies available with which to compare our results, but all were carried out in Queensland. However, very few details are given on the morphometric parameters and if some data are presented, no explanations are given relative to the way that they have been obtained (e.g., Fabbro and Duivenvoorden 1996). These last authors studied a bloom of *Cylindrospermopsis* in central Queensland with cell densities (15000 cells.mL⁻¹) corresponding more to those found in January here. They found that the number of trichomes was significantly increasing towards the surface. This was observed in our study during the February study and can be explained by the amount of light available. In January, the euphotic zone was above ca. 5 m while it was at 2.7 m in February, corresponding to the layers into which the bloom was located. McGregor and Fabbro (2000) also observed that strongly stratified waters, as we had in February, lead to the highest concentrations of cells.

Despite the different light and bloom conditions between January and February, the length of trichomes was less variable when the stratification was more marked (63.61 \pm 2.61 μm) than when the waters were well mixed as in January (71.10 \pm 7.10 μm). The width of the trichomes was comparable with 4.165 \pm 0.132 μm in January and 3.826 \pm 0.158 μm in February. This could be explained by a more uniform physiological stage of the trichomes during a well marked bloom

(February) compared with the situation of a well-mixed environment and low densities with trichomes probably at different stages of their growth (see results from growth experiment above). The trichome length of *Cylindrospermopsis raciborskii* was shown to change in response to light intensity in culture controlled conditions (Regel and Brookes 2005; see above).

4.4 Discussion and Conclusion

This study is the first to successfully use automatic acquisition of data from monocultures and natural samples of *Cylindrospermopsis raciborskii*, allowing enumeration and measurement of trichomes of a defined species. The large amount of data obtained and their statistical strength allowed insights into the morphometric changes of *Cylindrospermopsis raciborskii* both in cultures and in natural environments, and so into its ecology. This is important when considering the potential toxicity of this species.

Moreover, with trichomes such as those of *Cylindrospermopsis*, which even when said to be straight are often slightly bent, the measurement of the trichome length cannot be accurately achieved with an ocular micrometer. The programs written in this study, using the area and perimeter of the objects to calculate the fibre length and width, give a real advantage by providing more accurate results. This remark is extended to the calculation of total biomass in water from a much larger number of cells than when data are acquired manually. The guidelines are more and more giving alert levels in volume per volume unit, which, considering the relation between cell volume and toxin production, makes results in biomass more reliable. As we observed during this study and as it has been noted previously elsewhere (Bouaïcha and Nasri 2004), there is inherent difficulty in seeing the septa between vegetative cells, making it difficult to count them accurately and reproducibly, especially when multiple operators are involved. This reinforces the importance of using more robust measures such as biomass or biovolume when setting response triggers for toxic algae.

The results obtained with the image analysis system allowed us, for example, to conduct a detailed study of the different morphometric parameters of *C. raciborskii* in both cultures and in natural environments. As already observed by McGregor and Fabbro (2000), we also remarked that the width of cells in environmental samples were typically narrower than those of cultured cells: $3.94 \pm 0.36 \mu\text{m}$ to $4.87 \pm 0.09 \mu\text{m}$ in cultures compared with $3.83 \pm 0.16 \mu\text{m}$ to $4.16 \pm 0.13 \mu\text{m}$ in North Pine Dam. This may be a morphological indicator of the lower nutrient concentration in natural waters compared to culture media. Brookes et al. (1999) measured the Greatest Axial Linear Dimension (GALD) of *Anabaena circinalis* and showed that it was increasing with decreasing irradiance. The increase was due to aggregation of filaments in low light intensities. This supports a theory that filament aggregation may be a strategy to increase light exposure. Regel and Brookes (2005) found that trichomes of *C. raciborskii* were longer in low light which gave them a faster floating or sinking velocity. This may act to move trichomes away from high light to low light or conversely from darkness to low light. This was also noticeable in the work done in chapter 4.2.2. However, in natural habitats, the variations were not as clear.

5. Discussion

Noxious cyanobacteria are important to the water industry due to their potential impact on the quality of drinking and recreational waters (Falconer 2001). The water industry still relies on routine sampling and direct observation of water samples to determine the identity and the concentration of potentially toxic algae and cyanobacteria (Burch et al. 2003). These tasks require expertise and are quite time consuming. Moreover, the quality and accuracy of the results are impeded by inherent errors during enumeration and by the subjectivity of the operator. New, more efficient techniques, which could be rapid, inexpensive and user-friendly are required to improve the operation of routine water testing laboratories.

Image analysis, which was first developed in the 1950's, offers analytical laboratories a technique that is similar to microscopy currently in use. Although, image analysis has been well developed and is used routinely in pathology laboratories, for example with customized hardware and softwares (e.g., LifeSpan, Inc.), and in limnology and marine laboratories for research purposes (see Mueller et al. 2004), not many attempts have been made to develop a system dedicated to be used extensively in water analytical laboratories. Few projects have tried to make automation of counting and measurement of algae available to a broader audience. Algamica (Gosselain et al. 2000) was developed in the early 1980's, and was aiming to provide a user-friendly system to assist people with counting and calculating the biovolume of a large range of microplanktonic algae. However, this is not an image analysis system and is rather a utility to aid microscopists with data recording (the number of particular species and any measurements) and allows automated calculation of biovolumes for particular species based on predefined shapes.

Some studies have especially focussed on developing image analysis systems for cyanobacteria: Walsby and Avery (1996) developed a system that allowed the measurement of the total length of trichomes after transfer of filamentous cyanobacteria on filters. Each image had to be treated individually. A few years later, Congestri et al. (2000) published a system to measure individual filaments, but manual intervention on each image was necessary to alleviate the problems caused by the curvature of the filaments. Due to the difficulty of counting cells in a colony, there has only been one report tackling colonial genera such as *Microcystis* to measure the size of the colonies (Ishikawa et al. 2004).

This study is the first to have successfully customized an automated image analysis system to simultaneously acquire data on the density and the morphometry of two morphological types of cyanobacteria: *Microcystis* spp. (round/ellipsoid) and *Cylindrospermopsis raciborskii* (with straight/curved trichomes). The results showed that the programs developed are robust and solved problems such as separation of joining cells for *Microcystis* and counting of overlapping trichomes for *Cylindrospermopsis*. The criteria used for discriminating the objects of interest from background noise using morphometric parameters was also quite successful, with the exception of the case of *Microcystis* when using DIC optics with samples of low cell density but many artefacts (small, round) present. A way to alleviate this problem would be to scan the samples using higher magnification, but this would slow down the process. The use of fluorescence for counting *Microcystis* was revealed to be the most promising avenue. It would, however, be difficult to compare the results obtained with those from routine laboratories as fluorescence would only count living cells, or cells with pigments, instead of the classic live and dead cells. Fluorescence cannot easily be used when measurements are needed as a halo is present around the cells and additional processing steps would need to be taken to account for this in the measurement of the cell.

We showed that we could use our image analysis system for cultured organisms as well as organisms from natural samples. Each time a new type of sample is analysed however, the parameters of discrimination have to be tested and modified as required, necessitating the presence of someone with sufficient familiarity with the software to modify the programs accordingly. The help of a taxonomist is also required when the identity of a species has to be confirmed in a natural sample. The system, when set-up, appeared to be user-friendly and very little training was required to enable operators to acquire and analyse data.

The competitiveness of the image analysis system appeared to be maximum for its speed of operation, once the system was set-up for a particular type of sample, especially to measure cells but also to count samples of medium to high concentration. The quality and reproducibility of the data, acquired without any bias or subjectivity, are a huge advantage of the image analysis system

(Schröder and Krambeck 1991). A wider usage of the image analysis system, once calibrated, could allow for better comparisons between operators and laboratories.

Besides a clear advantage in the quality and quantity of data acquired, the type of data that can be easily acquired with the image analysis system is also important. This study showed that considering cells of *Microcystis* as ellipsoid instead of as a sphere led to more accurate calculations of biovolume. additionally, the ability of being able to measure the full length of trichomes following their curvature gave a better estimate of biovolume. More reliable methods for estimating biovolume will provide a more realistic way of setting alert levels since the toxin contents of cyanobacteria species is dependent of the physiological stage of the cells and thus of their volume (Burch et al. 2003). Such data, acquired during experiments, allowed an insight into the ecology of the organisms, such as insights into the relationship between light and trichome length.

6. Recommendations

Image analysis efficiency and advantages

The image analysis project revealed the potential of a customized and automatic system to rapidly measure the size and biovolume of ovoid and straight – curved filamentous cyanobacteria. It is the first time that such a system has been applied to automatically enumerate and measure two types of cyanobacteria from both cultures and environmental samples. The results obtained were comparable if not better in some instances with those obtained with the traditional microscopy method. The analysis system relieves the operators from biases resulting from fatigue and subjectivity. The speed due to automation of the system makes the acquisition and the analysis of the data carried out as well as the amount of data that can be acquired extremely competitive. Usage of such an image analysis system allows uniformity of the protocols and allows for comparisons of data between operators and laboratories.

Incorporation of biovolume into Guidelines

The image analysis system allows the simple acquisition of morphometric data, such as the length of trichomes and the accurate calculation of cell or trichome biovolume, which would be difficult and extremely labour intensive to gather using manual techniques such as classical microscopy. This is very important when considering that guidelines are based on cell densities and that it is difficult to accurately count the number of cells within trichomes. Moreover, the biovolume of trichomes, and presumably the level of risk of bloom toxicity, changes in response to physiological conditions and so we advocate the common usage of biovolume instead of cell numbers in the Guidelines. The same applies to ellipsoid-shaped cyanobacteria such as *Microcystis*, which can vary in size and shape (they are not spherical as assumed in traditional biovolume calculations), especially for cells undergoing cell division. The necessity of measuring two dimensions instead of one to accurately calculate cell or trichome biovolume was highlighted during this study, especially when comparing data obtained between different operators and between different laboratories.

Future directions

The image analysis system provides a research tool that can be used to assist with the collection of large amounts of data, which would not have been previously possible to readily obtain, for the study of the ecology and management of cyanobacteria. In addition, the system will provide a tool to assist laboratory analysts to more readily measure sample biovolume. However, the system is currently limited in its application and additional work is required in the following areas:

- Technology transfer is required for the use of the image analysis system
 - The system is currently not simple or “idiot” proof and requires a degree of understanding / expertise to use.
- Validation is required for the measurement of species other than those examined in this report. This may require new approaches to measure different shapes.
- Research is required to solve the problems associated with the measurement of coiled species (largely related to the measurement of coiled trichomes which exist in different focal planes).
- The system has limited utility for discrimination of similar shaped species. Additional research would be required to allow this (e.g. molecular probes would allow the definitive identification of a particular species).
- The system performed poorly for samples with low cell densities. Additional research is required to validate the use of concentration techniques, fluorescence and the rapid scan. Methods for processing fluorescence images are required to allow more accurate measurement of cell dimensions (or counting should be conducted under fluorescence and dimensions could then be measured under phase contrast or DIC).

7. Acknowledgements

The authors would like to thank Lynn Jarvis, Caroline Fazekas, Peter Hobson, Daniel Hoefel, Paul Rasmussen and the staff of the Biology laboratory at AWQC for their advice and technical assistance.

8. References

- Amaral, A.L., da Motta, M., Pons, M.N., Vivier, H., Roche, N., Mota, M. and Ferreira, E.C. (2004) Survey of Protozoa and Metazoa populations in wastewater treatment plants by image analysis and discriminant analysis. *Environmetrics* **15**, 381-390.
- Amaral, A.L., Baptiste, C., Pons, M.N., Nicolau, A., Lima, N., Ferreira, E.C., Mota, M. and Vivier, H. (1999) Semi-automated recognition of protozoa by image analysis. *Biotechnology Techniques* **13**, 111-118.
- Anonymous (2003) Blue-green algae (Cyanobacteria) in inland waters: Assessment and control of risks to Public Health – Compiled by the Scottish Executive Health Department – Blue Green Algae Working Group, Scottish Executive Health Department, 47 pp.
- Andreatta, S., Wallinger, M.M., Piera, J., Catalan, J., Psenner, R., Hofer, J.S. and Sommaruga, R. (2004) Tools for discrimination and analysis of lake bacterioplankton subgroups measured by flow cytometry in a high-resolution depth profile. *Aquatic Microbial Ecology* **36**: 107-115.
- Azevedo, S.M.F.O. (1996) Toxic cyanobacteria and the Caruaru tragedy. *Proceedings of the IV symposium of the Brazilian Society of Toxicology* **83**.
- Baker, P. (1991) Identification of common noxious cyanobacteria. Part 1 – *Nostocales*. UWRRA Research Report No. 29, Urban Water Research Association of Australia, Melbourne.
- Baker, P. (1992) Identification of common noxious cyanobacteria. Part II - *Chroococcales* and *Oscillatoriales*. Urban Water Research Association of Australia. Research Report No. 46.
- Baker, P.D., Steffensen, D.A., Humpage, A.R., Nicholson, B.C., Falconer, I.R., Lanthois, B., Fergusson, K.M. and Saint, C.P. (2001) Preliminary evidence of toxicity associated with the benthic cyanobacterium *Phormidium* in South Australia. *Environmental Toxicology* **16**, 506-511.
- Baker, P.D. and Fabbro, L.D. (2002) A guide to the identification of common blue-green algae (Cyanoprokaryotes) in Australian Freshwaters. Identification & Ecology Guide No. 25. Cooperative Research Centre for Freshwater Ecology, Ellis Street, Thurgoona, NSW, Australia.
- Bartram, J., Burch, M., Falconer, I. R., Jones, G. and Kuiper-Goodman, T. (1999) Situation Assessment, Planning and Management. pp 179-209 in *Toxic Cyanobacteria in Water. A guide to their public health consequences, monitoring and management*. Eds. I. Chorus and J. Bartram. 1999. E&FN Spon, London.
- Bellinger, E.G. (1974) A note on the use of algal sizes in estimates of population standing crop. *British Phycology Journal*
- Bjørnsen, P.J. (1989) Automatic determination of bacterioplankton biomass by image analysis. *Applied Environmental Microbiology* **51**, 1199-1204.
- Blackburn, N., Hagström, Å., Wikner, J., Cuadros-Hansson, R. and Bjørnsen, P.K. (1998) Rapid determination of bacterial abundance, biovolume, morphology, and growth by Neural Network-Based image analysis. *Applied and Environmental Microbiology* **64**, 3246-3255.
- Bláha, L., Sabater, S., Babica, P., Vilalta, E. and Mařálek, B. (2004) Geosmin occurrence in riverine cyanobacterial mats: is it causing a significant health hazard? *Water Science and Technology* **49**, 307-312.
- Bloem, J., Veninga, M. and Shepherd, J. (1995) Fully automatic determination of soil bacterium numbers, cell volumes, and frequencies of dividing cells by confocal laser scanning microscopy and image analysis. *Applied and Environmental Microbiology* **61**, 926-936.
- Bobrow, M.N.T., Harris, T.D., Shaughnessy, K.J. and Litt, G.J. (1989) Catalyzed reporter deposition, a novel method of signal amplification – II application to immunoassays. *Journal of Immunological Methods* **125**, 279-285.
- Borics, G., Grigorzi, I., Szabo, S. and Padisák, J. (2000) Phytoplankton associations under changing pattern of bottom-up vs. top-down control in a small hypertrophic fishpond in East Hungary. *Hydrobiologia* **424**, 79-90.
- Bouaïcha, N. and Nasri, A.-B. (2004) First report of cyanobacterium *Cylindrospermopsis raciborskii* from Algerian freshwaters. *Environmental Toxicology* **19**: 541-543.
- Boulos, L., Prevost, M., Barbeau, B., Coallier, J. and Desjardins, R. (1999) LIVE/DEAD® BacLight™: application of a new rapid staining method for direct enumeration of viable and total bacteria in drinking water. *Journal of Microbiological Methods* **37**, 77-86.
- Bouvy, M., Falcão, D., Marinho, M., Pagano, M. and Moura, A. (2000) Occurrence of *Cylindrospermopsis* (Cyanobacteria) in 39 Brazilian tropical reservoirs during the 1998 drought. *Aquatic Microbial Ecology* **23**, 13-27.

- Bouvy, M., Pagano, M. and Trousselier, M. (2001) Effects of a cyanobacteria bloom (*Cylindrospermopsis raciborskii*) on bacteria and zooplankton communities in Ingazeira reservoir (northeast Brazil). *Aquatic Microbial Ecology* **25**, 215-227.
- Box, J.D. (1981) Enumeration of cell concentrations in suspensions of colonial freshwater microalgae, with particular reference to *Microcystis aeruginosa*. *British Phycological Journal* **16**, 153-164.
- Briand, J.-F., Leboulanger, C., Humbert, J.-F., Bernard, C. and Dufour, P. (2004) *Cylindrospermopsis raciborskii* (Cyanobacteria) invasion at mid-latitudes: selection, wide physiological tolerance, or global warming? *Journal of Phycology* **40**, 231-238.
- Brookes, J.D., Ganf, G.G., Green, D. and Whittington, J. (1999) The influence of light and nutrients on buoyancy, filament aggregation and flotation of *Anabaena circinalis*. *Journal of Plankton Research* **21**, 327-341.
- Bruchet, A. and Duguet, J.P. (2004) Role of oxidants and disinfectants on the removal, masking and generation of tastes and odours. *Water Science and Technology* **49**, 297-306.
- Burch, M.D., Harvey, F.L., Baker, P.D. and Jones, G.J. (2003) National protocol for the monitoring of cyanobacteria and their toxins in surface waters. *ARMCANZ National Algal Management Report*, 73 pp.
- Campbell, S.E. (1985) '*Oscillatoria limnetica*' from Solar Lake, Sinai, is a *Phormidium* (Cyanophyta or Cyanobacteria). *Archiv fur Hydrobiology, Supplement* **71**, 175-190.
- Carmichael, W.W. (1992) A status report on planktonic cyanobacteria (blue-green algae) and their toxins. US Environmental Protection Agency, Cincinnati, USA.
- Carmichael, W.W. and Gorham, P.R. (1974) An improved method for obtaining axenic clones of planktonic blue-green algae. *Journal of Phycology* **10**, 238-240.
- Chonudomkul, D., Yongmanitchai, W., Theeragool, G., Masanobu, K., Kasai, F., Kaya, K. and Watanabe, M.M. (2004) Morphology, genetic diversity, temperature tolerance and toxicity of *Cylindrospermopsis raciborskii* (Nostocales, cyanobacteria) strains from Thailand and Japan. *FEMS Microbial Ecology* **48**: 345-355.
- Congestri, R., Federici, R. and Albertano, P. (2000) Evaluating biomass of Baltic filamentous cyanobacteria by image analysis. *Aquatic Microbial Ecology* **22**, 283-290.
- Congestri, R., Federici, R. and Albertano, P. (2003) Morphometric variability of the genus *Nodularia* (Cyanobacteria) in Baltic natural communities. *Aquatic Microbial Ecology* **22**, 283-290.
- Contreras, E.M., Giannuzzi, L. and Zaritzky, N.E. (2004) Use of image analysis in the study of competition between filamentous and non-filamentous bacteria. *Water Research* **38**, 2621-2630.
- Culverhouse, P.F., Herry, V., Reguera, B., S. González-Gil, S., Williams, R., Fonda, S., Cabrini, M., Parisini, T. and Ellis, R. (2001) Dinoflagellate Categorisation by Artificial Neural Network (DICANN). In: Harmful Algal Blooms. Hallegraeff, G., Blackburn, S., Lewis, R. and Bolch, C. (eds.). Intergovernmental Oceanographic Commission of UNESCO, pp. 195-198.
- Da Motta, M., Pons, M.N., Vivier, H., Amaral, A.L., Ferreira, E.C., Roche, N., Mota, M. (2001) The study of protozoa population in wastewater treatment plants by image analysis. *Brazilian Journal of Chemical Engineering* **18**, 103-111.
- Daims, H., Ramsing, N.B., Schleifer, K.H. and Wagner, M. (2001) Cultivation-independent, semiautomatic determination of absolute bacterial cell numbers in environmental samples by fluorescence in situ hybridization. *Applied and Environmental Microbiology* **67**, 5810-5818.
- Duguet, J.P., Mallevalle, J., Ho, J. and Suffet, I.H. (1995) Oxidation processes chlorine and chloramines. In: *Advances in Taste-and-Odor Treatment and Control*, I.H. Suffet, J. Mallevalle, Elizabeth Kawczynski (ed.), AWWARF-Lyonnaise des Eaux **3**, 75-113.
- Estep, K.W. and MacIntyre, F. (1989) Counting, sizing, and identification of algae using image analysis. *Sarsia* **74**, 261-268.
- Fabbro, L.D. and Duivenvoorden, L.J. (1996) Profile of a bloom of the cyanobacterium *Cylindrospermopsis raciborskii* (Woloszynska) Seenaya and Subba Raju in the Fitzroy river in Tropical Central Queensland. *Marine and Freshwater Research* **47**, 685-694.
- Falconer, I.R. (2001) Toxic cyanobacterial bloom problems in Australian waters: risks and impact on human health. *Phycologia* **40**, 228-233.
- Falconer, I.R., Burch, M.D., Steffensen, D.A., Choice, M. and Coverdale, O.R. (1994) Toxicity of the blue-green alga (Cyanobacterium) *Microcystis aeruginosa* in drinking water to growing pigs, as an animal model for human injury and risk assessment. *Environmental Toxicity and Water Quality* **9**, 131-139.

- Falconer, I., Bartram, J., Chorus, I., Kuiper-Goodman, T., Utkilen, H., Burch, M. and Codd, G.A. (1999) "Safe Levels and Safe Practices". Toxic Cyanobacteria in Water. A Guide to their Public Health Consequences, Monitoring and Management. Eds. Chorus I. and Bartram J., 155-178.
- Fuchs, B.M., Glöckner, F.O., Wulf, J. and Amann, R. (2000) Unlabeled helper oligonucleotides increase the in situ accessibility to 16S rRNA of fluorescently labelled oligonucleotide probes. *Applied and Environmental Microbiology* **66**, 3603-3607.
- Gagné, F., Ridal, J., Blaise, C. and Brownlee, B. (1999) Toxicological effects of geosmin and 2-methylisoborneol on rainbow trout hepatocytes. *Bulletin of Environmental and Contamination Toxicology* **63**, 174-180.
- Gaston K.J. and O'Neill, M.A. (2004) Automated species identification: why not? *Philosophical Transactions of the Royal Society in London* **359**, 655-667.
- Gilbert, J.J. (1996) Effects of food availability on the response of planktonic rotifers to a toxic strain of the cyanobacterium *Anabaena flos-aquae*. *Limnology and Oceanography* **42**, 1565-1572.
- Glasbey C.A. and Horgan, G.W. (1995) Image analysis for the biological sciences. Wiley, Chichester.
- Gliwicz, Z.M. and Lampert, W. (1990) Food thresholds in *Daphnia* species in the absence and presence of blue-green filaments. *Ecology* **71**, 691-702.
- Gorham, P.R., McLachlan, J., Hammer, U.T. and Kim, W.K. (1964) Isolation and culture of toxins strains of *Anabaena flos-aquae* (Lyngb.) de Breb. *Vereinigung für Theoretische und Angewandte Limnologie* **15**, 796-804.
- Gosselain, V., Hamilton, P.B. and Descy, J.-P. (2000) Estimating phytoplankton carbon from microscopic counts: an application for riverine systems. *Hydrobiologia* **438**, 75-90.
- Gragani, A., Scheffer, M. and Rinaldi, S. (1999) Top-down control of cyanobacteria: a theoretical analysis. *American Naturalist* **153**, 59-72.
- Hall, S.J., Keller, J. and Blackall, L.L. (2003) Microbial quantification in activated sludge: the hits and misses. *Water Science and Technology* **48**, 121-126.
- Hallegraeff, G.M. (1977) A comparison of different methods used for the quantitative evaluation of biomass of freshwater phytoplankton. *Hydrobiologia* **55**, 145-165.
- Hand D.J. 1981. Discrimination and classification, Wiley, USA.
- Hanninen, O., Ruuskanen, J.I. and Oksanen, J. (1993) A method for facilitating the use of algae growing on tree trunks as bioindicators of air quality. *Environmental Monitoring and Assessment* **28**, 215.
- Hašler, P. and Pouličková, A. (2003) Diurnal changes in vertical distribution and morphology of a natural population of *Planktothrix agardhii* (Gom.) Anagnostidis et Komarek (Cyanobacteria). *Hydrobiologia* **506**, 195-201.
- Hawkins, P.R. and Lampert, W. (1989) The effect of *Daphnia* body size on filtering rate inhibition in the presence of a filamentous cyanobacterium. *Limnology and Oceanography* **34**, 1084-1089.
- Hawkins, P.R., Runnegar, M.T.C., Jackson, A.R.B. and Falconer, I. (1985) Severe hepatotoxicity caused by the tropical cyanobacterium (blue-green alga) *Cylindrospermopsis raciborskii* (Woloszynska) Seenaya and Subba Raju isolated from a domestic supply reservoir. *Applied and Environmental Microbiology* **50**, 1292-1295.
- Hawkins, P.R., Putt, E., Falconer, I. and Humpage, A. (2001) Phenotypical variation in a toxic strain of the phytoplankton, *Cylindrospermopsis raciborskii* (Nostocales, Cyanophyceae) during batch culture. *Environmental Toxicology* **16**, 460-467.
- Hawkins, P.R., Chandrasena, N.R., Jones, G.J., Humpage, A.R. and Falconer, I.R. (1997) Isolation and toxicity of *Cylindrospermopsis raciborskii* from an ornamental lake. *Toxicon* **35**, 341-346.
- Hillebrand, H., Dürselen, C.-D., Kirschtel, D., Pollinger, U. and Zohary, T. (1999) Biovolume calculation for pelagic and benthic microalgae. *Journal of Phycology* **35**, 403-424.
- Holt, J.G., Krieg N.R., Sneath, P.H.A., Staley, J.T. and Williams, S.T. (1994) Group 11. Oxygenic phototrophic bacteria. In Hensyl, W.R. (ed), *Bergey's Manual of Determinative Bacteriology*, 9th ed., Williams & Wilkins, Baltimore, pp. 377-425.
- Hoogveld, H.L. and Moed, J.R. (1993) A digitising tablet for determining the length distribution of filamentous cyanobacteria. *European Journal of Phycology* **28**, 59-61.
- Hötzl, G. and Croome, R. (1999) A Phytoplankton Methods Manual for Australian Freshwaters. Land and Water Resources Research and Development Corporation, Canberra, Australia.
- Humpage, A.R., Fenech, M., Thomas, P. and Falconer, I.R. (2000) Micronucleus induction and chromosome loss in transformed human white cells indicate clastogenic and aneugenic action of the cyanobacteria toxin, cylindrospermopsin. *Mutation Research* **472**, 155-161.

- Humphries, S.E. and Widjaja, F. (1979) A simple method for separating cells of *Microcystis aeruginosa* for counting. *British phycological Journal* **14**, 313-316.
- Ishikawa, K., Walker, R.F., Tsujimura, S., Nakahara, H. and Kumagai, M. (2004) Estimation of *Microcystis* colony size in developing water blooms via image analysis. *Journal of Japan Society on Water Environment* **27**, 69-72.
- Izaguirre, G. and Taylor, W.D. (2004) A guide to geosmin- and MIB-producing cyanobacteria in the United States. *Water Science and Technology* **49**, 19-24.
- John, U., Cembella, A., Hummert, C., Elbrächter, M., Groben, R. and Medlin, L. (2003) Discrimination of the toxigenic dinoflagellates *Alexandrium tamarense* and *A. ostenfeldii* in co-occurring natural populations from Scottish coastal waters. *European Journal of Phycology* **38**, 1: 25-40.
- Kirchman D, Sigda J, Kapuscinski R, Mitchell R: (1982) Statistical analysis of the direct count method for enumerating bacteria. *Appl Environ Microbiol*, **44**(2):376-382.
- Komárek, J. and Kling, H. (1991) Variation in six planktonic cyanophyte genera in Lake Victoria (East Africa). *Algological Studies* **61**, 21-45.
- Korber, D.R., Lawrence, J.R., Cooksey, K.E., Cooksey, B. and Caldwell, D.E. (1989) Computer image analysis of diatom chemotaxis. *Binary – Computing in Microbiology* **1**, 155-168.
- Kurmayer, R. and Kutzenberg, T. (2003) Application of real-time PCR for quantification of microcystin genotypes in a population of the toxic cyanobacterium *Microcystis* sp. *Applied and Environmental Microbiology* **69**, 6723-6730.
- Kurmayer, R., Christiansen, G. and Chorus, I. (2003) The abundance of microcystin-producing genotypes correlates positively with colony size in *Microcystis* sp. And determines its microcystin net production in Lake Wannsee. *Applied and Environmental Microbiology* **69**, 787-795.
- Lagos, N., Onodera, H., Zagatto, P.A., Andrinolo, D., Azevedo, S.F.M.O. and Oshima, Y. (1999) The first evidence of paralytic shellfish toxins in the freshwater cyanobacterium *Cylindrospermopsis raciborskii*, isolated from Brazil. *Toxicon* **37**, 1359-1373.
- Laslett, G., Clark, R. and Jones, G. (1997) Estimating the precision of filamentous blue-green algae cell concentration from a single sample. *Environmetrics* **8**, 313-340.
- Lawton, L., Marsalek, B., Padisak, J. and Chorus, I. (1999) "Determination of Cyanobacteria in the Laboratory." Toxic Cyanobacteria in Water. A guide to their Public Health Consequences, Monitoring and Management. Eds Chorus, I. and Bartram, J., 347-367.
- Lelong, C., Boekema, E.J., Kruip, J., Bottin, H., Rögner, N. and Sétif, P. (1996) Characterization of a redox active cross-linked complex between cyanobacterial photosystem I and soluble ferredoxin. *European Molecular Biology Organization Journal* **15**, 2160-2168.
- Long, B.M., Jones, G.J. and Orr, P.T. (2001) Cellular microcystin content in N-limited *Microcystis aeruginosa* can be predicted from growth rate. *Applied and Environmental Microbiology* **67**, 278-283.
- Massana, R., Gasol, J.M., Bjørnsen, P.K., Blackburn, N., Hagström, A., Hietanen, S., Hygum, B.H., Kuparinen, J. and Pedrós-Alió, C. (1997) Measurement of bacterial size via image analysis of epifluorescence preparations: descriptions of an inexpensive system and solutions to some of the most common problems. *Sciencia marina* **61**, 397-407.
- McAlice, B. (1971) Phytoplankton sampling with the Sedgewick-Rafter cell. *Limnology and Oceanography* **16**, 19-28.
- McGregor, G.B. and Fabbro, L.D. (2000) Dominance of *Cylindrospermopsis raciborskii* (Nostocales, Cyanoprokaryota) in Queensland tropical and subtropical reservoirs: Implications for monitoring and management. *Lakes & Reservoirs: Research and Management* **5**, 195-205.
- Montagnes, D.J.S., Berges, J.A., Harrison, P.J. and Taylor, F.J.R. (1994) Estimating carbon, nitrogen, protein and chlorophyll a from volume in marine phytoplankton. *Limnology and Oceanography* **39**, 1044-1060.
- Mueller, L.N., de Brouwer, J.F.C., Xavier, J.B., Almeida, J.S. (2004) PHLIP: Image bioinformatics for the quantitative analysis of confocal laser scanning microscopy data. Proceedings IWA Biofilm Symposium. Las Vegas, Nevada.
- Necchi, O Jr., Sheath, R.G. and Cole, K.M. (1993) Systematics of freshwater *Audouinella* (Acrochaetiaceae, Rhodophyta) in North America. 1. The reddish species. *Archiv für Hydrobiologie Supplement* **98**, 11-28.
- Negri, A.P., Jones, G.J. and Hindmarsh, M. (1995) Sheep mortality associated with paralytic shellfish poisoning toxins from the cyanobacterium *Anabaena circinalis*. *Toxicon* **33**, 1321-1329.

- Ohtani, I., Moore, R.E. and Runnegar, M.T.C. (1992) Cylindrospermopsin: a potent hepatotoxin from the blue-green alga *Cylindrospermopsis raciborskii*. *Journal of the American Chemical Society* **114**, 7941-7942.
- Orr, P.T. and Jones, G.J. (1998) Relationship between microcystin production and cell division rates in nitrogen-limited *Microcystis aeruginosa* cultures. *Limnology and Oceanography* **43**, 1604-1614.
- Otsuka, S., Suda, S., Li, R., Matsumoto, S. and Watanabe, M.M. (2000) Morphological variability of colonies of *Microcystis* morphospecies in culture. *Journal of genetic and applied Microbiology* **46**, 39-50.
- Padisák, J. (1997) *Cylindrospermopsis raciborskii* (Woloszynska) Seenaya et Subba Raju, an expanding, highly adaptive cyanobacterium: worldwide distribution and review of its ecology. *Archiv fur Hydrobiology, Supplement* **4**, 563-593.
- Paerl, H.W., Fulton III, R.S., Moisander, P.H. and Dyble, J. (2001) Harmful freshwater algal blooms, with an emphasis on cyanobacteria. *TheScientific World* **1**, 76-113.
- Pernthaler, A., Pernthaler, J. and Amann, R. (2002) Fluorescence in situ hybridization and catalyzed reporter deposition for the identification of marine bacteria. *Applied and Environmental Microbiology* **68**, 3094-3101.
- Pernthaler, J., Alfreider, A., Posch, T., Anreatta, S. And Psenner, R. (1997) In situ classification and image cytometry of pelagic bacteria from a high mountain lake (Gossenköllesee, Austria). *Applied and Environmental Microbiology* **63**, 4778-4783.
- Pernthaler, J., Pernthaler, A. and Amann, R. (2003) Automated enumeration of groups of marine picoplankton after fluorescence in situ hybridization. *Applied and Environmental Microbiology* **69**, 2631-2637.
- Persson, P.-E. (1980) Muddy odour in fish from hypertrophic waters. *Developments in Hydrobiology* **2**, 203-208.
- Persson, P.-E. (1983) Off-flavours in aquatic ecosystems – an introduction. *Water Science and Technology* **15**, 1-11.
- Persson, P.-E. (1996) Cyanobacteria and off-flavours. *Phycologia* **35**, 168-171.
- Pilotto, L., Hobson, P., Burch, M.D., Ranmuthugala, G., Attewell, R. and Weightman, W. (2004) Acute skin irritant effects of cyanobacteria (blue-green algae) in healthy volunteers. *Australian and New-Zealand Journal of Public Health* **28**, 220-224.
- Poglazova, M.N., Mitskevitch, I.N., and Kuzhinovsky, V.A. (1996) A spectrofluorimetric method for determination of total bacterial counts in environmental samples. *Journal of Microbiological Methods* **24**, 211-218.
- Pons, M.N., Drouin, J.F., Louvel, L., Vanhoutte, B., Vivier, H. and Germain, P. (1998) Physiological investigation by image analysis. *Journal of Biotechnology* **65**, 3-14.
- Psenner, R. (1993) Determination of size and morphology of aquatic bacteria by automated image analysis. In: Kemp, P.F., Sherr, B.F., Sherr, E.B., Cole, J.J. (eds) *Handbook of Methods in Aquatic Microbial Ecology*. Lewis Publ., Boca Raton, 339-345.
- Regel, R. and Brookes, J. (2005) Light preference of *Cylindrospermopsis*. In: Reservoir management strategies for control and degradation of algal toxins. Brookes et al. (ed.), AWWA Research Foundation Project 2976, Second Periodic Report. Pp. 41-53.
- Reynolds, C.S. (1998) What factors influence the species composition of phytoplankton in lakes of different trophic status? *Hydrobiologia* **369/370**, 11-26.
- Reynolds, C.S. and Jaworski, G.H.M. (1978) Enumeration of natural *Microcystis* populations. *British Phycological Journal* **13**, 269-277.
- Rohlf, F.J. (1993) Relative warp analysis and an example of its application to mosquito wings. Pp. 131-159 in Marcus et al (eds.) *Contributions to morphometrics*. Musuo Nazionale de Ciencias Naturales.
- Ruffle, S.V., Mustafa, A.O., Kitmitto, A., Holzenburg, A. and Ford, R.C. (2000) The location of the mobile electron carrier ferredoxin in vascular plant photosystem I. *Journal of Biological Chemistry* **275**, 36250-36255.
- Russ, J.V. (1999) The image processing handbook. CRC Press, Raleigh, North Carolina, U.S.A.
- Saker, M.L. and Griffiths, D.J. (1999) Occurrence of blooms of the cyanobacterium *Cylindrospermopsis raciborskii* (Woloszynska) Seenayya and Subba in a north Queensland domestic water supply. *Marine and Freshwater Research* **52**, 907-915.
- Saker, M.L., Neilan, B.A. and Griffiths, D.J. (1999) Two morphological forms of *Cylindrospermopsis raciborskii* (Cyanobacteria) isolated from Solomon Dam, Palm Island, Queensland. *Journal of Phycology* **35**, 599-606.

- Schmid, M., Thill, A., Purkhold, U., Walcher, M., Bottero, J.Y., Ginestet, P., Nielsen, P.H., Wuertz, S. and Wagner, M. (2003) Characterization of activated sludge flocs by confocal laser microscopy and image analysis. *Water Research* **37**, 2043-2052.
- Schröder D. and Krambeck H.J. (1991) Advances in digital image analysis of bacterioplankton with epifluorescence microscopy. *Internationale Vereinigung für Theoretische und Angewandte Limnologie* **24**, 2601-2604.
- Seenaya, G. and Raju, N.S.S. (1972) On the ecology and systematics position of the alga known as *Anabaenopsis raciborskii* (Wolosz.) Elenk. And a critical evaluation of the forms described under the genus *Anabaenopsis*. In Desikachary, T.V. (ed.) *Taxonomy and Biology of Blue-Green Algae*. University of Madras, Madras, India, pp. 52-57.
- Sekar, R., Pernthaler, A., Pernthaler, J., Warnecke, F., Posch, T. and Amann, R. (2003) An improved protocol for quantification of freshwater *Actinobacteria* by fluorescence *in situ* hybridization. *Applied and Environmental Microbiology* **69**, 2928-2935.
- Shafik, H.M., Vörös, L., Spröber, P., Présing, M. and Kovács, A.W. (2003) Some special morphological features of *Cylindrospermopsis raciborskii* (isolated from Lake Balaton, Hungary) in batch and continuous cultures. *Hydrobiologia* **506**, 163-167.
- Shopov, A., Williams, S.C., Verity, P.G. (2000) Improvements in image analysis and fluorescence microscopy to discriminate and enumerate bacteria and viruses in aquatic samples. *Aquatic Microbial Ecology* **22**, 103-110.
- Sieracki, C.K., Sieracki M.E. and Yentsch, C.S. (1998) An imaging-in-flow system for automated analysis of marine microplankton. *Marine Ecology Progress Series* **168**, 285-296.
- Sieracki, M.E., Johnson, P.W. and Sieburth, J.McN. (1985) Detection, enumeration, and sizing of planktonic bacteria by image-analyzed epifluorescence microscopy. *Applied and Environmental Microbiology* **49**, 799-810.
- Sieracki, M.E., Viles, C.L. and Webb, L. (1989) Algorithm to estimate cell biovolume using image analyzed microscopy. *Cytometry* **10**, 551-557.
- Simpson, R.G., Williams, R., Ellis, R.E. and Culverhouse, P.F. (1992) Biological pattern recognition by neural networks. *Marine Ecology Progress Series* **79**, 303-308.
- Sorokin, Y.I. and Kadota, H. (1972) Techniques for the assessment of microbial production and decomposition in fresh waters. IBP Handbook N. 23. Blackwell Scientific Pub., London.
- Suffet, I.H. (1986) Removal of tastes and odors by ozone. Sem. Ozonation and Water Treatment. In: *Proceedings AWWA, Annual Conference*, Denver.
- Suller, M.T.E. and Lloyd, D. (1999) Fluorescence monitoring of antibiotic-induced bacterial damage using flow cytometry. *Cytometry* **35**, 235-241.
- Thomas, C. and Packer, H. (1990) Morphological and structural measurements on filamentous microorganisms. *Binary* **2**, 47-54.
- Vaitomaa, J., Rantala, A., Halinen, K., Rouhianen, L., Tallberg, P., Møkelke, L. and Sivonen, K. (2003) Quantitative real-time PCR for determination of microcystin synthetase E copy numbers for *Microcystis* and *Anabaena* in lakes. *Applied and Environmental Microbiology* **69**, 7289-7297.
- Vanrolleghem, P.A. and Lee, D.S. (2003) On-line monitoring equipment for wastewater treatment processes: state of the art. *Water Science and Technology* **2**, 1-34.
- Walker, R.F. (1999) Cyanobacteria detection and species classification by image analysis. Cyanobacteria Risk Assessment for Lake Biwa – *Report to the Science and Technology Agency (Japan)* – 13th April 1999, Otsu, Lake Biwa Research Institute.
- Walker, R.F. and Kumagai, M. (2000) Image analysis as a tool for quantitative phycology. A computational approach to cyanobacterial taxa identification. *Limnology* **1**, 107-115.
- Walker, R.F., Ishikawa, K. and Kumagai, M. (2002) Fluorescence-assisted image analysis of freshwater microalgae. *Journal of Microbiological Methods* **51**, 149-162.
- Walsby, A.E. and Avery, A. (1996) Measurement of filamentous cyanobacteria by image analysis. *Journal of Microbiological Methods* **26**, 11-20.
- Whitton B.A. (2000) Soils and rice fields. In: Whitton B.A., Potts M. (eds). *The ecology of cyanobacteria*. Kluwer Academic Publishing, Dordrecht, The Netherlands, pp. 233- 255.
- Wynn-Williams, D.D. (1994) Detection and simulation of environmental change in Antarctica by image analysis of soil algae. *Binary – Computing in Microbiology* **6**, 76-77.
- Young W.F., Horth, H., Crane, R., Ogden, T. and Arnott, M. (1996) Taste and odour threshold concentrations of potential potable water contaminants. *Water Research* **30**, 331-340.

CRC for Water Quality and
Treatment
Private Mail Bag 3
Salisbury SOUTH AUSTRALIA 5108
Tel: (08) 8259 0351
Fax: (08) 8259 0228
E-mail: crc@sawater.com.au
Web: www.waterquality.crc.org.au



CRC for Water Quality
and Treatment



The Cooperative Research Centre (CRC) for Water Quality and Treatment is Australia's national drinking water research centre. An unincorporated joint venture between 29 different organisations from the Australian water industry, major universities, CSIRO, and local and state governments, the CRC combines expertise in water quality and public health.

The CRC for Water Quality and Treatment is established and supported under the Federal Government's Cooperative Research Centres Program.

The Cooperative Research Centre for Water Quality and Treatment is an unincorporated joint venture between:

- ACTEW Corporation
- Australian Water Quality Centre
- Australian Water Services Pty Ltd
- Brisbane City Council
- Centre for Appropriate Technology Inc
- City West Water Limited
- CSIRO
- Curtin University of Technology
- Department of Human Services Victoria
- Griffith University
- Melbourne Water Corporation
- Monash University
- Orica Australia Pty Ltd
- Power and Water Corporation
- Queensland Health Pathology & Scientific Services
- RMIT University
- South Australian Water Corporation
- South East Water Ltd
- Sydney Catchment Authority
- Sydney Water Corporation
- The University of Adelaide
- The University of New South Wales
- The University of Queensland
- United Water International Pty Ltd
- University of South Australia
- University of Technology, Sydney
- Water Corporation
- Water Services Association of Australia
- Yarra Valley Water Ltd